UNIVERSIDADE NOVA DE LISBOA

Imperial College London

REGULATION AND FUNCTION OF THE CELL WALL POLYMER LIPOTEICHOIC ACID IN *STAPHYLOCOCCUS AUREUS*

CAROLINA PIÇARRA CASSONA

A THESIS SUBMITTED FOR THE DEGREE OF MASTER IN MEDICAL MICROBIOLOGY

External supervisor: Dr. Angelika Gründling
Internal supervisor: Prof. Dr. Hermínia de Lencastre

Experimental work performed at the Centre for Molecular Bacteriology and Infection, Imperial College London, Flowers Building London SW7 2AZ, UK

LONDON, SEPTEMBER 2013

Bibliographic elements resulting from this dissertation:

Published paper

Reichmann, N. T., Picarra Cassona, C. & Gründling, A. (2013). Revised mechanism of D-alanine incorporation into cell wall polymers in Gram-positive bacteria. *Microbiology* **159**, 1868-1877.

Acknowledgments

First, I would like to thank Angelika for the opportunity to work in her laboratory for her good supervision and guidance, and for all I have learned during this year.

I would like to thank everyone from CMMI3 who received me so well, and particularly to the members of Angelika's lab: Rebecca, Matt, Ivan, Marta and Lauren and, although she is not in the lab anymore, to Nathalie, for all the help, good ideas and support she gave me during this year. Everyone made me fell part of the group and helped me when I needed advices.

I wish to thank my family and friends, especially Tiago, Joana, Verónica and Gabriela for all the support and friendship during this year.

I also thank Jan Marchant from the cross faculty NMR Centre at Imperial College London for running the NMR samples.

Finally, I would like to thank the Scientific Committee of the MSc in Medical Microbiology of UNL for the organization of this master's course.

Abstract

Lipoteichoic acid (LTA) is an important polymer present in the envelope of various Gram-positive bacteria. In *Staphylococcus aureus* it is composed of a polyglycerolphosphate chain synthesised by the enzyme LtaS, and is anchored to the membrane via a glycolipid anchor. Depletion of LTA is known to cause growth arrest, aberrant positioning of septa and enlargement of cells leading to eventual cell lysis. This highlights the importance of LTA for bacterial growth and also suggests a possible link between LTA synthesis and cell division. Although key enzymes required for LTA synthesis have been identified, how this process is regulated has not been elucidated. This study investigates the mechanisms of regulation of LTA synthesis, as well as provides further insights into the roles of LTA in *S. aureus*.

In this study, nuclear magnetic resonance (NMR) was used to experimentally confirm a function for LTA in the incorporation of D-alanines into a second polymer, wall teichoic acid (WTA). LTA was also shown to be essential not only for bacterial growth, but also for bacterial survival, as cells become bactericidal in its absence. Furthermore, fluorescence microscopy using a GFP-tagged version of the synthase enzyme indicated that LtaS localises to the septum, suggesting a possible role for LTA in cell division.

Regarding LTA regulation, this work has shown that the *ltaS* gene has two promoters and a large upstream UTR, but that only one promoter is essential and sufficient for expression. Studying the effect of salt stress on LTA production has also revealed that an increase the NaCl concentration in the media causes a reduction in the levels of LTA produced, which in turn has an effect on growth. However this is not due to a decrease in the levels of LtaS, reflecting a possible ionic or osmotic effect on LtaS enzymatic activity.

Resumo

O ácido lipoteicóico (LTA) é um importante polímero presente no envelope de varias bactérias Gram-positivas. Em *Staphylococcus aureus* é composto por uma cadeia de poliglicerolfosfato sintetizada pela enzima LtaS e está ancorado na membrana através de uma âncora glicolipídica. Sabe-se que na ausência de LTA há interrupção do crescimento bacteriano, o septo deslocaliza e as células aumentam o seu tamanho e eventualmente lisam. Estas observações, mostram a importância do LTA para o crescimento bacteriano e sugerem uma ligação entre a sua síntese e a divisão celular. Apesar das principais enzimas necessárias para a síntese de LTA serem conhecidas, a regulação deste processo permanece por elucidar. Este estudo investiga a regulação da síntese do LTA e fornece novas perspectivas sobre as suas funções em *S. aureus*.

Neste estudo, ressonância magnética nuclear foi utilizada para confirmar experimentalmente a função do LTA na incorporação de D-alanina num segundo polímero, o ácido teicóico da parede (WTA). Mostrou-se também que o LTA não só é essencial para o crescimento, mas também para a sobrevivência bacteriana, tendo a sua ausência um efeito bactericida. Adicionalmente, microscopia de fluorescência utilizando fusões da sintase à proteína de fluorescência GFP, demonstrou que LtaS localiza no septo, sugerindo uma possível função do LTA na divisão celular.

Relativamente à regulação da produção de LTA, este trabalho mostrou que o gene *ltaS* tem dois promotores e uma grande região não traduzida a montante, mas apenas um dos promotores é essencial e suficiente para ocorrer expressão. O estudo do efeito do aumento da salinidade na produção de LTA mostrou que o aumento da concentração de NaCl causa uma redução nos níveis de LTA, causando uma redução no crescimento. No entanto, esta observação não se deve a uma diminuição nos níveis de LtaS, reflectindo um possível efeito iónico ou osmótico na actividade enzimática de LtaS.

Symbols and Abbreviations

%	Percentage
°C	Degrees Celsius
Δ	Deletion
Ω	Ohm
A	Ampere
Amp	Ampicillin
Atet	Anhydrotetracycline
ATP	Adenosine triphosphate
bp	Base pairs
BSA	Bovine serum albumin
c-di-AMP	Cyclic diadenosine monophosphate
CDP-Gro	Cytidine diphosphoglycerol
D-Ala	D-alanine
D-Gln	D-glutamine
D-Lac	D-lactate
D_2O	Deuterium oxide
DAG	Diacylglycerol
ddH_2O	Double distilled water
DMSO	Dimethyl sulfoxide
DNA	Deoxyribonucleic acid
DNase	Deoxyribonuclease
dNTP	Deoxyribonucleotide triphosphate
ECL	Enhanced chemi-luminescence
EDTA	Ethylenediaminetetraacetic acid
Erm	Erythromycin
F	Farad
FucNAc	N-acetyl-L-fucosamine
g	Gram
GFP	Green fluorescent protein
Glc-1-P	Glucose-1-phosphate
Glc-6-P	Glucose-6-phosphate
Glc_2-DAG	Diglucosyldiacylglycerol
GlcNAc	N-acetylglucosamine
GlcNAc-1-P	N-acetylglucosamine-1-phosphate
GroP	Glycerol phosphate
h	Hour(s)
HRP	Horseradish peroxidase

IgG	Immunoglobulin G
IPTG	Isopropyl β-D-thiogalactosidase
Kan	Kanamycin
kb	Kilo base pair
kDa	Kilodalton
L	Liter
L-Lys	l-lysine
LA	Luria Bertani agar
LB	Luria Bertani broth
LTA	Lipoteichoic acid
Lys-PG	Lysyl-phosphatidylglycerol
M	Molar
ManNAc	N-acetylmannosamine
ManNAcA	N-acetylmannosaminuronic acid
MBOAT	Membrane-bound O-acetyltransferases
MIC	Minimum inhibitory concentration
min	Minute(s)
MOPS	3-(N-morpholino)propanesulfonic acid
MRSA	Methicillin resistant *Staphylococcus aureus*
MSSA	Methicillin sensitive *Staphylococcus aureus*
MU	4-methylumbilliferone
MUG	β-D-galactopyranoside
MurNAc	N-Acetylmuramic acid
NMR	Nuclear magnetic resonance
nt	Nucleotide(s)
OD	Optical density
P-C_{55}	Undecaprenyl phosphate
PBP	Peptidoglycan binding protein
PBS	Phosphate buffered saline
PCR	Polymerase chain reaction
PG	Phosphatidylglycerol
PGN	Peptidoglycan
PGP	Polyglycerolphosphate
PVDF	Polyvinylidene difluoride
RboP	Ribitol phosphate
rpm	Rotations per minute
s	Second(s)
SDS	Sodium dodecyl sulfate
SDS-PAGE	Sodium dodecyl sulfate polyacrylamide gel electrophoresis

SOE PCR	Splicing by overlap extension polymerase chain reaction
TA	Teichoic acids
TCA	Trichloroacetic acid
Tris	Tris(hydroxymethyl)aminomethane
TSA	Tryptic soy agar
TSB	Tryptic soy broth
U	Unit(s)
UDP	Uridine diphosphate
UDP-Glc	Uridine diphosphate glucose
UDP-GlcNAc	Uridine diphosphate N-acetylglucosamine
UDP-MurNAc	Uridine diphosphate N-Acetylmuramic acid
UTR	Untranslated region
V	Volt
VISA	Vancomycin-intermediate *Staphylococcus aureus*
VRSA	Vancomycin-resistant *Staphylococcus aureus*
WT	Wild-type
WTA	Wall teichoic acid
X-Gal	5-bromo-4-chloro-3-indolyl-β-D-galactopyranoside
xg	Times gravity

Table of Contents

List of Figures

Page

List of Tables

Page

1. Introduction

1.1. *Staphylococcus aureus*

Staphylococcus aureus is a Gram-positive bacterium that is able to colonise and infect human and animal hosts. It is non-motile, non-sporeforming, facultative anaerobe and a member of the Firmicutes that is distinguishable from other staphylococcal species by its ability to produce coagulase (coagulase-positive), a secreted protein that promotes clumping of the human blood cell (Gotz *et al.*, 2006). *S. aureus* cells are 0.5-1.5 μm in diameter and can occur in various forms: singly, in pairs, tetrads or as grape-like clusters, which are formed by cells that fail to fully separate (Gotz *et al.*, 2006; Tzagoloff & Novick, 1977). Cell division occurs in three orthogonal planes and the future cell division site is perpendicular to the previous septum (Tzagoloff & Novick, 1977).

On agar plates *S. aureus* forms golden-yellow round colonies, which is due to its ability to produce a carotenoid pigment, staphyloxanthin, that is important for its virulence and to evade the host innate immune system (Liu *et al.*, 2005). Like other staphylococcal species, it has a low guanine and cytosine content in its genome (30-39 mol %) and the genome is approximately 3000 kb in size (Gotz *et al.*, 2006).

S. aureus mainly colonises the nasal passages transiently, sometimes permanently, and is a potential pathogen, which is able to cause both superficial skin infections as well as invasive infections such as toxic shock syndrome, endocarditis and osteomyelitis (Foster, 2005; Lowy, 2003).

The introduction of penicillin in the 1940s quickly promoted the proliferation of resistant *S. aureus* strains expressing β-lactamase (Barber & Rozwadowska-Dowzenko, 1948), making the development of antibiotics against this Gram-positive pathogen a challenge. β-lactamase is encoded by *blaZ* that is part of a transposable element in a large plasmid. This enzyme acts by hydrolysing the β-lactam ring inactivating the antibiotic (Bondi & Dietz, 1945; Rowland & Dyke, 1989). With the introduction in the 1950s of the first semisynthetic penicillin, methicillin, methicillin-resistant *S. aureus* (MRSA) became a concern and the foremost cause of bacterial infections at a global scale (Fuda *et al.*, 2005). MRSA strains were initially found to be hospital associated

(HA-MRSA), where the majority of infections still occur, but nowadays it is also community associated (CA-MRSA) (Fey *et al.*, 2003; Okuma *et al.*, 2002). β-lactam antibiotics act by mimicking the substrate of penicillin-binding proteins (PBPs) and, consequently, acylate and inactivate the PBPs, which are essential for the last steps of peptidoglycan synthesis (Chambers, 2003). The resistance mechanism in MRSA strains is due to the acquisition of an extra PBP, PBP2A encoded by the *mecA* gene (Beck *et al.*, 1986). This PBP is able to perform the normal functions of the other PBPs in cell wall biosynthesis, but has low affinity for all β-lactam antibiotics (Beck *et al.*, 1986; de Jonge *et al.*, 1992). PBP2A acts by compensating for PBP2 transpeptidase (TPase) function, though the transglycosylase (TGase) function of PBP2 is still required (Pinho *et al.*, 2001) (see section 1.2.2. Peptidoglycan structure and synthesis).

The glycopeptide antibiotic vancomycin started to be used as an alternative treatment for MRSA infections. However, vancomycin-intermediate *S. aureus* (VISA) and fully vancomycin-resistant *S. aureus* (VRSA) have now been already detected. In VISA strains there is an increase in the quantity of peptidoglycan, which results in an increase of D-Ala-D-Ala residues exposed and, since these are the targets for vancomycin, the access to the bacterial target is prevented (Sieradzki & Tomasz, 1999). VRSA strains, on the other hand, emerged due to the acquisition of the *vanA* gene from vancomycin resistant enterococci. In these isolates, the terminal dipeptide in the peptidoglycan is D-Ala-D-Lac instead of D-Ala-D-Ala, the synthesis of which is catalysed by a ligase encoded by *vanA* (Showsh *et al.*, 2001).

Given the emergence of resistance mechanisms to the available antibiotics, there has been a growing interest in studying the staphylococcal cell surface in order to find novel antibiotic targets.

1.2. Components of the *S. aureus* cell wall

The wall of Gram-positive bacteria is characterised by a thick layer of cross-linked peptidoglycan (PGN) that enables these bacteria to survive in harsh environments, even lacking the outer membrane characteristic of Gram-negative bacteria (Silhavy *et al.*, 2010) (Figure 1). Besides peptidoglycan other components are required to maintain the envelope structure and function, including the teichoic acids

(TAs). TAs are composed of polyol-phosphate subunits and can be grouped into wall teichoic acids (WTAs), which are covalently attached to the peptidoglycan and lipoteichoic acids (LTAs), which are anchored to the cell membrane via a glycolipid anchor (Fischer, 1994; Neuhaus & Baddiley, 2003; Reichmann & Gründling, 2011; Xia *et al.*, 2010) (Figure 1).

The surface of Gram-positive bacteria also contains proteins that can be associated with the membrane through membrane spanning domains or attached to lipid anchors (Silhavy *et al.*, 2010). Proteins can also be associated to the peptidoglycan layers or to other polymers such as TAs and polysaccharides (Navarre & Schneewind, 1999) (Scott & Barnett, 2006). It is still worth noting that the presence of a low-density region that can be considered to be the Gram-positive periplasm has been identified in these bacteria (Matias & Beveridge, 2005; Matias & Beveridge, 2006; Matias & Beveridge, 2008) (Figure 1).

The membrane is a phospholipidic bilayer with integrated membrane proteins and other components such as LTA and lipoproteins. In *S. aureus*, the four major lipids making up the membrane are diglucosyl diacylglycerol (Glc_2-DAG), phosphatidyl glycerol (PG), diacylglycerol (DAG) and a lysyl-phosphatidyl glycerol (Lys-PG) (Koch *et al.*, 1984; White & Frerman, 1967). LTA represents 6% of the membrane composition and its synthesis is closely interconnected with the synthesis of the other membrane lipids (Koch *et al.*, 1984) (see section 1.2.3.2 LTA structure and synthesis).

In the majority of the *S. aureus* strains there is also a polysaccharide capsule external to the peptidoglycan layer that has been shown to be important for virulence, colonisation and biofilm formation (O'Riordan & Lee, 2004).

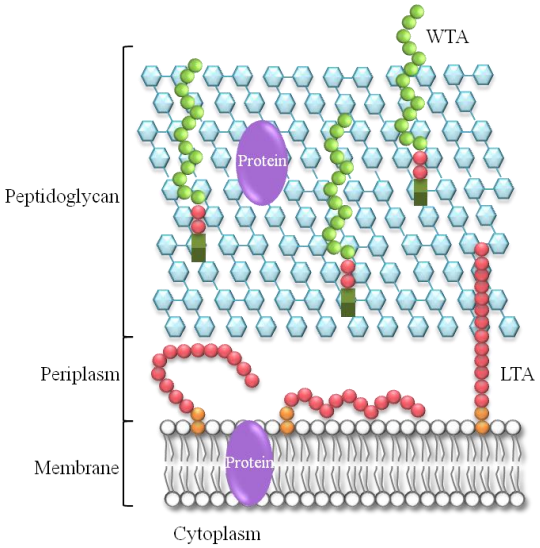

Figure 1 – Schematic representation of the cell wall in Gram-positive bacteria. The cell wall in Gram-positive bacteria is mainly composed of cross-linked peptidoglycan (blue hexagons), teichoic acids that can be divided into wall teichoic acids (WTAs) (green circles) and lipoteichoic acids (LTAs) (pink circles). Additionally, there are proteins associated to the membrane or to the peptidoglycan layer (purple). Adapted from Reichmann and Gründling, 2011.

1.2.1. The polysaccharide capsule

A capsule usually surrounds microorganisms that cause invasive infections. Encapsulation is an important characteristic as it enhances virulence and protects the bacteria from phagocytic uptake (O'Riordan & Lee, 2004). In *S. aureus*, polysaccharide capsules are grouped into serotypes and, although there are 11 serotypes, the serotype 5 and 8 are the most predominant ones in clinical isolates (Hochkeppel *et al.*, 1987; Roghmann *et al.*, 2005; Sompolinsky *et al.*, 1985).

Of the *S. aureus* strains where the capsule biochemical structure has been ascertained all contain hexosaminuronic acids. Although types 5 and 8 belong to different serotypes, they have similar structures: both have a residue of N-acetylmannosaminuronic acid (ManNAcA) and two residues of N-acetyl-L-fucosamine (FucNAc) and they only differ in the way the sugars are linked and in the site of O-acetylation of the N-acetylamannosaminuronic acid residues (Fournier *et al.*, 1984; Fournier *et al.*, 1987).

The proteins required for the synthesis of serotypes 5 and 8 capsules are encoded in the gene clusters *cap5* and *cap8*, respectively. These clusters contain homologous genes (*cap5A*, *cap5G* and *cap5L-P* are very similar to *cap8A*, *cap8G* and *cap8L-P*) but

also contain type-specific genes. The functions of these genes have not been experimentally demonstrated but the majority are likely to be involved in sugar synthesis, transfer, chain-length regulation and polymerisation (Sau *et al.*, 1997).

It has been shown that the environment has an influence on polysaccharide capsule production. For example, growth in low concentrations of iron and on solid medium enhances the production of the serotype 8 capsule (Lee *et al.*, 1993; Poutrel *et al.*, 1995). Furthermore, serotype 5 capsule production is downregulated by CO_2 levels (serotype 8 capsule production is also regulated by CO_2 levels but in a genetic background dependent manner between different strains) and enhanced by NaCl concentration (Herbert *et al.*, 2001; Sompolinsky *et al.*, 1985).

1.2.2. Peptidoglycan structure and synthesis

The peptidoglycan structure is common to most bacteria, both Gram-positive and Gram-negative (Silhavy *et al.*, 2010). It is composed of disaccharide-peptide repeats linked through glycolipid bonds [β-1,4 linkages between N-acetylmuramic acid (MurNAc) and N-acetylglucosamine (GlcNAc) subunits] forming glycan strands, which in turn are cross-linked through peptide stems attached to the MurNAc subunits (Ghuysen & Strominger, 1963; Navarre & Schneewind, 1999). This results in a structure that is flexible enough to ensure that the cell can resist changes in the internal osmotic pressure (Scheffers & Pinho, 2005). Although this structure is well dispersed amongst bacteria, its length is variable and in *S. aureus* most of the glycan strands have 3 to 10 subunits, but can reach up to 26 subunits (Navarre & Schneewind, 1999; Scheffers & Pinho, 2005).

The peptide stems also vary significantly, though they all consist of a pentapeptide chain containing L- and D-amino acids and one dibasic amino acid (L-lysine in many Gram-positive bacteria), which allows the formation of the peptide cross bridge. In *S. aureus*, the pentapeptide is composed of L-alanine (L-Ala), D-glutamine (D-Gln), L-lysine (L-Lys) and two D-alanine residues (D-Ala-D-Ala). The peptides are connected through a pentaglycine structure extending from the L-Lys residue and connecting it to the penultimate D-Ala residue in the neighbouring peptide (Navarre &

Schneewind, 1999). *S. aureus* has a high degree of cross-linking when compared with other Gram-positive bacteria (up to 90% comparing with 56 to 63% in *B. subtilis*, for example), which is mainly attributed to PBP4 (Scheffers & Pinho, 2005).

As described below, the biosynthesis of peptidoglycan can be divided into three stages:

a) The first stage takes place in the cytoplasm and generates the precursors UDP-N-acetylmuramyl-pentapeptide (UDP-MurNAc-pentapeptide) and UDP-N-acetylglucosamine (UDP-GlcNAc). These steps involve the GlmM, GlmS and GlmU and the MurA-F proteins in a well known pathway (reviewed in Barreteau *et al.*, 2008).

b) The second stage occurs in the cytoplasmic membrane, where precursor lipid intermediates are synthesised. Phospho-MurNAc-pentapeptide is transferred from UDP-MurNAc-pentapeptide to the membrane acceptor bactoprenol producing MurNAc-(pentapeptide)-pyrophosphoryl-undecaprenol, also called lipid I . The addition of GlcNAc to lipid I then yields GlcNAc-β-(1,4)-MurNAc-(pentapeptide)-pyrophosphoryl-undecaprenol, commonly known as lipid II (Scheffers & Pinho, 2005). The five glycine residues involved in cross-linking are added to the L-Lys residue by the nonribosomal peptidyl transferases Fem A, Fem B and Fem X (Berger-Bachi & Tschierske, 1998; Ton-That *et al.*, 1998). These precursors are then translocated across the hydrophobic membrane to the outer leaflet of the membrane prior to being incorporated into the growing peptidoglycan chains (Scheffers & Pinho, 2005).

c) The last steps involve two reactions, transglycosylation and transpeptidation, which are catalysed by the PBPs (Sauvage *et al.*, 2008). Transglycosylation is the transference of the C-4 carbon from the glucosamine residue of the lipid-linked precursor to the MurNAc of the nascent peptidoglycan with the release of undecaprenyl-pyrophosphate, leading to the incorporation of precursor subunits into the growing peptidoglycan strand (Scheffers & Pinho, 2005). The transpeptidation reaction leads to formation of peptide bonds between the peptide stems. Firstly, the D-Ala-D-Ala linkage is cleaved resulting in an enzyme-substrate intermediate with the PBP. This releases the energy necessary for the transfer of a peptidyl moiety to a glycine on the pentaglycine bridge of a neighbouring peptide stem, resulting in a cross-bridge between the peptidoglycan subunits (Scheffers & Pinho, 2005).

In methicillin susceptible *S. aureus* strains (MSSA) there are four native PBPs, which catalyse these reactions. PBP1 has an essential role in cell division and its transpeptidase domain has been shown to play a vital role during cell separation (Pereira *et al.*, 2009). PBP2 has both TGase and TPase activity and localises at the cell division site (Scheffers & Pinho, 2005). However, in the presence of oxacillin, a β-lactam antibiotic which binds to the transpeptidase domain, PBP2 delocalises, indicating that binding to its substrate is necessary for correct localisation (Pinho & Errington, 2005). In methicillin resistant *S. aureus* strains there is an additional PBP, the PBP2A, which is encoded by the *mecA* gene (Beck *et al.*, 1986; Hartman & Tomasz, 1984) and is able to restore PBP2 localisation even in the presence of oxacillin (Pinho & Errington, 2005). This extra PBP acts as a surrogate for the TPase activity of PBP2 in the presence of β-lactam antibiotics, but the TGase activity of the native PBP2 is still needed (Pinho *et al.*, 2001). PBP3 is encoded by *pbpC* and its absence does not cause a change in peptidoglycan composition. However, the mutant of PBP3, once grown in the presence of sub-MIC levels of methicillin, displays increased cell size, aberrant cell shape and misplacement of the septa, indicating a role in cell division (Pinho *et al.*, 2001). Finally, PBP4 is non-essential, is responsible for the high degree of peptidoglycan cross-linking observed in *S. aureus* and its mutant was found to be more susceptible to β-lactams (Memmi *et al.*, 2008; Wyke *et al.*, 1981).

Besides the enzymes necessary for PG synthesis it is also important not to forget that PG hydrolases have a vital role in cell growth, since it is important to cleave old PG in order to incorporate new material. Therefore, it has been proposed that PG synthases form a multienzyme complex together with hydrolases in order to maintain the equilibrium between these two activities (Scheffers & Pinho, 2005).

1.2.3. Teichoic acids

The cell surface of most Gram-positive bacteria including *S. aureus* and *B. subtilis* also contain TAs. These components have a zwitterionic character and perform crucial roles in bacterial survival and cellular processes (Kohler *et al.*, 2009; Xia *et al.*, 2010). TAs act as a layer of protection to the PG layer from small harmful molecules and other environmental stresses but, since these are the more external components (at

least in *S. aureus*), and given its charge distribution, they are also possibly involved in regulating cation concentrations and enzymatic activities at the cell surface and in mediating interactions with receptors and biomaterials, which is relevant in biofilm formation (Schirner *et al.*, 2009; Weidenmaier & Peschel, 2008; Xia *et al.*, 2010).

TAs are composed of repeating polyol phosphate subunits such as ribitol phosphate (RboP) or glycerol phosphate (GroP) and can be grouped into WTA that is covalently linked to the peptidoglycan, and LTA that is anchored to the membrane through a glycolipid anchor and extends into the wall (Xia *et al.*, 2010).

1.2.3.1. WTA structure, synthesis and functions

WTA is structural diverse in Gram-positive bacteria due to the nature of its monomeric forms and to modifications with glycosyl substituents and D-alanyl esters (Neuhaus & Baddiley, 2003). The monomers are polyol phosphate residues, which form linear chains covalently linked to the peptidoglycan through a phosphodiester bond. In the majority of *S. aureus* strains, the chains consist of RboP subunits, while in *B. subtilis* WTA is made up of GroP residues (Bertram *et al.*, 1981; Sanderson *et al.*, 1962). *S. aureus* WTA is covalently linked to the C6 hydroxyl group of MurNAc of peptidoglycan, through a disaccharide, composed of N-acetylglucosamine-1-phosphate (GlcNAc-1-P) and N-acetylmannosamine (ManNAc), and two GroP residues (Figure 2) (Brown *et al.*, 2008; Xia *et al.*, 2010).

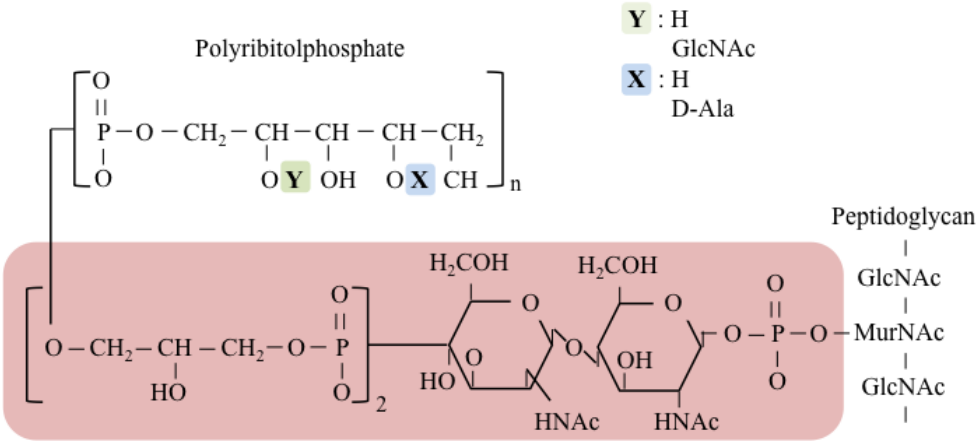

Figure 2 – WTA chemical structure in *S. aureus*. The RboP chain can be modified with a D-alanyl ester (blue) or glycosyl group (green) and is linked to the peptidoglycan via a disaccharide composed of N-acetylglucosamine-1-phosphate (GlcNAc-1-P) and N-acetylmannosamine (ManNAc), and two GroP residues (pink).

The steps for *S. aureus* WTA synthesis are known and begin at the inner leaflet of the cytoplasmic membrane where the disaccharide linkage unit is produced. First, GlcNAc-1-P and ManNAc are transferred from UDP-activated precursor molecules to undecaprenylphosphate (C_{55}-P), by TagO and TagA, respectively (Brown *et al.*, 2008; Xia *et al.*, 2010). This first step is followed by the addition of the GroP residues, involving TagB that adds the first GroP subunit to the disaccharidic linker, and TarF, which adds the second GroP subunit. The substrate used by these enzymes is the activated precursor cytidine diphosphoglycerol **(**CDP-Gro), which is generated by TagD (Badurina *et al.*, 2003). TarL then polymerises the poly-RboP chain (Brown *et al.*, 2008), using as its substrate the TarIJ generated precursor, CDP-Rbo (Meredith *et al.*, 2008). Finally, this structure is transported to the outside of the cell through a two-component transporter (TagG and TagH), where it can be attached to the peptidoglycan (Brown *et al.*, 2008). Besides D-alanylation, *S. aureus* WTA is also modified with α- or β-O-acetylgucosamine residues, which are added due the action of TarM and TarS as recently shown (Brown *et al.*, 2012).

Although WTA is not essential for viability in both *S. aureus* and *B. subtilis* (D'Elia *et al.*, 2006; Weidenmaier *et al.*, 2004a), it has important roles in virulence. WTA protects the cell from the host immune defences such as lysozyme, possibly by preventing the enzyme from reaching the glycan strands of PG (Bera *et al.*, 2007), and also from antimicrobial fatty acids due to its hydrophilic properties (Kohler *et al.*, 2009), which makes WTA important for infection, especially for skin infection. Furthermore, WTA is important for adherence to epithelial and endothelial cells (Weidenmaier *et al.*, 2004a; Weidenmaier *et al.*, 2005). These functions make WTA vital during host infection and colonisation. Besides this, WTA, being at the surface, is also important for phage binding, which makes it relevant for phage typing (Pantucek *et al.*, 2004).

1.2.3.2. LTA structure and synthesis

LTA consists of a polyglycerolphosphate (PGP) chain that is linked through a glycolipid anchor to the bacterial membrane and extends into the cell wall (Figure 3) (Archibald *et al.*, 1968; Fischer, 1994). In staphylococci, bacilli and streptococci the glycolipid anchor is glucosyl (β1-6) glucosyl (β1-3) diacylglycerol (Glc_2-DAG) (Neuhaus & Baddiley, 2003; Reichmann & Gründling, 2011). Although LTA has a well-defined structure there is still variability due to glycosyl and D-alanine substitutions, fatty acid composition and length of the PGP chain (Neuhaus & Baddiley, 2003).

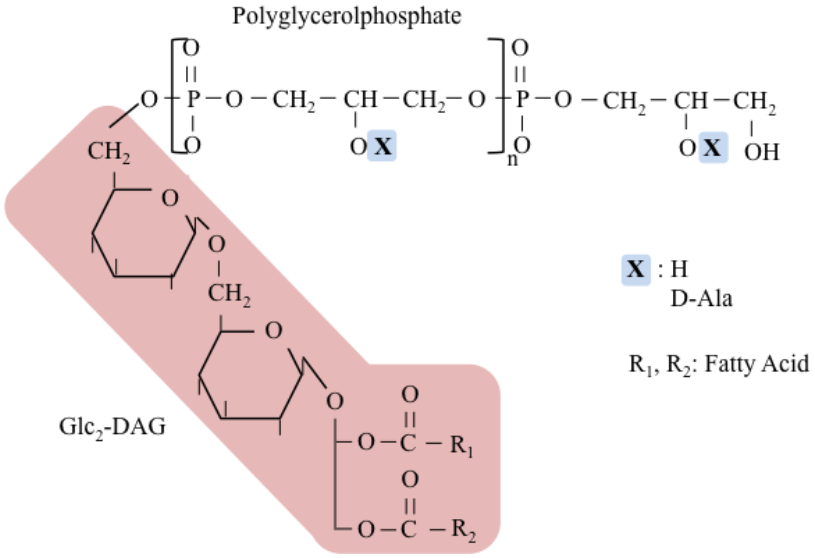

Figure 3 – LTA chemical structure in *S. aureus*. The polyglycerolphosphate (PGP) chain is linked to the membrane through a glycolipid anchor (Glc_2-DAG) (pink). The PGP chain can be modified at the C2 position with D-alanine residues, as shown in blue. Adapted from Reichmann & Gründling, 2011.

LTA synthesis can be mainly divided into three steps: the glycolipid anchor synthesis (Figure 4, steps 1 to 4), the PGP chain polymerization (Figure 4, step 5) and the addition of D-alanine residues (Figure 4, step 6) (Fischer, 1994).

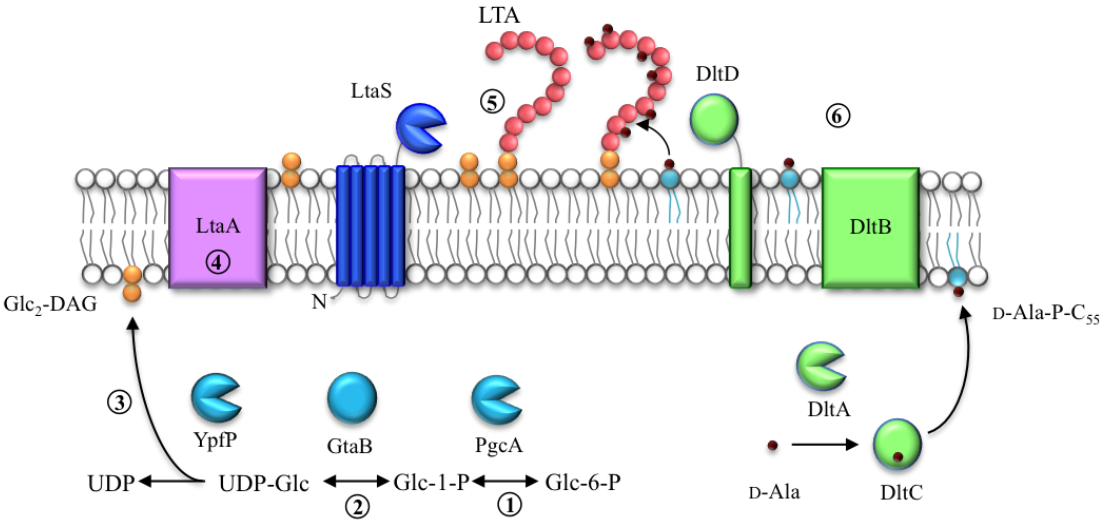

Figure 4 – Schematic representation of LTA synthesis in *S. aureus*. The glycolipid anchor (orange) is synthesised in the cytoplasm of the cell by PgcA, GtaB and YpfP (blue) (steps 1 to 3), and translocated across the membrane, which possibly involves LtaA (violet) (step 4). The polyglycerolphosphate chain (pink circles) is synthesised by the LTA synthase, LtaS (dark blue) (step 5). The DltA-D proteins (green) (step 6) are essential for the incorporation of D-alanine esters (dark red) into the LTA chain.

In *S. aureus* and *B. subtilis*, the Glc_2-DAG anchor is synthesised in the cytoplasm and this process involves the transference of two glucose moieties from uridine diphosphate glucose (UDP-Glc) to DAG (Fischer, 1994; Kiriukhin *et al.*, 2001) (Figure 4). For this to occur, the action of three enzymes is required: PgcA (or Pgm), a α-phosphoglucomutase, which converts glucose-6-phosphate (Glc-6-P) to glucose-1-phosphate (Glc-1-P) (Gründling & Schneewind, 2007a; Lazarevic *et al.*, 2005; Lu & Kleckner, 1994); GtaB (or GalU), which transfers UDP to glucose-1-phosphate, giving rise to UDP-Glc (Gründling & Schneewind, 2007a; Pooley *et al.*, 1987); and YpfP (or UgtP), a processive glycosyltransferase which transfers two glucose moieties from UDP-Glc to DAG, generating Glc_2-DAG and releasing UDP (Gründling & Schneewind, 2007a; Jorasch *et al.*, 1998; Kiriukhin *et al.*, 2001) (Figure 4, steps 1 to 4). Lastly, Glc_2-DAG needs to be transported across the membrane to the outer leaflet of the membrane, where the PGP chain will be polymerised on this glycolipid. It is thought that in *S. aureus* LtaA a member of a major facilitator superfamily clan, and encoded in the same operon as *ypfP* (Gründling & Schneewind, 2007a) is involved in this flipping reaction (Figure 4, step 5).

All the enzymes involved in this process are not essential for cell viability since its mutants are still able to synthesise LTA but without a glycolipid anchor, resulting in LTA directly anchored to DAG (Gründling & Schneewind, 2007a; Lazarevic *et al.*, 2005). Cells from *S. aureus ypfP* mutants were shown to be misshaped and enlarged (Kiriukhin *et al.*, 2001) but still viable. However, these mutants demonstrate varying phenotypes depending on the strain background. For instance, RN4220 *ypfP* mutants produce a slightly increased amount of PGP-LTA that is released into the supernatant (Kiriukhin *et al.*, 2001) while SA113 Δ*ypfP* contains significantly reduced amounts of LTA (Fedtke *et al*., 2007).

As mentioned above, the PGP chain is polymerised on the outside of the cell and the LTA synthase (LtaS) is responsible for this reaction (Gründling & Schneewind, 2007b) (Figure 4). LtaS is a polytopic membrane protein with five N-terminal transmembrane helices (5TM domains) and a C-terminal extracellular enzymatic domain (eLtaS) (Gründling & Schneewind, 2007b; Lu *et al.*, 2009) (Figure 4). This enzyme is cleaved in the linker region between these two domains by the protease SpsB, which is thought to inactivate the enzyme that is only active when in its full-length form (Wörmann *et al.*, 2011b).

For LTA synthesis it has been proposed that the GroP subunits are derived from the head group of the membrane lipid phosphatidylglycerol (PG), which was first suggested by pulse-chase experiments (Koch *et al.*, 1984). More recently an experiment using fluorescently labelled PG showed that LtaS is able to cleave GroP from PG in order to form DAG (Karatsa-Dodgson *et al.*, 2010). The GroP subunits are then added to the distal end of the growing chain. Although in *S. aureus* LtaS is able to start and extend the PGP chain, it is important to note that in *L. monocytogenes* there is an LTA primase (LtaP), which is necessary to add the first GroP subunit to the glycolipid anchor (Webb *et al.*, 2009). Similarly, *B. subtilis* expresses an enzyme with primase activity, YvgJ (Wörmann *et al.*, 2011a). In fact, in *B. subtilis* there are four enzymes able to hydrolyse PG from membrane lipids: LtaS, YqgS, YvgJ and YfnI. The reason for the presence of multiple enzymes to synthesise LTA in *B. subtilis* comparing with the one-enzyme system in *S. aureus* may be due to an interconnection between LTA synthesis, and environmental conditions and developmental processes, such as sporulation (Wörmann *et al.*, 2011a).

In *S. aureus*, LtaS depletion results in inability to synthesise LTA and growth arrest associated with severe envelope and division defects (Gründling & Schneewind, 2007b). In these conditions, cells present aberrant positioning of the septa, altered cell morphology and even lysed cells without cytoplasm or nucleic acids (Gründling & Schneewind, 2007b).

1.2.3.3. The function and localisation of lipoteichoic acid

In addition to WTA, LTA is also important to maintain the cell wall structure and has important functions in helping cells to adapt to different environmental factors. In *S. aureus* it has been shown that LTA is important to protect the cell in low osmolarity conditions, given the fact that an LtaS depleted strain is only able to survive at 37°C at high salt (7.5%) or sucrose (40%) (Oku *et al.*, 2009). This may indicate that LTA act as an osmoprotectant under normal growth conditions.

As described above, *S. aureus* mutants with depleted LtaS have misplaced division septa, which seems to indicate a role in cell division (Gründling & Schneewind, 2007b; Oku *et al.*, 2009). This may be due to interactions with the membrane-bound division machinery (Xia *et al.*, 2010). Although in *S. aureus* it is still not proved that LtaS localises at the division septa, in *B. subtilis* both LtaS and YqgS localise to the site of cell division and the absence of LtaS results in FtsZ delocalisation and subsequent misplacement of septa (Schirner *et al.*, 2009). Also, the YpfP homolog in *B. subtilis*, UgtP, was shown to have a septal localisation, which is dependent on the presence of UDP-Glc, the substrate for this enzyme (Weart *et al.*, 2007). Together, this data seem to indicate a link between LtaS and cell division.

LTA, together with WTA, also has an important role in regulating autolytic activity in *S. aureus*, since in the absence of LtaS there is a decrease in autolytic activity (Oku *et al.*, 2009). Furthermore, an LTA suppressor strain with mutations affecting the levels of the signalling molecule cyclic diadenosine monophosphate (c-di-AMP) was obtained (Corrigan *et al.*, 2011) and in this strain there is a reduction in the levels of hydrolytic enzymes that were increased by the re-introduction of *ltaS* and consequent LTA production (Corrigan *et al.*, 2011). Once again these observations support the role

of LTA in autolysis regulation and may be related to the fact that LTA is essential for ion binding, particularly Mg^{2+} ions (Heptinstall *et al.*, 1970).

Suggested function of LTA in the cell is closely related to its location and some suggested roles for this polymer are based on the assumption that this is a cell-surface exposed molecule. However, LTA is detected in the membrane and the detection of this polymer in whole cells of *S. aureus* is variable between strains (Aasjord & Grov, 1980). Furthermore, labelling experiments with positively charged gold nanoparticles suggested that the periplasmic space in *B. subtilis* is occupied by negatively charged components (Matias & Beveridge, 2008). These components could not be removed by protease treatment, indicating that these are not proteinaceous components, and could be detected by an LTA-specific monoclonal antibody (Matias & Beveridge, 2008). These data suggest that LTA might be the major component of the Gram-positive periplasm. Additionally, LTA PGP chain synthesis by LtaS that uses PG as a substrate, and D-alanylation by Dlt proteins suggests that LTA needs to remain close to the membrane during and after its synthesis (Reichmann & Gründling, 2011). However, it is important not to forget the possibility that LTA is also involved in WTA D-alanylation (Haas *et al.*, 1984), which implies flexibility in the positioning of the LTA molecule.

It has also been suggested that LTA has roles in adherence, biofilm formation and interactions with the molecules from the host immune system (Xia *et al.*, 2010) but these are not compatible with the idea that LTA is not exposed at the cell surface. These roles might be related with the fact that LTA is also released from the bacterial cell and found in the supernatant (Fischer, 1988).

1.2.3.4. D-Alanine incorporation into teichoic acids

Both LTA and WTA are modified with D-alanine esters and this process, adding positive charges to the otherwise negatively charged polymers, is important to modulate envelope properties (Neuhaus & Baddiley, 2003).

The enzymes involved in LTA D-alanylation are encoded in the *dlt* operon (Neuhaus *et al.*, 1996; Perego *et al.*, 1995). In *S. aureus* the *dlt* operon consists of five genes, *dltX*, *A*, *B*, *C* and *D* (Fischer, 1994). The *dltX* gene encodes DltX, which is a very

small protein with an expected size of 5.9 kDa and has been annotated to belong to the DUF3687 superfamily (Reichmann *et al.*, 2013). In *S. aureus* and other gram-positive bacteria, this protein is encoded immediately upstream of *dltA*, but whether if functions in the D-alanylation process it is still unknown (Koprivnjak *et al.*, 2006). The *dltA* gene encodes the D-alanine-D-alanyl carrier protein ligase (DltA) (Baddiley & Neuhaus, 1960), which belongs to a family of enzymes that activate and transfer amino or fatty acids to a thiol group of the 4-phosphopantetheine prosthetic group of a carrier protein (Du *et al.*, 2008; Osman *et al.*, 2009). In the process of D-alanylation, its role is to ligate D-alanine to the 4-phosphopantetheine of the carrier protein DltC, leading to the release of adenosine monophosphate (AMP) (Heaton & Neuhaus, 1994; Neuhaus *et al.*, 1996). DltB and DltD, encoded by *dltB* and *dltD*, respectively, have more questionable roles. DltB is predicted to be a polytopic membrane protein with 12 transmembrane domains and belongs to the membrane-bound O-acetyltransferases (MBOAT) family (Hofmann, 2000). DltD is also a membrane protein that is likely to be anchored to the membrane via its N-terminus (Perego *et al.*, 1995). The roles these enzymes play in the process of D-alanylation are divergent between two proposed models, one forward by Fisher and colleagues (1995) and the alternative proposed by Neuhaus & Baddiley (2003).

In the first model (Figure 4) it was proposed that DltB acts as a facilitator to transfer D-alanines from the carrier protein, DltC, to undecaprenyl phosphate, C_{55}-P, forming the lipid linked intermediate D-Ala-P-C_{55} (Perego *et al.*, 1995). As a second role for DltB this protein would aid in traversing the intermediate to the outer leaflet of the membrane. In a final step, DltD would act on the outside of the cell and, with its positive charge, would be able to detect the negatively charged PGP from LTA and bring it in close proximity to the intermediate D-Ala-P-C_{55} (Perego *et al.*, 1995). The second model, on the other hand, proposes that DltD acts in the cytoplasm by bringing in close proximity DltA and DltC, which would result in the efficient charging of DltC with D-alanines (Neuhaus & Baddiley, 2003). This hypothesis was made based on experiments using purified proteins from *Lactobacillus rhamnosus*, which showed a two-fold increase in the rate of ligation of D-alanines from DltA to DltC in the presence of DltD. Furthermore, this model proposes that DltC, once charged with D-alanines, is translocated across the membrane through a channel formed by DltB, before the D-alanines are transferred to LTA on the outer leaflet of the membrane (Neuhaus &

Baddiley, 2003). Only recently it has been shown, using protein localisation and membrane topology analysis in *S. aureus*, that DltC remains within the cell, while DltD has an N-terminal embedded in the membrane and a C-terminus on the outer side of the membrane. These observations are in agreement with the model proposed by Fisher and colleagues (Reichmann *et al.*, 2013).

For WTA D-alanylation it is known that the *dlt* operon is also necessary for this process, since it is abolished in *B. subtilis dlt* mutants (Perego *et al.*, 1995). However, it has been proposed that the Dlt proteins may not be directly involved and instead D-Ala-LTA is the D-alanine donor for WTA (Haas *et al.*, 1984). Pulse-chase experiments using [^{14}C]-alanine showed that a decrease in radioactivity in LTA is coupled with an increase in radioactivity in WTA (Haas *et al.*, 1984; Koch *et al.*, 1985). However, there is still no direct evidence that D-Ala-LTA is the donor for WTA D-alanylation.

1.2.3.5. Functions of D-alanine esters in teichoic acids

Given the negative charges in TAs, their decoration with positively charged D-alanine residues plays an important role in the function of these cell wall components. In the absence of D-alanylation the cell wall net charge at the surface becomes more negative and this has the effect of making the cell more susceptible to positively charged molecules such as cationic antimicrobial peptides (CAMPs), defensins and nisin (Fabretti *et al.*, 2006; Kovács *et al.*, 2006; Kramer *et al.*, 2008; Peschel *et al.*, 1999), as well as to cells from the host immune system such as phagocytes and neutrophils, highlighting the importance of D-alanylation during infection (Collins *et al.*, 2002; Kristian *et al.*, 2005; Poyart *et al.*, 2003; Walter *et al.*, 2007). In *S. aureus*, it has also been observed that *dlt* mutants have an impaired ability to form biofilms and a reduced adherence to epithelial cells (Gross *et al.*, 2001; Weidenmaier *et al.*, 2004b).

The important role of TAs in scavenging ions, especially Mg^{2+} is related to D-alanylation (Fischer *et al.*, 1981; Koprivnjak *et al.*, 2006). In fact, the *dlt* operon in *S. aureus* is downregulated in the presence of Mg^{2+} and also by an increase in NaCl concentration, as well as pH and temperature (Boyd *et al.*, 2000; Koprivnjak *et al.*, 2006; Novitsky *et al.*, 1974). Although in *S. aureus* it is still not known how this process is regulated, it is known that in *Streptococcus agalactiae* and *S. gordonii*, the expression

of the *dlt* gene is under the control of the two-component systems DltRS and LiaRS, respectively (McCormick *et al.*, 2011; Poyart *et al.*, 2001).

1.3. Objectives of this study

Through the analysis of mutants defective in LTA synthesis, various functions have been attributed to this zwitterionic polymer. However, most of these roles are based on phenotypic analysis of mutants with altered LTA glycolipid anchor (Fedtke *et al.*, 2007; Gründling & Schneewind, 2007a; Kiriukhin *et al.*, 2001), since strains lacking the PGP chain are only viable under osmoprotective conditions or by the acquisition of suppressor mutations (Corrigan *et al.*, 2011; Oku *et al.*, 2009). Therefore little is known about the function of the PGP chain of LTA in *S. aureus*, including whether effects observed are direct or indirect, and so one key aim of this research was to provide further insights into roles of LTA. One such role is during D-alanine incorporation into WTA, whereby D-Ala-LTA has been proposed to act as the D-alanine donor (Haas *et al.*, 1984). However, direct experimental evidence is lacking, and so this study investigated this hypothesis.

Under normal growth conditions, LTA is essential for *S. aureus* growth (Gründling & Schneewind, 2007b), though it is still not known if cells enter starvation and growth arrest under these circumstances or if the absence of this polymer causes actual cell death. In this study it is investigated whether the absence of LTA in *S. aureus* is bacteriostatic or bactericidal, which may indicate if LTA is a suitable target for new antimicrobials. Furthermore, due to its role in Mg^{2+} binding and predicted function in cation homeostasis, the influence of LTA depletion on membrane potential was investigated. It was also previously shown that in the absence of LTA *S. aureus* cells present misplaced septa, cell enlargement and eventually lyse (Gründling & Schneewind, 2007b). Additionally, in *B. subtilis* it was found that both UgtP, involved in glycolipid anchor synthesis, and LtaS localise at the site of cell division (Schirner *et al.*, 2009). These seem to be good indications for a role of LTA in cell division. The localisation of LTA in *S. aureus* has been studied and is proposed to be an important component of the Gram-positive periplasm (Matias & Beveridge, 2008) being maintained in close proximity to the cell membrane without reaching the cell surface as

usually represented. At this location LTA is likely to have a physiological function during bacterial growth and cell division since the division machinery is mainly kept close to the membrane (Reichmann & Gründling, 2011). Therefore, in this study the localisation of LTA synthase, LtaS, was investigated using fusions to a green fluorescent protein (GFP).

Nowadays, the process for LTA synthesis is mostly defined, as well as the enzymes involved in the process. However, the regulation of this process in accordance with the cell needs is mainly unknown. Another aim of this study is to determine if LTA production is regulated during growth or under stress conditions. Since LtaS is the enzyme responsible for the PGP chain polymerisation (Gründling & Schneewind, 2007b) and is essential for LTA synthesis, regulation studies focused on the expression of the *ltaS* gene as well as LTA production levels.

2. Materials and Methods

2.1. Bacterial strains, growth conditions and storage

E. coli and *S. aureus* strains used in this study are shown in Table 1 with the respective references when applicable. The *E. coli* strain XL1 Blue was used for cloning and plasmid propagation. Strains were stored at -80°C by mixing 500 µl overnight culture with 500 µl freezer medium that consists of 10% bovine serum albumin and 10% monosodium glutamate. *E. coli* strains were grown at 37°C with shaking at 180 rpm in Luria Bertani (LB) broth or on LB agar. When necessary the medium was supplemented with the following antibiotics and inducers: Ampicillin (Amp), 100 µg/ml; Kanamycin (Kan), 30 µg/ml; 5-bromo-4-chloro-3-indolyl-β-D-galactopyranoside (X-gal), 40 µg/ml.

S. aureus strains were grown at 37°C with shaking at 180 rpm in Tryptic Soy Broth (TSB) or on Tryptic Soy Agar (TSA). When necessary the medium was supplemented with the following antibiotics, inducers and indicators: Chloramphenicol (Cam), 5 to 10 µg/ml; Erythromycin (Erm), 10 µg/ml; Anhydrotetracycline (Atet), 100 to 200 ng/ml; Isopropyl β-D-thiogalactosidase (IPTG), 1 mM; 5-bromo-4-chloro-3-indolyl-β-D-galactopyranoside (X-gal), 100 µg/ml.

All optical density (OD) was measured using the Biochrom Libra S11 spectrophotometer.

2.2. Recombinant DNA techniques

2.2.1. Purification of plasmid DNA from *E. coli*

Plasmid DNA was extracted from 5 ml *E. coli* overnight cultures using the Macherey-Nagel plasmid DNA purification kit, following the manufacturer's instructions. The plasmid DNA was eluted in 40 µl ddH_2O. When higher amounts were needed plasmid DNA was isolated from 200 ml overnight cultures using the QIAGEN

plasmid midi kit, following the manufacturer's instructions. The DNA was rehydrated in 150 µl ddH_2O. Plasmid DNA was stored at -20°C.

2.2.2. Isolation of chromosomal DNA from *S. aureus*

In order to isolate *S. aureus* chromosomal DNA, a 4 ml overnight culture was centrifuged for 20 min at 1,303 xg. The pellet was suspended in 50 µl TSM buffer (50 mM Tris HCl pH 7.5, 0.5 M sucrose, 10 mM $MgCl_2$ filter sterilised) and the cell wall was digested for 30 min at 37°C using lysostaphin (AMBI Products) at a final concentration of 100 µg/ml. The subsequent steps of the chromosomal DNA isolation were performed using the Wizard Genomic DNA Purification kit (Promega, Madison USA) and following the manufacturer's protocol. The DNA was rehydrated in 40 µl ddH_2O for 1 h at room temperature and stored at -20°C.

2.2.3. Polymerase Chain Reaction (PCR)

All the primers used in this study were ordered from Sigma Aldrich and can be found in Table 2. In general all the reactions were performed in a total volume of 50 µl, adding 2 µl of 40 mM dNTPs, 1 µl of each primer at a concentration of 10 mM, 50 to 100 ng of template DNA, polymerase enzymes with their respective buffers, where for cloning 1 µl Herculase II (Agilent) was used with 10 µl 5X Herculase buffer and for all other PCR reactions, 0.5 µl Taq (New England Biolabs) with 5 µl 10X Taq buffer, and ddH_2O to obtain the final volume. In order to fuse different fragments Splicing by Overlap Extension PCR (SOE PCR) was used. In these reactions 2 µl from each PCR product was used as the DNA template.

The PCR program consisted of an initial denaturation step at 94°C for 2 min, followed by 5 cycles of denaturation at 94°C for 30 seconds, annealing at 45°C for 30 seconds and extension at 72°C for a time dependent on the length of the product (1 min per 1 kb). Subsequently, these conditions were repeated for another 25 cycles, but this time with an annealing temperature of 53°C. A final extension at 72°C for 7 min was performed and the reaction was held at 10°C, ready for use or to be store at -20°C. All

PCR products were purified using the QIAquick Gel Extraction kit or the QIAquick PCR purification kit (QIAGEN) following the manufacturer's instructions and eluted in 50 µl 5mM Tris HCl pH 8.

2.2.4. Restriction digests of plasmids and PCR fragments

Plasmid DNA was digested with restriction enzymes from New England Biolabs for cloning or to check inserts sizes in plasmids after cloning. For cloning, reactions were prepared using 10 µg DNA, 2 µl enzyme, 10 µl 10X enzyme buffer, 1 µl 100X BSA (when necessary) and ddH_2O to obtain a final volume of 100 µl. The reaction was incubated for 4 h at 37°C (except for *Sal*I and *Bgl*II digests where the reactions were incubated for 16 h). In order to check inserts in plasmids, reactions were prepared using 0.1-1 µg DNA, 0.25 µl enzyme, 2 µl 10X enzyme buffer, 0.2 µl 100X BSA (when necessary) and ddH_2O to obtain a final volume of 20 µl. The reactions were incubated for 2 h at 37°C.

Ligation reactions were prepared in a final volume of 25 µl using a molar ratio of 1:3 vector to insert, 1 µl T4 DNA ligase (New England Biolabs), 2.5 µl 10X T4 DNA ligase buffer and ddH_2O to obtain the right volume. The reaction was incubated at 17°C for 16 h and heat-inactivated for 20 min at 65°C.

2.2.5. Sequencing of clones

After cloning all plasmid inserts were sequenced at the MRC CSC Genomics Core Laboratory at the Hammersmith Campus (Imperial College London) using fluorescent automated sequencing. The inserts of interest were PCR amplified using 25 µl Taq polymerase and purified using the QIAquick Gel Extraction kit or the QIAquick PCR purification kit (QIAGEN). Reactions for sequencing were prepared adding 10 ng per 100 bp of PCR product, 2 µl primer (10 mM) and ddH_2O to give a total volume of 10 µl. The sequencing results were analysed by aligning the result with a predicted sequence using the program SeqMan from Lasergene 8, DNASTAR.

2.2.6. Preparation and transformation of chemically competent *E.coli* cells

In order to prepare chemically competent *E. coli* cells, 20 ml of an overnight culture was back diluted 1:100 in 1 L PSI broth (5 g/L bacto yeast extract, 20 g/L bacto tryptone, pH 7.6, 20 mM $MgSO_4$). The culture was incubated at 37°C with shaking at 180 rpm until an OD_{600nm} of 0.5-0.7. Once grown, the culture was incubated on ice for 15 min and centrifuged at 3,847 xg for 10 min. The pellet was suspended in 200 ml sterile TfbI buffer (15% glycerol, 30 mM potassium acetate, 100 mM rubidium chloride, 10 mM calcium chloride, 50 mM manganese chloride) and incubated on ice for 15 min. The suspension was centrifuged at 3,847 xg for 10 min. The pellet was suspended in 20 ml sterile TbfII buffer (15% glycerol, 10 mM MOPS, 75 mM calcium chloride, 10 mM rubidium chloride) and incubated on ice for 15 min. The cell suspension obtained was separated into 500 µl aliquots, snap frozen in a dry ice/ethanol bath and stored at -80°C.

In order to transform chemically competent *E. coli* cells, 12.5 µl of heat-inactivated ligation mixture was added to 100 µl competent cells and incubated on ice for 30 min. The mixture was submitted to a heat shock by incubating at 42°C for 45 seconds and then incubated on ice for 5 min. Nine hundred µl SOC medium (5 g/L bacto yeast extract, 20 g/L bacto tryptone, 3.6 g/L glucose, 2.5 mM KCl, pH 7.0) was added to the cells, which were recovered by incubation at 37°C for 1 h. One hundred µl from the suspension was spread on LB agar with the appropriate antibiotics. The remaining cell suspension was pelleted at 17,000 xg for 5 min, 750 µl of the supernatant was removed, and the pellet was suspended in the remaining liquid and plated on LB agar plates with the appropriate antibiotics. Plates were incubated at 37°C overnight to obtain single colonies.

2.2.7. Preparation and electroporation of electrocompetent *S. aureus* cells

In order to prepare electrocompetent *S. aureus* cells, an overnight culture was grown shaking at 37°C in TSB with the appropriate antibiotics (when necessary). The following day, the culture was back diluted 1:100 in 150 ml TSB and incubated at 37°C

shaking at 180 rpm until an OD_{600nm} of around 2.1. The cells were then centrifuged at 6,000 xg for 10 min at 4°C. The pellet was washed twice with 150 ml sterile 0.5 M sucrose and once with 75 ml sterile 0.5 M sucrose. The final pellet was suspended in 1.5 ml sterile 0.5 M sucrose. The cell suspension obtained was separated in 230 µl aliquots that were snap frozen in a dry ice/ethanol bath before storage at -80°C.

Aliquots of 110 µl of cells were pipetted into 1 mm electroporation cuvettes (Biorad) and 20 µl of plasmid DNA in a concentration range of 300-600 ng/µl previously dialysed against ddH_2O was added. For electroporation, a Biorad Gene Pulser with 100 Ω, 2.5 kV and 25 µF settings was used. After electroporation, cells were recovered with 900 µl BHI 0.5 M sucrose medium, incubated for 1 h at 37°C and 100 µl cells were spread on TSA plates with the appropriate antibiotics. The remaining cell suspension was pelleted at 10,000 xg for 3 min and 750 µl from the supernatant was removed. The pellet was suspended in the remaining liquid and plated on TSA with the appropriate antibiotics. Plates were incubated at 37°C overnight and single colonies were re-streaked twice on TSA plates. Single colonies were used to inoculate TSB media with the appropriate antibiotics to grow overnight and freeze the cultures the next day.

2.2.8. Phage transduction in *S. aureus* cells

2.2.8.1. Preparation of phage lysates

For the preparation of phage lysates, the donor strains were grown in 4.5 ml LB/TSB in a ratio of 2:1 supplemented with 5 mM $CaCl_2$ and incubated shaking at 37°C overnight. The next day, the culture was diluted 1:50 into new media with the same composition and grown for 3 h shaking at 37°C. A lysate of the transducing phage 85 was diluted in 10-fold dilutions from 10^{-1} to 10^{-6} in TMG buffer (10 mM Tris-HCl pH 7.4, 10 mM $MgSO_4$, 0.1% gelatin) and 100 µl of each dilution was incubated with 500 µl of culture from the donor strain at room temperature for 30 min to enable phage adsorption. To each mixture, 5 ml top agar cooled to 42°C (0.8% NaCl, 0.8% Bacto-agar) was added. Thin TSA plates pre-warmed to 37°C supplemented with the

appropriate antibiotics were overlaid with 5.5 ml cells in top agar and incubated with the lid side up at 37°C overnight. The next day, the plate with a semi-confluent layer of plaques was overlaid with 4 ml TMG buffer and incubated for 20 min at room temperature. The liquid was pipetted into a 15 ml tube and centrifuged for 20 min at 3,220 xg to pellet cellular debris and the supernatant was sterile filtered using a 0.22 mm filter. The phage lysates were stored at 4°C.

2.2.8.2. Phage transduction of *S. aureus*

The recipient strains were grown overnight in 24 ml LB/TSB in a ratio 2:1 supplemented with 5 mM $CaCl_2$. The following day, cells were harvested by centrifugation for 20 min at 3,220 xg and suspended in 4.5 ml LB/TSB in a ratio 2:1. To a 250 µl aliquot of cells, 200 µl lysate was added and incubated at 37°C shaking for 20 min. Cells were placed on ice and 24 µl 1 M sodium citrate was added to inhibit infection. Cells were pelleted at 10,000 xg for 3 min and washed twice with 1 ml 40 mM sodium citrate. The final pellet was suspended in 300 µl 40 mM sodium citrate, and 100 µl and 200 µl were spread on TSA supplemented with 40 mM sodium citrate and the appropriate antibiotics. The TSA plates were incubated for 48 h at 37°C and single colonies were streaked twice on new TSA plates supplemented 40 mM sodium citrate and the appropriate antibiotics.

2.3. Strain and plasmid construction

2.3.1. *ltaS* promoter-*lacZ* fusions constructs

For LacZ fusions to the *ltaS* promoter region, different sized fragments were cloned into the vector pCL55i*TET*-*lacZ* upstream of the *lacZ* gene. The full-length 5' UTR region (700 bp) and truncated versions (473 bp, 400 bp, 300 bp, 200bp and 100 bp) were amplified from *S. aureus* RN4220 chromosomal DNA using primer pairs 1058/1052, 1047/1052, 1048/1052, 1049/1052, 1050/1052 and 1051/1052, respectively.

All the PCR products and pCL55i*TET-lacZ* were digested with *Kpn*I/*Sal*I and ligated. The resulting plasmids (pCL55*p700ltaS-lacZ*, pCL55*p473ltaS-lacZ*, pCL55*p400ltaS-lacZ*, pCL55*p300ltaS-lacZ*, pCL55*p200ltaS-lacZ* and pCL55*p100ltaS-lacZ*) were first obtained in *E. coli* XL1 Blue yielding strains ANG2028, ANG2029, ANG2030, ANG2031, ANG2032 and ANG2033, respectively. The plasmids were then introduced into *S. aureus* RN4220 yielding strains ANG2866, ANG2867, ANG2868, ANG2869, ANG2870 and ANG2871, respectively. Similarly, the plasmids integrated into the chromosome were transduced into *S. aureus* LAC* generating strains ANG2964, ANG2965, ANG2966, ANG2967, ANG2968 and ANG2969, and into *S. aureus* Newman resulting in strains ANG2970, ANG2971, ANG2972, ANG2973, ANG2974 and ANG2975, respectively.

In order to delete the bases from 400 to 30 from the full-length UTR producing pCL55*pΔ400-30ltaS-lacZ*, two fragments were amplified from pCL55*p700ltaS-lacZ* using primer pairs 1058/1232 and 1233/817 and the PCR fragments were fused by SOE PCR using primer pair 1058/817. For the deletion of the P2 region, the bases 294 to 30 were deleted, constructing pCL55*pΔ294-30ltaS-lacZ* by amplifying two fragments from pCL55*p700ltaS-lacZ* with primer pairs 1058/1234 and 1235/817, and these PCR fragments were fused by SOE PCR using primer pair 1058/817. In order to mutate the transcriptional start site located 294 bp upstream of the start codon and obtain pCL55*pΔ294ltaS-lacZ*, two fragments were amplified from pCL55*p700ltaS-lacZ* using primer pairs 1058/1236 and 1237/817, and these PCR fragments were fused by SOE PCR using primer pair 1058/817. All PCR products and pCL55i*TET-lacZ* were digested with *Kpn*I/*Sal*I before ligation. The plasmids pCL55*pΔ400-30ltaS-lacZ* and pCL55*pΔ294ltaS-lacZ* were first obtained in *E. coli* XL1 Blue yielding strains ANG2204 and ANG2206, and afterwards introduced into *S. aureus* RN4220Δ*spa* yielding strains ANG2961 and ANG2963. The plasmid pCL55*pΔ294-30ltaS-lacZ* was electroporated directly into *S. aureus* RN4220Δ*spa* generating strain ANG2962. The three plasmids were also introduced into *S. aureus* LAC* yielding strains ANG2976, ANG2977 and ANG2978 and into *S. aureus* Newman yielding strains ANG2979, ANG2980 and ANG2981.

2.3.2. Construction of *gfp*$_{P7}$-*ltaS*$_{S218P}$ fusions

For the LtaS localisation studies, a fast folding version of GFP (GFP$_{P7}$) was fused to the N-terminal end of the non-cleavable LtaS$_{S218P}$ variant, with and without a 3x EAAAK amino acid linker region. These fusions were expressed either form the *ltaS* native promoter or the Atet inducible i*TET* promoter.

For construction of pCL55*pltaS-gfp*$_{P7}$-*ltaS*$_{S218P}$, the promoter sequence of *ltaS* was amplified from Newman chromosomal DNA using primer pair 1334/1697 and *gfp*$_{P7}$ was amplified from pTrc99A-*gfp*$_{P7}$ using primer pair 1698/1699. These PCR products were fused by SOE PCR using primer pair 1334/317, resulting in the *pltaS-gfp*$_{P7}$ fragment. The gene *ltaS*$_{S218P}$ was amplified from pOK-*ltaS*$_{S218P}$ using primer pair 1700/317 and fused to *pltaS-gfp*$_{P7}$ using primer pair 1334/317, giving rise to *pltaS-gfp*$_{P7}$-*ltaS*$_{S218P}$. The final PCR product and pCL55 were digested with *Eco*RI/*Kpn*I and ligated. The plasmid pCL55*pltaS-gfp*$_{P7}$-*ltaS*$_{S218P}$ was initially obtained in *E. coli* XL1 Blue yielding the strain ANG2990 and subsequently introduced into *S. aureus* strains RN4220Δ*spa*, LAC* and LAC*-i*ltaS* yielding strains ANG3018, ANG3022 and ANG3026 respectively.

For construction of a *pltaS-gfp*$_{P7}$-linker-*ltaS*$_{S218P}$ fusion, the promoter sequence of *ltaS* was amplified from Newman chromosomal DNA using primer pair 1334/1697 and *gfp*$_{P7}$ was amplified from pTrc99A-*gfp*$_{P7}$ using primer pair 1698/1699. These PCR products were fused by SOE PCR using primer pair 1334/1701, giving rise to *pltaS-gfp*$_{P7}$. The gene *ltaS*$_{S218P}$ was amplified from pOK-*ltaS*$_{S218P}$ using primer pair 1700/317 and both *pltaS-gfp*$_{P7}$ and *ltaS*$_{S218P}$ were digested with *Sac*II and ligated. The ligation product was amplified using primer pair 1334/317 to yield the fusion *pltaS-gfp*$_{P7}$-linker-*ltaS*$_{S218P}$. The final PCR product and pCL55 were digested with *Eco*RI/*Kpn*I and ligated. The plasmid pCL55*pltaS-gfp*$_{P7}$-linker-*ltaS*$_{S218P}$ was initially obtained in *E. coli* XL1 Blue yielding the strain ANG2991 and subsequently introduced into *S. aureus* strains RN4220Δ*spa*, LAC* and LAC*-i*ltaS* yielding strains ANG3019, ANG3023 and ANG3027 respectively.

For construction of pCL55i*TET-gfp*$_{P7}$-*ltaS*$_{S218P}$ fusion, *gfp*$_{P7}$ was amplified from pTrc99A-*gfp*$_{P7}$ using primer pair 1702/1699 and *ltaS*$_{S218P}$ was amplified from pOK-*ltaS*$_{S218P}$ using primer pair 1700/319. The *gfp*$_{P7}$-*ltaS*$_{S218P}$ fragment was fused by SOE

PCR using primer pair 1702/319. The final PCR product and the plasmid pCL55i*TET* were digested with *Avr*II/*Bgl*II and ligated. The plasmid pCL55i*TET-gfp*$_{P7}$-*ltaS*$_{S218P}$ was initially obtained in *E. coli* XL1 Blue yielding strain ANG2992 and subsequently introduced into *S. aureus* strains RN4220Δ*spa*, LAC* and LAC*-i*ltaS* yielding strains ANG3020, ANG3024 and ANG3028 respectively.

For construction of pCL55i*TET-gfp*$_{P7}$-linker-*ltaS*$_{S218P}$ fusion, *gfp*$_{P7}$ was amplified from pTrc99A-*gfp*$_{P7}$ using primer pair 1702/1701 and *ltaS*$_{S218P}$ was amplified from pOK- *ltaS*$_{S218P}$ using primer pair 1337/319. Both PCR products were digested with *Sac*II and ligated. The ligation product was amplified using primers 1702/319 to yield fusion i*TET-gfp*$_{P7}$-linker-*ltaS*$_{S218P}$. The final PCR product and pCL55i*TET* were digested with *Avr*II/*Bgl*II and ligated. The plasmid pCL55i*TET-gfp*$_{P7}$-linker-*ltaS*$_{S218P}$ was initially obtained in *E. coli* XL1 Blue yielding strain ANG2993 and subsequently introduced into *S. aureus* strains RN4220Δ*spa*, LAC* and LAC*-i*ltaS* yielding strains ANG3020, ANG3024 and ANG3028 respectively.

2.4. *S. aureus* growth curves

RN4220 (ANG113), RN4220Δ*spa* (ANG314), LAC* (ANG1575), RN4220-i*ltaS* (ANG499) and LAC*-i*ltaS* (ANG 2505) *S. aureus* strains and the remaining strains of interest for fluorescence microscopy were grown overnight at 37°C with shaking in TSB or LB supplemented with the appropriate antibiotics and 1 mM IPTG for the inducible strains. The next day, 1 ml culture was washed three times in TSB or LB and diluted 1:100 into 5 ml TSB or LB medium with and without IPTG, supplemented with the appropriate antibiotics. The cultures were grown at 37°C with shaking and bacterial growth was monitored by determining OD_{600nm} every 2 h until the 8 h timepoint. At the 4 h time point, cultures were diluted 1:100 into fresh TSB or LB medium to maintain bacteria in the exponential growth phase.

2.5. Live/Dead bacterial viability assay

The same *S. aureus* strains as used for growth curves (see section 2.4. *S. aureus* growth curves) were grown overnight at 37°C with shaking in TSB supplemented with the appropriate antibiotics and 1 mM IPTG for the inducible strains. The next day 1 mL culture was washed three times in TSB and diluted 1:400 into 25 ml TSB medium with and without IPTG, supplemented with the appropriate antibiotics. Cultures were grown at 37°C with shaking and bacterial growth was monitored by determining OD_{600nm} every 2 h until the 6 h timepoint. From the overnight culture and at each time point, a 1 ml sample was centrifuged at 10,000 xg for 3 min and suspended in a volume of 0.85% NaCl normalised for OD_{600nm} readings (where a culture with OD_{600nm} of 0.5 was suspended in 100 µl 0.85% NaCl).

In order to distinguish between living and dead cells, the Live/Dead Baclight Bacterial Viability Kit (Invitrogen) was used. Following the manufacturer's instructions, equal volumes of component A (SYTO 9 dye) and component B (propidium iodide) were mixed and diluted 1:10 in DMSO (dimethyl sulfoxide). Of this mixture, 3 µl was added to 100 µl bacterial culture (suspended in 0.85% NaCl). Four µl was spotted on the slide and covered with a coverslip, before observation using a Nikon Eclipse E600 microscope equipped with a Nikon Digital DXM1200 camera and Digital Sight ACT-1 software. Cells were counted using the Image J software.

2.6. Membrane potential assay

Changes in membrane potential were determined as previously described with slight modifications (Li *et al.*, 2009). The same strains, which were analysed in the Live/Dead assay experiment (see section 2.5. Live/dead bacterial viability assay) were used and the cultures were prepared following the same procedure, with the exception that Mueller-Hinton broth (Fluka) supplemented with 25 mg/L Ca^{2+} and 12.5 mg/L Mg^{2+} (CA-MHB) was used for growth. At each time point, a 1 ml sample was centrifuged at 10,000 xg for 3 min and washed once with 1 ml buffer A (5mM HEPES pH 7.2, 5mM glucose). The cell suspension was centrifuged again at 10,000 xg for 3

min, suspended in 1 ml buffer B (5mM HEPES pH 7.2, 5mM glucose, 100mM KCl) and diluted in the same buffer for a final OD_{600nm} of 0.05. Two hundred µl of this suspension were added to a black 96-well polystyrene fluorescence MaxiSorp plate (Thermo Scientific Nunc) plate. The membrane potential-sensitive fluorescent dye 3,3'-dipropylthiadicarbocyanine iodide (DiSC3(5), Invitrogen) was added at a final concentration of 2 µM and the samples were incubated for 15 min to enable dye uptake and fluorescence quenching. Buffer B only and buffer B with dye was used as background and positive controls respectively. To one sample with wild-type bacteria, nisin, a pore forming peptide, was added at a final concentration of 10 µg/ml in order to guarantee fluorescence can be detected when there is no dye uptake. The fluorescence was measured at an excitation wavelength of 622 nm and emission wavelength of 670 nm.

2.7. β-Galactosidase activity assay in *S. aureus*

S. aureus strains of interest were grown overnight in 4 ml TSB supplemented with the appropriate antibiotics at 37°C with shaking. The following day cultures were diluted 1:100 into 5 ml fresh TSB medium and grown at 37°C with shaking and as negative control, *S. aureus* RN4220 pCL55i*TET* was grown in the presence of 200 ng/ml Atet.

Cultures were grown without inducer for 4 h and with inducer for 5 h. The OD_{600nm} was recorded, 1 ml from each culture centrifuged at 17,000 xg for 10 min and pellets were subsequently suspended in 1 ml ABT buffer (60 mM K_2HPO_4, 40 mM $KHPO_4$, 100 mM NaCl, pH 7.0, 1% Triton X-100) containing 20 µg/ml lysostaphin and incubated at 37°C for 30 min to allow cell lysis. Cell debris were pelleted by centrifugation at 17,000 xg for 10 min and 100 µl supernatant was incubated for 1 h at room temperature in the dark with 20 µl 0.4 mg/ml 4-methyl umbelliferyl β-D-galactopyranoside (MUG) in a black 96-well polystyrene fluorescence MaxiSorp plate (Thermo Scientific Nunc). As a background control it was used 100 µl ABT buffer. Following the incubation, 20 µl was mixed with 180µl ABT buffer and the fluorescence was measured at an excitation wavelength of 336 nm and emission wavelength of 445 nm. In order to obtain a standard curve, 2-fold serial dilutions of 4-methylumbilliferone

(MU) in ABT buffer at known concentrations were made and subsequently these values were used to determine the concentration (in μM) of product in each sample.

2.8. Sodium Dodecyl Sulphate Polyacrylamide Gel Electrophoresis (SDS-PAGE) and western immunoblot

In order to separate proteins and LTA prior to western immunoblot analysis, sodium dodecyl sulphate polyacrylamide gel electrophoresis (SDS-PAGE) was performed using 10 % or 15 % polyacrylamide gels produced as previously described (Sambrook *et al*., 1989). In order to estimate protein size, 5 μl of protein ladder (BenchMarkTM Prestained, Invitrogen or PageRuler Plus Prestained Protein Ladder, Thermo Scientific) was loaded beside 10 μl of the different samples, and separated by electrophoresis at 200 V (with the exception of LtaS samples that were separated at 100 V) using a Hoefer Mini Protein Electrophoresis system in 1X SDS buffer (14.4 g/L glycine, 3 g/L Tris-base, 1 g/L SDS).

All the western immunoblot procedures were performed using polyvinylidene difluoride (PVDF) membranes activated in methanol. Proteins and LTA were transferred for 1 h with a constant current of 1000 mA using a Hoefer electrophoretic transfer cell system filled with transfer buffer [3 g/L Tris-base, 14.5 g/L glycine, 20 % (v/v) methanol]. After the transference, the membranes were blocked for 1 h at room temperature in 5% (w/v) milk in 1X TBST (50 mM Tris-base, 150 mM NaCl, 0.1% tween, pH 7.4). When necessary, 10 μg/ml human IgG was added to all incubation steps, in order to inhibit the binding of *S. aureus* protein A. Following the blocking step, membranes were incubated with the primary antibody overnight at 4°C in 5% (w/v) milk in TBST. The following day the membranes were washed three times with 20 ml TBST for 10 min, prior to incubation with the secondary antibody, when necessary, which was performed for 3 h in 5% (w/v) milk in TBST. The membranes were washed as previsously prior to detection. Detection was performed by incubating the membranes for 2 min with ECL (100 mM Tris-HCl pH 8.5, 2.5 mM luminol, 2.5 mM P-coumaric acid) containing 0.009 % (v/v) hydrogen peroxide, with the exception of the LtaS protein prepared from strains with inducible *ltaS*, where the signal was detected

using the Amersham ECL Prime Western Blotting Detection Kit (GE Healthcare), following the manufacturer's instructions. The chemiluminescent signal was detected in an ECL Hyperfilm (GE Healthcare) and the film was developed using AGFA-Healthcare N. V. automated developer. Exposure time was variable depending on signal strength.

2.8.1. Preparation of samples and detection of LTA by western immunoblot

In order to obtain LTA samples for immunoblot analysis, the same *S. aureus* strains as used for growth curves (see section 2.4. *S. aureus* growth curves) were grown overnight at 37°C with shaking in TSB supplemented with the appropriate antibiotics and 1 mM IPTG for the inducible strains. The following day 1 ml culture was washed three times in TSB and diluted 1:100 into 5 ml TSB medium with and without IPTG for the inducible strains and supplemented with the appropriate antibiotics. Cultures were grown for 4 h at 37°C with shaking and bacterial growth was monitored by determining OD_{600nm} every 2 h. Cells were lysed by adding 1 ml culture to 0.5 ml of 0.1 mm glass beads and vortexing upside down for 45 min at 4°C. In order to settle the beads, the samples were centrifuged for 1 min at 200 xg and the supernatant containing lysed bacteria was transferred into a fresh eppenford tube. Bacterial debris was collected by centrifuging for 15 min at 17,000 xg. The pellet containing LTA was suspended in 2 % SDS-containing sample buffer normalised for OD_{600nm} readings (where a culture with OD_{600nm} of 3 was suspended in 90 µl buffer). Samples were boiled for 20 min and centrifuged for 5 min at 17,000 xg, before loading 10 µl onto a 15% polyacrylamide gel.

Following SDS-PAGE and transfer to a PVDF membrane, LTA was detected using a 1:5000 dilution of mouse monoclonal LTA antibody (HyCult Biotechnology) and a 1:10000 dilution of horseradish peroxide HRP-conjugated anti-mouse secondary antibody as described in section 2.8.

2.8.2. Preparation of samples and detection of LtaS by western immunoblot

In order to obtain samples for LtaS immunoblot analysis, cells were grown following the same procedure as for LTA samples (see section 2.8.1. Preparation of samples and detection of LTA by western immunoblot). To prepare the cell fraction (containing the cell wall, cell membrane and cytoplasm), 1 ml cell culture was pelleted by centrifugation at 17,000 xg for 5 min. The pellet was suspended in cell lysis buffer (100 mM Tris-HCl pH 7.5, 10mM $MgCl_2$, 200 µg/ml lysostaphin, 100 µg/ml DNase) normalised for OD_{600nm} reading (where a culture with OD_{600nm} of 3 was suspended in 45 µl buffer). After incubation for 30 min at 37°C, 2 % SDS-containing sample buffer was added (same volume as cell lysis buffer). Samples were boiled for 15 min, centrifuged at 17,000 xg for 5 min and 10 µl aliquots were separated on 10 % polyacrylamide gels for western blot analysis.

For LtaS detection, a 1:20000 dilution of a rabbit polyclonal LtaS antibody was used prior to incubation with an HRP-conjugated anti-rabbit IgG antibody at a 1:10000 dilution as described in section 2.8.

2.9. Preparation of cell wall and WTA purification for analysis by NMR

Purification of peptidoglycan-WTA complexes purification was performed as previously described (Bernal *et al.*, 2009; Kopp *et al.*, 1996; Stranden *et al.*, 1997) with slight modifications. Overnight cultures of *S. aureus* were diluted into 1 L TSB to obtain an initial OD_{600nm} of approximately 0.06 (5 L batches were used for each strain) and grown at 37°C with shaking until an OD_{600nm} of approximately 3. Bacteria were collected by centrifugation at 6,000 xg for 10 min and washed once with 1 M NaCl. Cells were disrupted with 0.1 mm glass beads and the broken cells were collected by centrifugation for 40 min at 13,300 xg. The cell wall material was washed once with 1 M NaCl, three times with 0.5 % (w/v) sodium dodecyl sulphate (SDS) and three times with water. The material in solution was incubated with gentle stirring for 30 min at

60°C, removing non-covalently bound components. The cell wall material was recovered by centrifugation at 34,572 xg for 20 min, washed with water once and recovered again by centrifugation. The pellet was suspended in 0.15 mM Tris-HCl pH 7.0 with trypsin (0.2 mg/ml) and incubated at 37°C for 18 h to remove cell wall proteins. The material was recovered by centrifugation and washed with 1 M Tris-HCl pH 7.0, 1 M Tris-HCl pH 7.0 containing 1 M NaCl, 1 M Tris-HCl pH 7.0 and three times with water. In order to hydrolyse WTA from peptidoglycan, the cell wall material was incubated in 10 % (w/v) TCA at 4°C for 18 h. The peptidoglycan was removed by centrifugation at 9,690 xg for 45 min. WTA was precipitated with 0.1 volumes 3 M sodium acetate pH 5.2 and 3 volumes 95 % ice cold ethanol and held overnight at -80°C. The following day, the WTA was precipitated by centrifugation at 9,690 xg for 30min and was washed five times with 95 % ethanol. Following the final wash, the ethanol was evaporated and the WTA was suspended in 500 µl water and lyophilised overnight.

For NMR analysis, 6 mg WTA was suspended twice in 99.96 % D_2O and lyophilised, prior to suspension in 99.99 % D_2O. Spectra were acquired on a 600 MHz Bruker AVANCE III spectrometer equipped with TCI cryoprobe, and processed using Bruker TopSpin 3.1 software.

2.10. Fluorescence microscopy

Strains were prepared for fluorescence microscopy by growing the different *S. aureus* strains in 5 ml TSB supplemented with the appropriate antibiotics at 37°C with shaking overnight. The next day, cultures were diluted 1:1000 into 5 ml TSB without antibiotics and grown to an OD_{600nm} of 0.8 (mid-exponential phase). A 1 ml aliquot was pelleted by centrifugation at 17,000 xg for 1 min and suspended in 25 µl PBS (phosphate buffered saline). Two µl was spotted on 1.2% PBS agarose slides and covered with a coverslip before observation by Dr. Nathalie Reichmann in Dr. Mariana Pinho's laboratory (Instituto de Tecnologia Química e Biológica, Portugal) on a Zeiss Axio Observer microscope equipped with a Phtometrics CoolSNAP HQ2 camera (Roper Scientific) and Metamorph software.

Table 1 - Strains used in this study

Strain	Relevant features	Reference
	***Escherichia coli* strains**	
XL1 Blue	Cloning strain. TetR – ANG 127	Stratagene
ANG 243	pCL55 in XL1 Blue; *S. aureus* single site integration vector. AmpR	(Lee *et al.*, 1991)
ANG 284	pCL55i*TET* in XL1 Blue; pCL55 containing Atet inducible promoter. AmpR	(Gründling & Schneewind, 2007b)
ANG 286	pCL55i*TET-lacZ* in XL1 Blue; AmpR	Lab strain collection
ANG 1242	pOK-$ltaS_{S218P}$ in XL1 Blue. KanR	(Wörmann *et al.*, 2011b)
ANG 2028	pCL55*p700ltaS-lacZ* in XL1 Blue; AmpR	Lab strain collection
ANG 2029	pCL55*p473ltaS-lacZ* in XL1 Blue; AmpR	Lab strain collection
ANG 2030	pCL55*p400ltaS-lacZ* in XL1 Blue; AmpR	Lab strain collection
ANG 2031	pCL55*p300ltaS-lacZ* in XL1 Blue; AmpR	Lab strain collection
ANG 2032	pCL55*p200ltaS-lacZ* in XL1 Blue; AmpR	Lab strain collection
ANG 2033	pCL55*p100ltaS-lacZ* in XL1 Blue; AmpR	Lab strain collection
ANG 2204	pCL55*pΔ400-30ltaS-lacZ* in XL1 Blue; AmpR	Lab strain collection
ANG 2206	pCL55*pΔ294ltaS-lacZ* in XL1 Blue; AmpR	Lab strain collection
ANG 2956	pTrc99A-gfp_{P7} in	(Fisher & DeLisa, 2008)
ANG 2990	pCL55*pltaS-*gfp_{P7}*-*$ltaS_{S218P}$ in XL1 Blue; AmpR	This study
ANG 2991	pCL55*pltaS-*gfp_{P7}-linker-$ltaS_{S218P}$ in XL1 Blue; AmpR	This study
ANG 2992	pCL55i*TET-*gfp_{P7}*-*$ltaS_{S218P}$ in XL1 Blue; AmpR	This study
ANG 2993	pCL55i*TET-*gfp_{P7}-linker-$ltaS_{S218P}$ in XL1 Blue; AmpR	This study
	***Staphylococcus aureus* strains**	
RN4220	Transformable laboratory strain – ANG 113	(Kreiswirth *et al.*, 1983)
SEJ1	RN4220Δ*spa* – ANG314	(Gründling & Schneewind, 2007a)
AH1263	LAC* - ANG1575	(Boles *et al.*, 2010)
ANG 467	Newman ΔΦ4	(Corrigan *et al.*, 2013)
ANG499	RN4220-i*ltaS*; strain with IPTG-inducible *ltaS* expression; ErmR, IPTG	(Gründling & Schneewind, 2007b)
ANG1786	4S5; derivative of RN4220Δ*spa* Δ*ltaS* with suppressor mutations, lacking LTA	(Corrigan *et al.*, 2011)
ANG2505	LAC*-i*ltaS*; strain with IPTG-inducible *ltaS* expression; ErmR, IPTG	Lab strain collection
ANG2392	pCL55*ltaS-gfp-*$ltaS_{S218P}$ integrated in strain ANG1575; CamR	Lab strain collection
ANG 2398	pCL55i*TET* integrated in strain ANG 1575; CamR	Lab strain collection
ANG 2866	pCL55*p700ltaS-lacZ* integrated in strain ANG 113; CamR	Lab strain collection
ANG 2867	pCL55*p473ltaS-lacZ* integrated in strain ANG 113; CamR	Lab strain collection
ANG 2868	pCL55*p400ltaS-lacZ* integrated in strain ANG 113; CamR	Lab strain collection
ANG 2869	pCL55*p300ltaS-lacZ* integrated in strain ANG 113; CamR	Lab strain collection
ANG 2870	pCL55*p200ltaS-lacZ* integrated in strain ANG 113; CamR	Lab strain collection
ANG 2871	pCL55*p100ltaS-lacZ* integrated in strain ANG 113; CamR	Lab strain collection
ANG 2961	pCL55*pΔ400-30ltaS-lacZ* integrated in strain ANG 314; AmpR	This study
ANG 2962	pCL55*pΔ294-30ltaS-lacZ* integrated in strain ANG 314; AmpR	This study
ANG 2963	pCL55*pΔ294ltaS-lacZ* integrated in strain ANG 314; AmpR	This study
ANG 2964	pCL55*p700ltaS-lacZ* integrated in strain ANG 1575; CamR	This study
ANG 2965	pCL55*p473ltaS-lacZ* integrated in strain ANG 1575; CamR	This study
ANG 2966	pCL55*p400ltaS-lacZ* integrated in strain ANG 1575; CamR	This study
ANG 2967	pCL55*p300ltaS-lacZ* integrated in strain ANG 1575; CamR	This study
ANG 2968	pCL55*p200ltaS-lacZ* integrated in strain ANG 1575; CamR	This study

ANG 2969	pCL55*p100ltaS-lacZ* integrated in strain ANG 1575; CamR	This study
ANG 2970	pCL55*p700ltaS-lacZ* integrated in strain ANG 467; CamR	This study
ANG 2971	pCL55*p473ltaS-lacZ* integrated in strain ANG 467; CamR	This study
ANG 2972	pCL55*p400ltaS-lacZ* integrated in strain ANG 467; CamR	This study
ANG 2973	pCL55*p300ltaS-lacZ* integrated in strain ANG 467; CamR	This study
ANG 2974	pCL55*p200ltaS-lacZ* integrated in strain ANG 467; CamR	This study
ANG 2975	pCL55*p100ltaS-lacZ* integrated in strain ANG 467; CamR	This study
ANG 2976	pCL55*pΔ400-30ltaS-lacZ* integrated in strain ANG 1575; CamR	This study
ANG 2977	pCL55*pΔ294-30ltaS-lacZ* integrated in strain ANG 1575; CamR	This study
ANG 2978	pCL55*pΔ294ltaS-lacZ* integrated in strain ANG 1575; CamR	This study
ANG 2979	pCL55*pΔ400-30ltaS-lacZ* integrated in strain ANG 1575; CamR	This study
ANG 2980	pCL55*pΔ294-30ltaS-lacZ* integrated in strain ANG 1575; CamR	This study
ANG 2981	pCL55*pΔ294ltaS-lacZ* integrated in strain ANG 1575; CamR	This study
ANG 3018	pCL55*pltaS-gfp*$_{P7}$-*ltaS*$_{S218P}$ integrated in strain ANG 314; CamR	This study
ANG 3019	pCL55*pltaS-gfp*$_{P7}$-linker-*ltaS*$_{S218P}$ integrated in strain ANG 314; CamR	This study
ANG 3020	pCL55i*TET-gfp*$_{P7}$-*ltaS*$_{S218P}$ integrated in strain ANG 314; CamR	This study
ANG 3021	pCL55i*TET-gfp*$_{P7}$-linker-*ltaS*$_{S218P}$ integrated in strain ANG 314; CamR	This study
ANG 3022	pCL55*pltaS-gfp*$_{P7}$-*ltaS*$_{S218P}$ integrated in strain ANG 1575; CamR	This study
ANG 3023	pCL55*pltaS-gfp*$_{P7}$-linker-*ltaS*$_{S218P}$ integrated in strain ANG 1575; CamR	This study
ANG 3024	pCL55i*TET-gfp*$_{P7}$-*ltaS*$_{S218P}$ integrated in strain ANG 1575; CamR	This study
ANG 3025	pCL55i*TET-gfp*$_{P7}$-linker-*ltaS*$_{S218P}$ integrated in strain ANG 1575; CamR	This study
ANG 3026	pCL55*pltaS-gfp*$_{P7}$-*ltaS*$_{S218P}$ integrated in strain ANG 2505; CamR	This study
ANG 3027	pCL55*pltaS-gfp*$_{P7}$-linker-*ltaS*$_{S218P}$ integrated in strain ANG 2505; CamR	This study
ANG 3028	pCL55i*TET-gfp*$_{P7}$-*ltaS*$_{S218P}$ integrated in strain ANG 2505; CamR	This study
ANG 3029	pCL55i*TET-gfp*$_{P7}$-linker-*ltaS*$_{S218P}$ integrated in strain ANG 2505; CamR	This study

Table 2 - Primers used in this study

Number	Primer	Sequence
ANG 317	3-KpnI-SAV719	GGGGTACCCCGAGTTCGTGTTTAAATATTATTTTTTAG
ANG 319	3-BglII-SAV719	GAAGATCTCCGAGTTCGTGTTTAAATATTATTTTTTAG
ANG 817	pLKC480 rev (LacZ)	GCCTCTTCGCTATTACGCCAGCTGG
ANG 1047	5-KpnI-P473-LtaS	GGGGTACCTATTTGGTACGTAGCTCATACTCG
ANG 1048	5-KpnI-P400-LtaS	GGGGTACCTTTTATCTGCGAAATGTATCATTTTCTAATTC
ANG 1049	5-KpnI-P300-LtaS	GGGGTACCATTAATTGAGCTATGCTTATTATTAC
ANG 1050	5-KpnI-P200-LtaS	GGGGTACCGTTGTAGCCCAAAATACTTGTTAAATC
ANG 1051	5-KpnI-P100-LtaS	GGGGTACCAACTTTTAAACGCACTTATTAATTAAC
ANG 1052	3-Biotin-Sal-LtaS-3AA	Biotin-ACGCGTCGACTGAACTCATGATTCTTTCCCCCG
ANG 1058	5-KpnI-P700-LtaS	GGGGTACCCTATTATCCTATTAAATGATCATTATACGC
ANG 1232	3-Upstr-RM -400 to 30	TTAGATAATAAATCACAGTATTATTTCATTATACATTAGG
ANG 1233	5-Down-RM -400 to 30	AATAATACTGTGATTTATTATCTAAATAACGG
ANG 1234	3-Upstr-RM -294 to 30	TTAGATAATAAATGCATAGCTCAATTAATAAATATAGAG
ANG 1235	5-Down-RM -294 to 30	ATTGAGCTATGCATTTATTATCTAAATAACGG
ANG 1236	3-Upstr-RM P294	CAATTAATACCACACGAGTAATTTTAGTCAAAATT CAAG
ANG 1237	5- Down-RM P294	ATTACTCGTGTGGTATTAATTGAGCTATGCTTATTA TTAC
ANG 1334	5'-EcoRI-pltaS for	CCGGAATTCGGAATAGAATATAGAATGCAATTAG
ANG 1337	SacII-linker-LtaS for	GGCCGCGGCTAAAGAAGCTGCCGCAAAAAGTTCACA AAAAAAGAAAATTAGTC
ANG 1697	3-pltaS GFPmut2	TCCTTTACTCATGATTCTTTCCCCCGTTATTTAG
ANG 1698	5-pltaS GFPmut2	GGGGAAAGAATCATGAGTAAAGGAGAAGAACTTTTC ACTGG
ANG 1699	3-GFPmut2-LtaS	TTTTTGTGAACTTTTGTATAGTTCATCCATGCCATGTG
ANG 1700	5-GFPmut2-LtaS	GAACTATACAAAAGTTCACAAAAAAAGAAAATT AGTCTTTTTGC
ANG 1701	3-GFPmut2-linker-SacII	TCCCCGCGGCTTCTTTCGCAGCTGCTTCTTTGTATAG TTCATCCATGCCATGTGTAATC
ANG 1702	5-AvrII-LtaS rbs-GFPmut2	CCGCCTAGGCTAAATAACGGGGGAAAGAATCATG AGTAAAGGAGAAGAACTTTTCACTGG

Restriction sites are underlined in the primer sequences.

3. Results

3.1. Cellular functions of LTA

3.1.1. LTA is required for efficient incorporation of D-alanines into WTA

The DltABCD proteins are responsible for D-alanylation of LTA (Fischer, 1994; Neuhaus *et al.*, 1996; Perego *et al.*, 1995) and it was found that in a *dlt* operon mutant D-alanylation is abolished in both, LTA and WTA (Perego *et al.*, 1995). Furthermore it was found when using [^{14}C]-alanine that when the radioactivity is lost from the LTA fraction it increases in the WTA fraction (Haas *et al.*, 1984; Koch *et al.*, 1985), which would indicate that D-Ala-LTA acts as the donor of D-alanine residues for WTA.

In order to further investigate the possibility that D-Ala-LTA is the donor for D-alanines on WTA, the D-alanine content in WTA was determined in an LTA negative (RN4220Δ*spa* Δ*ltaS*) *S. aureus* strain (4S5) (Corrigan *et al.*, 2011). This strain is able to grow in the absence of LTA almost normally due to second site suppressor mutations that result in increased levels of c-di-AMP (Corrigan *et al.*, 2011). A whole genome sequence analysis was previously performed on strain 4S5, which revealed that this strain contains an intact *dlt* operon (Corrigan *et al.*, 2011). The wild-type *S. aureus* control strain (RN4220Δ*spa*) and LTA negative 4S5 strain were grown to mid-log phase and cell wall material containing WTA isolated as described in section 2. Materials and Method. WTA was hydrolysed from peptidoglycan in acidic conditions to retain the D-alanine modifications. The purified WTA material was subsequently analysed by 1D proton NMR. Clear signals derived from protons from the D-alanine and N-acetyl-glucosamine (GlcNAc) modifications were observed in WTA samples isolated from the wild-type strain (Figure 5). As previously reported (Bernal *et al.*, 2009), the ratio of the signal from the three methyl groups protons of D-Ala at 1.6 ppm to GlcNAc at 2.1 ppm was 0.54 ± 0.08 for WTA isolated from a wild-type strain (Figure 5). On the other hand, the reduction in the D-alanine specific signal in WTA isolated from the LTA negative strain was drastic and statistically significant, yielding a D-Ala to GlcNAc ratio

of 0.11 ± 0.01 (Figure 5). These results support a model whereby D-Ala-LTA acts as the donor of D-alanines for WTA.

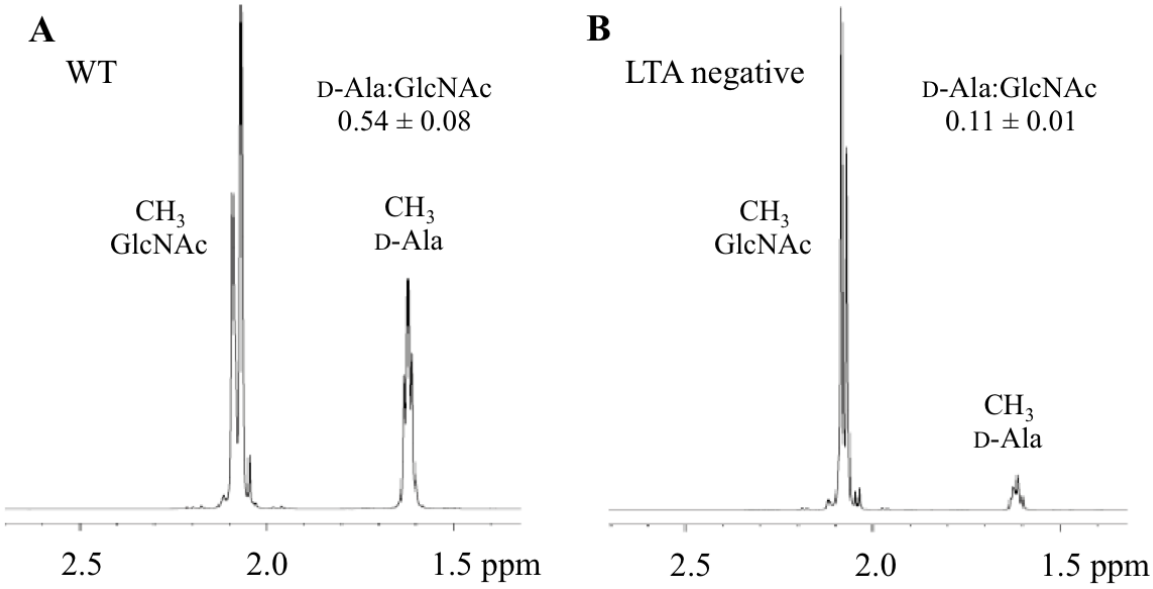

Figure 5 - NMR analysis of WTA isolated from WT and LTA negative *S. aureus* strains. *S. aureus* strains RN4220Δ*spa* (WT) and 4S5 (LTA negative) where grown to mid-log phase and WTA purified as described in the section 2. Materials and Methods. Six mg of dried WTA were suspended in 99.99 % D_2O and 1-D proton spectra acquired at 600 MHz. The experiment was performed in triplicate and representative spectra are shown. The ratio of the D-Ala to GlcNAc signal is 0.54 ± 0.08 for WTA isolated from a WT strain and 0.11 ± 0.01 for WTA isolated from the LTA negative strain. A 2-tailed unequal variance T-test indicated a $p<0.01$ indicating statistically significant differences. Peaks are annotated as previously described (Bernal *et al.*, 2009) and full spectra are shown in Annex 1.

3.1.2. Depletion of LTA is bactericidal

The LTA synthase enzyme LtaS is responsible for the synthesis of the LTA polyglycerolphosphate (PGP) chain in *S. aureus* (Gründling & Schneewind, 2007b). Using an inducible *ltaS* strain, it was previously shown that this enzyme is essential for bacterial growth as in the absence of the inducer cells are no longer able to grow (Gründling & Schneewind, 2007b). However, it is not known whether the cells are no longer able to grow but are still viable (bacteriostatic effect), or if the cells lose their viability and are in fact dying in the absence of LTA (bactericidal effect). Here it was further studied if the absence of LTA is bacteriostatic or bactericidal.

In order to do this the wild-type *S. aureus* strains RN4220 and LAC* and the isogenic inducible *ltaS* strains RN4220-i*ltaS* and LAC*-i*ltaS* were grown overnight in TSB medium. The next day, the cultures were washed with fresh medium and back diluted into TSB and grown for 6 h at 37°C. In the case of the inducible *ltaS* strains, cultures were grown with and without inducer. Samples were taken every 2 h, normalised for OD_{600nm} readings (Figure 6A, 6B), stained with the live/dead stains and analysed by microscope (Figure 6C). The live/dead microscopic viability assay uses two stains that differ in their ability to penetrate cells: SYTO 9, a green-fluorescent nucleic acid stain that penetrates all cells in a population, the ones with intact membranes (living cells) and the ones with damaged membranes (dead cells) and propidium iodide, a red-fluorescent nucleic acid stain that is only able to penetrate dead cells and, when used with SYTO 9, reduces the green fluorescence. Therefore, living cells are stained green and damaged cells are stained red.

The growth curves seem to indicate that the uninduced RN4220-i*ltaS* ceases to grow earlier than the uninduced MRSA strain LAC*-i*ltaS* (Figures 6A, 6B). However, the live/dead assay shows similar results for both strains (Figure 7A, 7B). As seen in Figure 6C, the majority of wild-type cells, as well as RN4220-i*ltaS* grown with IPTG remain alive during the 6 h of growth. However, in the absence of IPTG, cell death is observed at both the 4 h and 6 h time points. It is important to note that, although all the samples were normalised for OD_{600nm} readings, most of the cells are enlarged and misshaped especially after 4 h of IPTG removal in the i*ltaS* strain (Gründling & Schneewind, 2007b). This may influence the optical density and in this way influence the number of cells per field. The images presented correspond to the results obtained in the *S. aureus* RN4220 strains, but similar results were observed using LAC* strains.

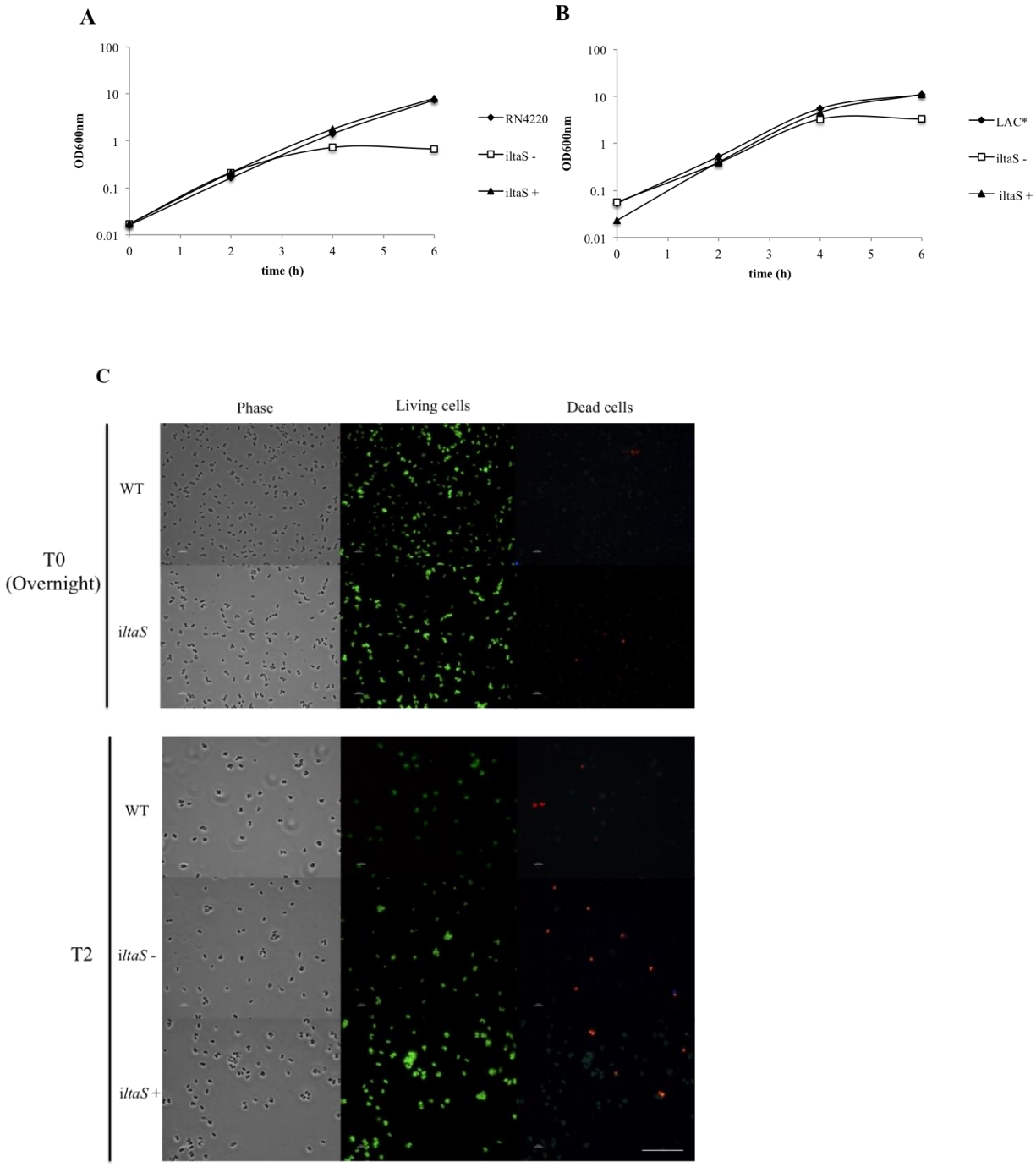
A
B
C
OD600nm
time (h)
RN4220
iltaS -
iltaS +
LAC*
Phase
Living cells
Dead cells
T0
(Overnight)
WT
iltaS
T2
WT
iltaS -
iltaS +

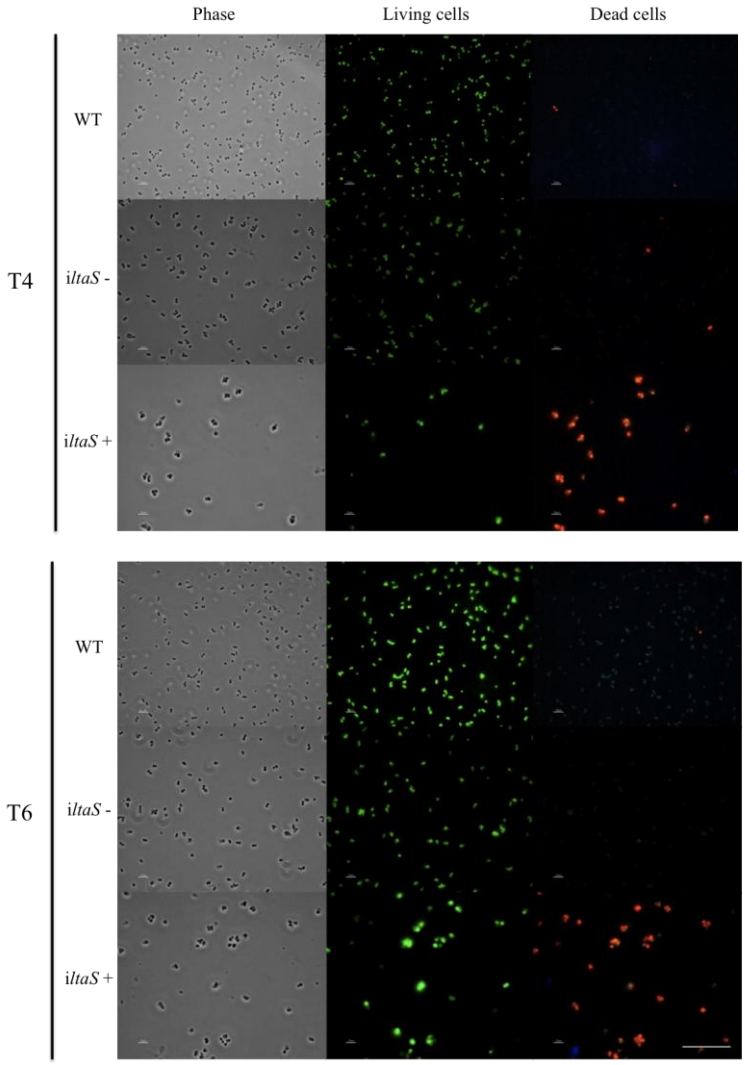

Figure 6 – Determination of bacterial viability using a live/dead staining assay. (**A, B) Bacterial growth curves.** The *S. aureus* WT strains RN4220 or LAC*, and the inducible *ltaS* strains RN4220-i*ltaS* or LAC*-i*ltaS* were grown overnight, washed and back diluted 1:400 into fresh medium with or without IPTG for the inducible strains. OD_{600nm} readings were determined and plotted every 2 h. The experiment was performed in triplicate and representative growth curves are shown. **(C) Microscopic images for RN4220 and RN4220-i*ltaS* samples.** Samples were taken every 2 h, normalised for OD_{600nm} readings and stained with a 1:1 mixture of SYTO 9 (green) and propidium iodide (red) from the Live/Dead Baclight Bacterial Viability Kit. A Nikon Eclipse E600 microscope equipped with a Nikon Digital DXM1200 camera and Digital Sight ACT-1 software was used to acquire the images. In a population living cells are stained green, while dead cells are stained red. The experiment was performed in triplicate and representative images are presented. Scale bar = 50μm.

After microscopic observation, three fields of each sample in each experiment were analysed using Image J software in order to quantify the results. The cells observed by phase contrast were considered the number of total cells in order to calculate percentages (Figure 7A, 7B). The quantification confirmed what was observed in the microscopy images: in the LtaS depleted strains there is a significant decrease in

living cells from the 4 h time point, while the wild-type and induced strains maintain a high level of living cells.

These results indicate that the absence of LTA is indeed bactericidal for *S. aureus* cells for both the laboratory strain RN4220 and the MRSA strain LAC*, confirming that LtaS activity is necessary for bacterial survival.

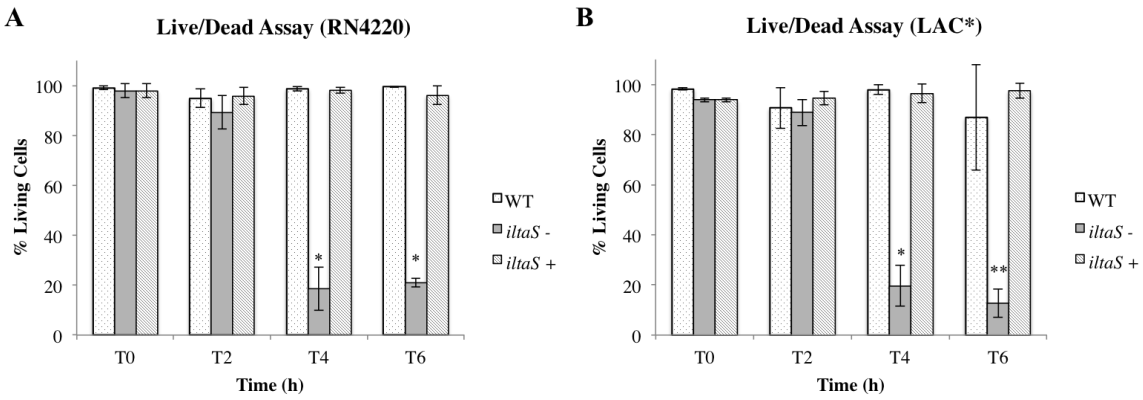

Figure 7 - Quantification of the live/dead assay. In each experiment cells from three different fields were counted. Cells from the phase contrast images were considered the total number to calculate the percentage of living cells. The assay was performed in triplicate and the mean and standard deviation are shown in the graph. A 2-tailed unequal variance T-test analysis was performed and results that have statistically significant differences comparing with the WT strain are indicated with asterisks (*p<0.01; **p<0.05).

3.1.3. Depletion of LTA causes membrane depolarisation

In the cell envelope, the membrane potential is an important determinant in maintaining the charge equilibrium at the surface, since it regulates the binding of ions (Neuhaus & Baddiley, 2003). Given the zwitterionic properties of LTA, it could be expected that its absence would also have an influence on the membrane potential. Furthermore, it was shown by electron microscopy that in the absence of LtaS cells become misshaped and have deformed membranes (Gründling & Schneewind, 2007b). Also, as referred to in the previous section, cells actually die in the absence of LtaS, which would be expected to be reflected in membrane depolarisation.

Therefore it was decided to investigate how the membrane potential changes in the absence of LtaS. For this purpose, and similarly to the procedure used for the

live/dead assay, the wild-type *S. aureus* strains RN4220 and LAC*, and the inducible *ltaS* strains RN4220-i*ltaS* and LAC*-i*ltaS* were grown overnight in Mueller-Hinton broth. The following day the cultures were washed in fresh medium and back diluted into medium with or without inducer for the inducible *ltaS* strain. The strains were grown for 6 h taking samples every 2 h. The samples were washed in a glucose-containing buffer, suspended in the same buffer with additional KCl and diluted to a final OD_{600nm} of 0.05. In order to measure changes in the membrane potential, the samples were incubated with 3,3'-dipropylthiadicarbocyanine iodide, [$DiSC_3(5)$], a positively charged dye. Under normal conditions, where the membrane potential is negative inside, the dye accumulates inside the cell, resulting in the formation of non-fluorescent aggregates. On the other hand, when there is membrane depolarisation the dye does not efficiently penetrate the cell, which results in an increase in fluorescence, and the opposite occurs when there is membrane hyperpolarisation (Sip *et al.*, 1990). As a positive control, the wild-type strains were incubated with nisin, an antimicrobial that is known to form pores in the membrane and thereby abolishes the membrane potential (Li *et al.*, 2009).

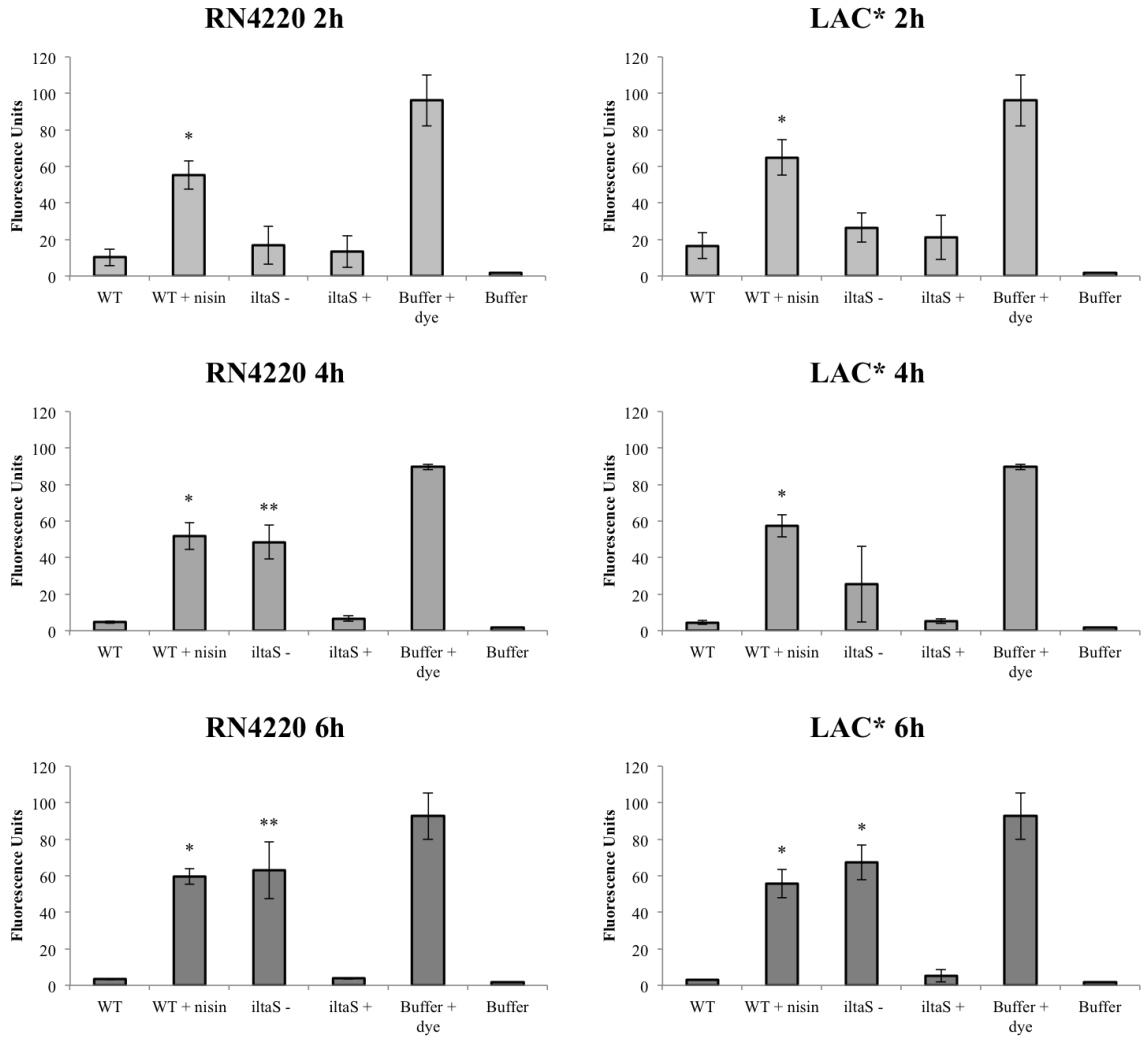

Figure 8 – Membrane potential changes in RN4220-i*ltaS* (A) and LAC*-i*ltaS* (B). The *S. aureus* WT strains RN4220 or LAC*, and the inducible strains RN4220-i*ltaS* or LAC*-i*ltaS* were grown overnight, washed and back diluted 1:400 into fresh medium with or without IPTG for the inducible strains. Samples were taken every 2 h and normalised for OD_{600nm} readings in buffer containing glucose and KCl. The samples were incubated with the dye $DiSC_3(5)$ to allow dye uptake and fluorescence quenching. For the positive controls, the WT strains were incubated with nisin. The fluorescence was measured at an excitation wavelength of 622 nm and emission wavelength of 670 nm. A 2-tailed unequal variance T-test analysis was performed and results that have statistically significant differences comparing with the WT are indicated with asterisks (* $p<0.01$; ** $p<0.05$).

At the 2 h time point there is a low level of fluorescence in both wild-type strains RN4220 and in LAC*, and a low level of fluorescence is also observed for the inducible *ltaS* strains with inducer (Figure 8), indicating that this is the fluorescence detected when the membrane potential is maintained at its wild-type level. However, the inducible *ltaS* strains without IPTG show a slight increase but this is not statistically

significant (Figure 8). This is in agreement with the live/dead assay, where only a slight decrease in the percentage of living cells is observed after 2 h of growth without inducer. At the 4 h time point there are differences between both strains: the laboratorial strain RN4220-i*ltaS* without inducer showed a significant increase in fluorescence, indicating membrane depolarisation, while for the MRSA strain LAC*-i*ltaS* there is also an increase in fluorescence but this is less significant and more variable (Figure 8). This may indicate that it takes longer in the MRSA strain for the membrane potential to change in the absence of LTA. At the 6 h time point similar results were obtained for both strains and a significant increase in fluorescence for the LtaS depleted strains, indicating membrane depolarisation (Figure 8).

These results indicate that in the absence of LTA, membrane depolarisation occurs, which happens at the same time point as when there is a significant increase in the number of dead cells (see section 3.1.2. Depletion of LTA is bactericidal).

3.1.4. LtaS localisation studies

In *S. aureus* it has been shown that in the absence of LtaS cells display aberrant positioning of the cell division septa (Gründling & Schneewind, 2007b). Furthermore, in *B. subtilis* it was previously shown that an LtaS homologue localises at the cell division site and the deletion of *ltaS* in *B. subtilis* leads to mislocalisation of FtsZ, a key cell division protein (Schirner *et al.*, 2009). These data indicate that LtaS may localise at the division septum in *S. aureus*, which may suggest a role in cell division. In order to observe the localisation of LtaS in *S. aureus*, fusions between the "superfast-folding" version of the green fluorescent protein (GFP) (Fisher & DeLisa, 2008) and $LtaS_{S218P}$, the less cleaved version of LtaS (Wörmann *et al.*, 2011b) were produced (Figure 9).

LtaS has five transmembrane helices linked to an extracellular enzymatic domain. The extracellular domain (eLtaS) is cleaved by the signal peptidase SpsB in the linker region after an AXA motif and released into the culture supernatant (Wörmann *et al.*, 2011b). It has been previously shown that the substitution of the serine residue following the cleavage site with a proline ($LtaS_{S218P}$) reduces the level of LtaS cleavage, resulting in higher amounts of full-length protein (Wörmann *et al.*, 2011b). The

cleavage of LtaS would lead to the rapid degradation of the fluorescent protein fusion and accumulation of the cleaved product in the cytoplasm. Fluorescent protein fusions to wild-type LtaS were previously constructed and resulted in high cytoplasmic fluorescence (Reichmann *et al*., unpublished results). Therefore, to minimise the degradation of the fusion proteins, GFP was fused to the $LtaS_{S218P}$ variant (Wörmann *et al.*, 2011b). Given the fact that the C-terminal end of LtaS is localised on the outside of the membrane, only N-terminal fusions were designed. Furthermore, in order to improve the fluorescence signal, $LtaS_{S218P}$ was fused to a "superfast-folding" variant of GFP (named GFP_{P7}). The "superfast-folding" variant of GFP is an improved variant of GFPmut2 (Cormack *et al.*, 1996) which has additional point mutations and the protein displays increased folding kinetics, slower unfolding and increased stability during equilibrium unfolding (Fisher & DeLisa, 2008).

Four different fusions were constructed: with and without a 3x EAAAK amino acid linker region between GFP_{P7} and $LtaS_{S218P}$, and expressed either from the native *ltaS* promoter or the Atet inducible i*TET* promoter (Figure 9). The introduction of the EAAAK linker would be expected to provide space and flexibility between GFP_{P7} and $LtaS_{S218P}$, perhaps improve protein folding and stabilise the fluorescent protein (Arai *et al.*, 2001). Furthermore, the utilisation of an inducible promoter allows control of the expression levels of the fusion proteins. However the utilisation of the native promoter provides more similar expression levels to those obtained under natural conditions. These fusions were cloned into the integration vector pCL55, enabling stable expression of the fusions from the chromosome after integration of the vector into the lipase gene locus *geh*. All plasmids were introduced into *S. aureus* RN4220Δ*spa* and subsequently transduced into LAC* and LAC*-i*ltaS* for fluorescence microscopy and functionality studies.

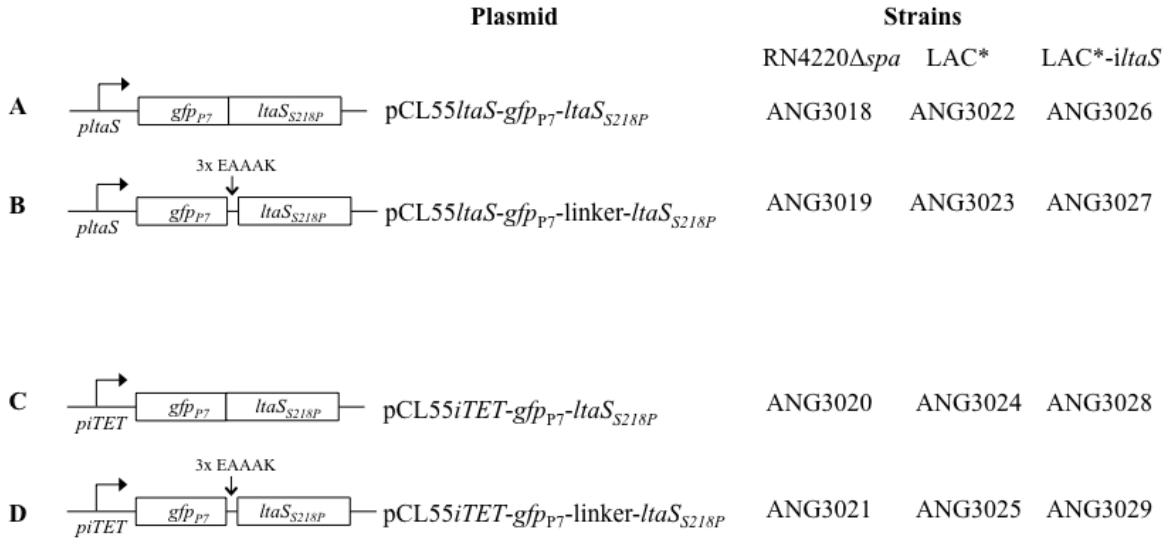

Figure 9 - Schematic representation of fluorescent protein fusions to the *S. aureus* $LtaS_{S218P}$ protein. The fluorescent protein GFP_{P7} was fused to the N-terminus of a less cleaved version of LtaS ($LtaS_{S218P}$) under the LtaS native promoter control (A, B) or the Atet inducible i*TET* promoter control (C, D). In two of the constructions a 3x EAAAK amino acid linker region was cloned between LtaS and the fluorescent protein GFP (B, D). Plasmid names and *S. aureus* strain numbers are given on the right.

Once the GFP_{P7} fusions to $LtaS_{S218P}$ were made, it was important to determine whether the fusion proteins were functional. In order to do this, each construction was introduced into the inducible *ltaS* strain, LAC*-i*ltaS*. Therefore, in the absence of IPTG, only strains expressing a functional *ltaS* gene are able to grow and produce LTA (Figure 10A). The *S. aureus* LAC*-i*ltaS* strains with the different GFP_{P7} constructs were then grown in absence of IPTG and constructions with Atet inducible i*TET* promoter were grown in the absence or presence of Atet. The LAC*-i*ltaS* strain grown in the absence of IPTG was used as the negative control, while the LAC* wild-type strain was used as a positive control since it produces wild-type levels of LTA.

Growth was restored in all four strains expressing the fusion proteins, and although at 6 h they did not reach the wild-type level, at 8 h they were all like the wild-type strain (Figure 10B). Of note, the fusions under the control of the Atet inducible i*TET* promoter, even in the absence of inducer were able to partially restore growth, indicating that expression from this system is "leaky".

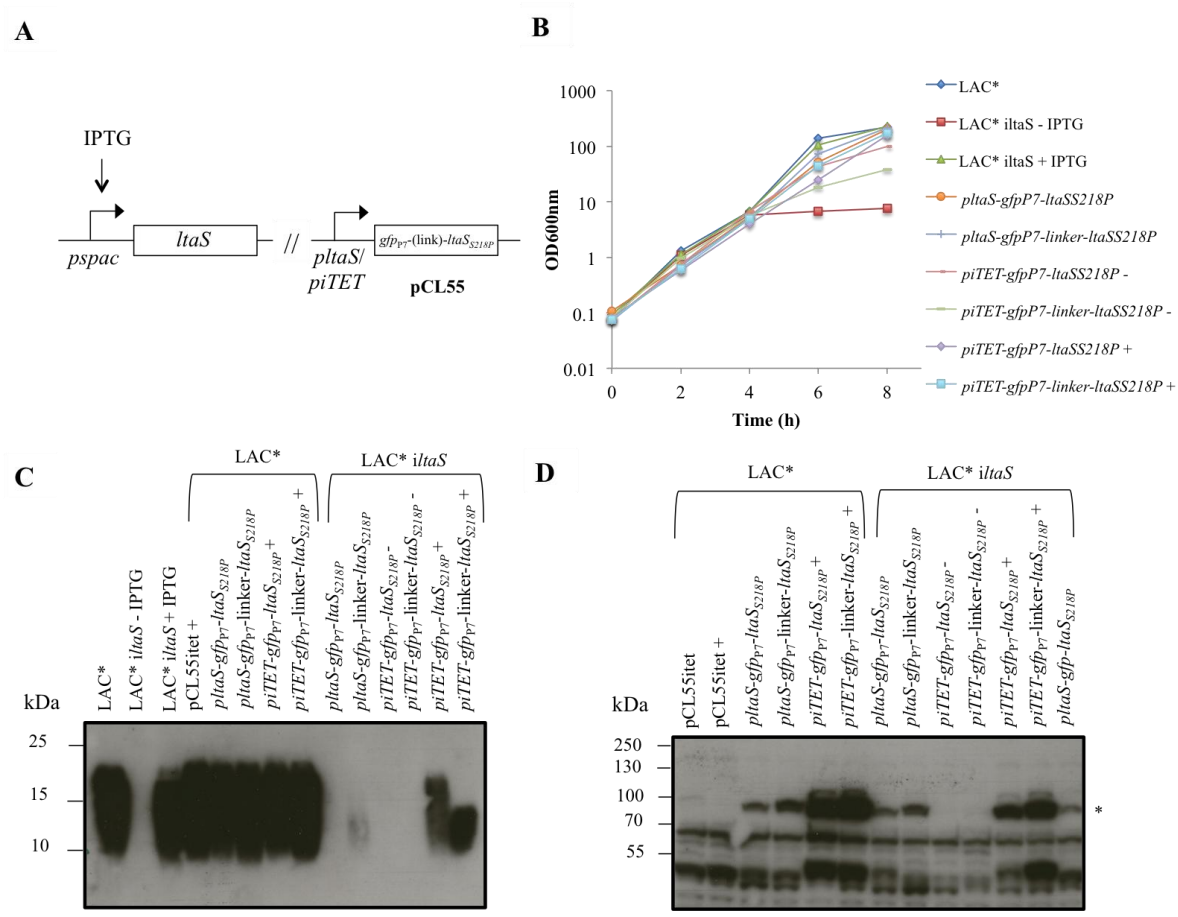

Figure 10 - LtaS complementation analysis as assessed by LTA and LtaS western blot analysis and bacterial growth complementation analysis. (A) Schematic representation of the *S. aureus* strains LAC*-i*ltaS*. The chromosomal copy of *ltaS* is expressed from the IPTG inducible *spac* promoter. GFP_{P7} fusions cloned into pCL55 that integrates into the chromosome in the lipase gene, *geh*, and are under the native *ltaS* or the Atet inducible i*TET* promoter control. In the absence of IPTG, LTA is no longer produced and cells cease to grow, unless complemented with a functional copy of $ltaS_{S218P}$ from pCL55. **(B) Bacterial growth curves**. The *S. aureus* LAC*-i*ltaS* strains were grown in absence of IPTG, with the exception of the LAC*-i*ltaS* control strain without any fusion that was grown the in absence (-) or presence (+) of 1mM IPTG. The constructions with Atet inducible i*TET* promoter were grown in the absence (-) or presence (+) of 100 ng/ml Atet. At the 4 h all strains were back-diluted 1:100. **(C) Detection of LTA production by western blot.** *S. aureus* LAC* and LAC*-i*ltaS* strains were grown in the same way as for the bacterial growth curves. At the 4 h time-point samples were prepared for western blot analysis and the LTA detected using a mouse monoclonal LTA antibody and HRP-conjugated anti-mouse IgG antibody at 1:5000 and 1:10000 dilutions, respectively (see section 2.Materials and Methods). **(D) Detection of LtaS production by western blot.** *S. aureus* LAC* and LAC*-i*ltaS* strains were grown in the same way as for the bacterial growth curves. At the 4 h time-point samples were prepared for western blot analysis and LtaS detected using a rabbit polyclonal LtaS antibody and HRP-conjugated anti-rabbit IgG antibody at 1:20000 and 1:10000 dilutions, respectively (see section 2. Materials and Methods section). The full-length fusions are indicated with an asterisk (*). The experiments were performed once.

At the 4 h time point, samples were prepared for LTA and LtaS analysis by western blot. In addition, LAC* strains containing the empty pCL55i*TET* vector or

GFP_{P7}-$LtaS_{S218P}$ fusions were grown for 4 h and prepared in a similar manner. As expected, all the LAC* strains with the fusion protein had a wild-type level of LTA since in this strain *ltaS* is produced from its native *locus*, however, that was not observed for the LAC*-i*ltaS* strains where none of the strains expressing the fusion proteins were able to produce wild-type levels of LTA: the strain containing pCL55*ltaS-gfp*$_{P7}$-*ltaS*$_{S218P}$ did not produce detectable amounts of LTA, while the strains containing pCL55*ltaS-gfp*$_{P7}$-linker-*ltaS*$_{S218P}$, pCL55i*TET-gfp*$_{P7}$-*ltaS*$_{S218P}$ and pCL55i*TET-gfp*$_{P7}$-linker-*ltaS*$_{S218P}$ produced LTA but not at the wild-type levels (Figure 10C). This indicates that the GFP_{P7}-$LtaS_{S218P}$ fusion is partially functional when expressed under the control of the inducible promoter, while the GFP_{P7}-linker-$LtaS_{S218P}$ is partially functional when expressed from the native and inducible promoters, however, producing higher levels of LTA under the control of the inducible promoter. Together with the bacterial complementation growth curves, these results indicate LTA is being produced at levels that although not wild-type, can still complement growth, indicating that the fusions are partially functional.

In order to use these fluorescent protein fusions in microscopy experiments, the full-length fusions need to be expressed. Therefore, western blot analysis was also performed and the LtaS protein detected using a rabbit polyclonal LtaS antibody. The *S. aureus* LAC* strain containing the empty vector pCL55i*TET* was used as a negative control, while the LAC* strain expressing the GFP-$LtaS_{S218P}$ under the native promoter control, previously constructed and analysed in the laboratory, was used as a positive control. All four strains were able to express the full-length fusions in the LAC* and LAC*-i*ltaS* strains (Figure 10D).

Next, the localisation of the fusion proteins was assessed by fluorescence microscopy. From studies that previously took place in our laboratory it was already known that the resolution of the images obtained at Imperial College London would be too low for analysis. Therefore, the strains were sent to Dr. Mariana Pinho's laboratory at the Instituto de Tecnologia Química e Biológica, a research group that has localised cell division proteins by fluorescence microscopy in *S. aureus*, and images were taken by Dr. Nathalie Reichmann. In this analysis, all strains were grown to mid-exponential phase, mounted on a 1.2 % PBS agarose slide and observed using a Zeiss Axio Observer Z1 microscope equipped with a Photometrics CoolSNAP HQ2 camera (Roper

Scientific) (see section 2. Materials and Methods). The image acquisition was performed with this microscope using Metamorph software. The preliminary data indicates that $LtaS_{S218P}$ displays concentrated fluorescence at the septum (Figure 11), suggesting that LtaS may localise mainly at the site of cell division in *S. aureus*, in agreement with studies in *B. subtilis* (Schirner *et al.*, 2009).

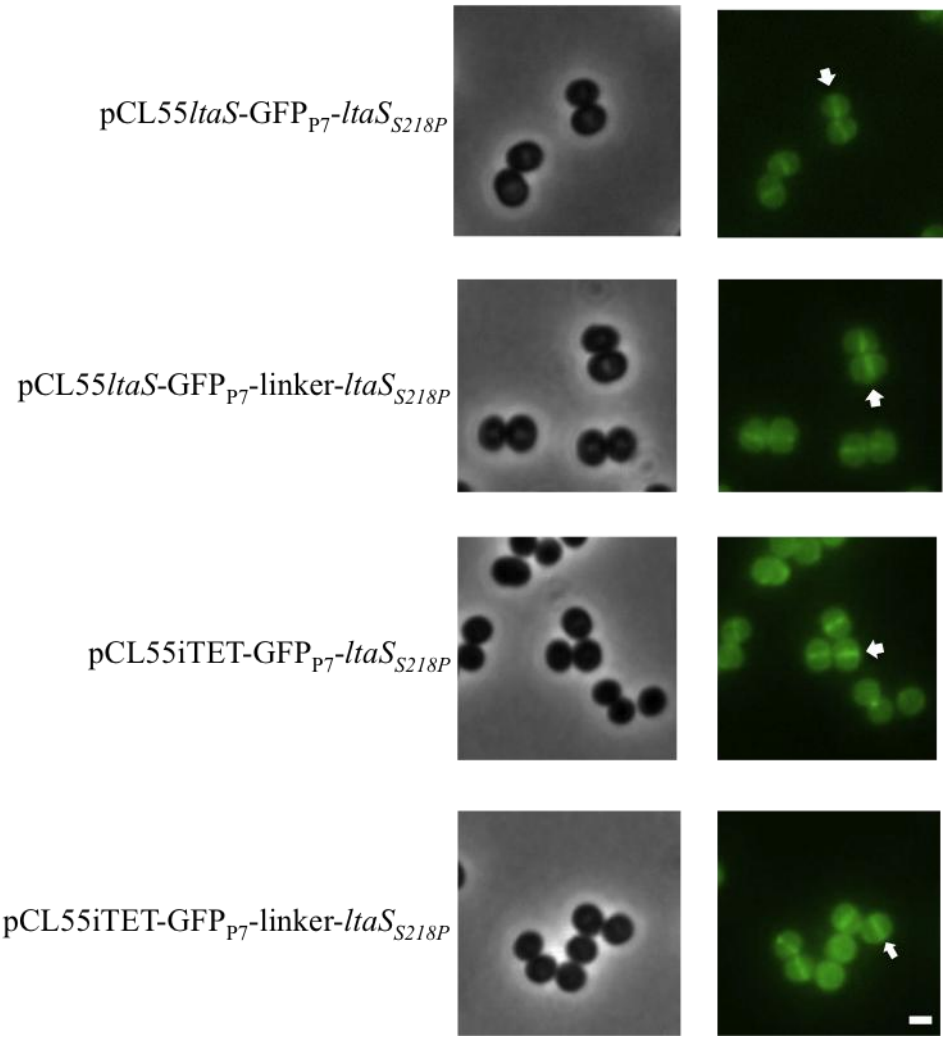

Figure 11 - Localisation of LtaS in *S. aureus* as assessed by fluorescence microscopy. The *S. aureus* LAC* strains with the different fusions were grown to mid-exponential phase and suspended in PBS. Cells were mounted on a 1.2% PBS agarose slide and subsequently observed using a Zeiss Axio Observer Z1 microscope equipped with a Photometrics CoolSNAP HQ2 camera (Roper Scientific). Images were acquired using Metamorph software. Phase contrast and GFP images are shown at the left and right, respectively, and the arrows point to the septum. Scale bar = 1 µm. This experiment was performed once.

3.2. Regulation of *ltaS* expression and LTA production

3.2.1. Mapping and activity analysis of two *ltaS* promoters

Although the reactions and enzymes involved in LTA synthesis are known, how this process is regulated is still mainly unknown. As LtaS is the key enzyme necessary for LTA synthesis (Gründling & Schneewind, 2007b), it would be of interest to study its promoter or *cis* elements in order to understand the regulation of LTA synthesis.

Previously in our laboratory the *ltaS* promoters were mapped using PCR Rapid Amplification of cDNA Ends (RACE) and primer extension. Both techniques enabled the identification of two transcriptional start sites 408 and 294 bases in front of the start codon of the *ltaS* gene (hereafter named P1 and P2 promoter, respectively) in *S. aureus* strains RN4220 and Newman (Figure 12) (Gründling, unpublished results). These results indicate a presence of a long 5' untranslated region (UTR) between the promoters and the initiation codon of *ltaS*, which is unusual and can indicate an intricate regulatory network.

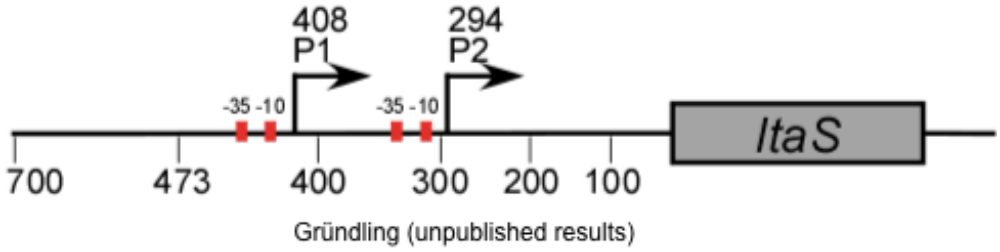

Figure 12 – Schematic representation of *ltaS* promoter region. Previously, two transcriptional start sites 408 and 294 bases in front of *ltaS* gene in *S. aureus* strains RN4220 and Newman were identified by A. Gründling (unpublished results) using PCR RACE and primer extension techniques.

In order to study the functionality of the two promoters and to further understand the transcriptional regulation of *ltaS* in *S. aureus*, a series of different promoter fusions to the reporter gene *lacZ* were constructed. Different portions of the *ltaS* UTR were fused to the *lacZ* gene using the plasmid pCL55i*TET-lacZ* (Figure 13A). The gene *lacZ* works as a reporter gene that enables the evaluation of expression from

the promoters of interest. Fragments with 700 bp, 473 bp, 400 bp, 300 bp, 200 bp and 100 bp from the *ltaS* start codon were amplified from *S. aureus* chromosomal DNA and then inserted into pCL55i*TET-lacZ* upstream of *lacZ*, and transformed into the *E. coli* XL1 Blue strain. The resulting plasmids were then introduced into *S. aureus* strains RN4220, LAC* and Newman. The *S. aureus* RN4220 strain with the empty plasmid pCL55i*TET* was used as a negative control, while the strains bearing the largest insert (700 bp) were used as a positive control for *ltaS*-driven *lacZ* expression (Figure 13B).

The β-galactosidase activity was evaluated and the results obtained indicate that the constructs with 700 bp, 473 bp and 400 bp from the upstream region of *ltaS* fused to *lacZ* have higher level of expression, compared to the constructs with 300 bp, 200 bp and 100 bp (Figure 13B). This indicates that in the absence of the P1 promoter there is still expression, but when the P2 promoter is deleted there is no longer expression. This may suggest that the P2 promoter is not only essential but also sufficient for expression. Of note, in all three background strains there is an increase in activity in the fusion containing 473 bp when compared with the construct with the largest insert, however this difference is not statistically significant.

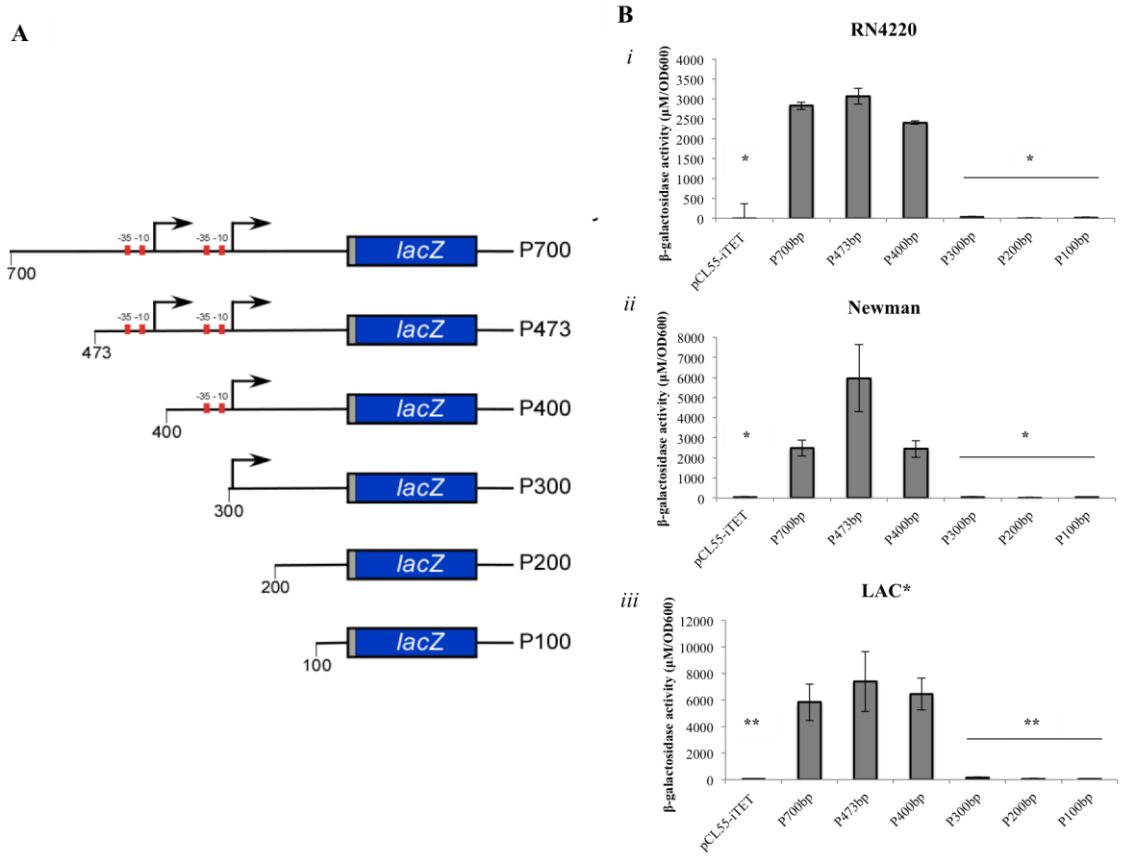

Figure 13 - Mapping and activity analysis of two *ltaS* promoters as assessed by *lacZ* fusions and β-galactosidase activity. (A) Schematic representation of the *lacZ* fusion constructs. The *ltaS* UTR region was cloned into pCL55i*TET-lacZ*. Six different constructions were made, where fragments with 700 bp, 473 bp, 400 bp, 300 bp, 200 bp and 100 bp from *ltaS* UTR were fused to *lacZ*. **(B) Determination of β-galactosidase activity.** S. *aureus* strains RN4220 (*i*), Newman (*ii*) and LAC* (*iii*) containing pCL55i*TET* with the different fusions and the *S. aureus* strain RN4220Δ*spa* containing the empty vector pCL55i*TET* (negative control) were grown for 4 h at 37°C and samples were prepared as described in the section 2. Materials and Methods. The assay was performed in triplicate and the mean and standard deviation are shown. Activity is given as Units per OD_{600nm}. A 2-tailed unequal variance T-test analysis was performed and values that have statistically significant differences comparing with the full-length UTR fusion (P700 bp) are indicated with asterisks (* $p<0.01$; ** $p<0.05$).

Given these results and to try to understand the role of the region between the P2 promoter and the translational start site and between both promoters, additional fusions were constructed. Firstly, a construction lacking the region from -400 bp to -30 bp (PΔ400-30) (the numbers are relative to the *ltaS* start codon) was made to determine the role of the region between the P1 promoter and the transcriptional start site. A construction with a deletion of the region from -294 bp to -30 bp (PΔ294-30) was designed to investigate a possible function of the region between the P2 promoter and the transcriptional start site. Lastly, a construction where the P2 promoter was mutated (PΔ294) by modifying the conserved -10 region was used to investigate if there is expression even in the absence of the P2 promoter but in the presence of only the P1 promoter (Figure 14A). Once again different fragments were amplified from *S. aureus* chromosomal DNA, assembled by SOE PCR in order to obtain the necessary deletions and inserted into pCL55i*TET-lacZ*. The plasmids were first obtained into the *E. coli* XL1 Blue strain and finally transformed into the *S. aureus* strains RN4220Δ*spa*, LAC* and Newman. The same negative and positive controls were used as in the experiment above (Figure 14B).

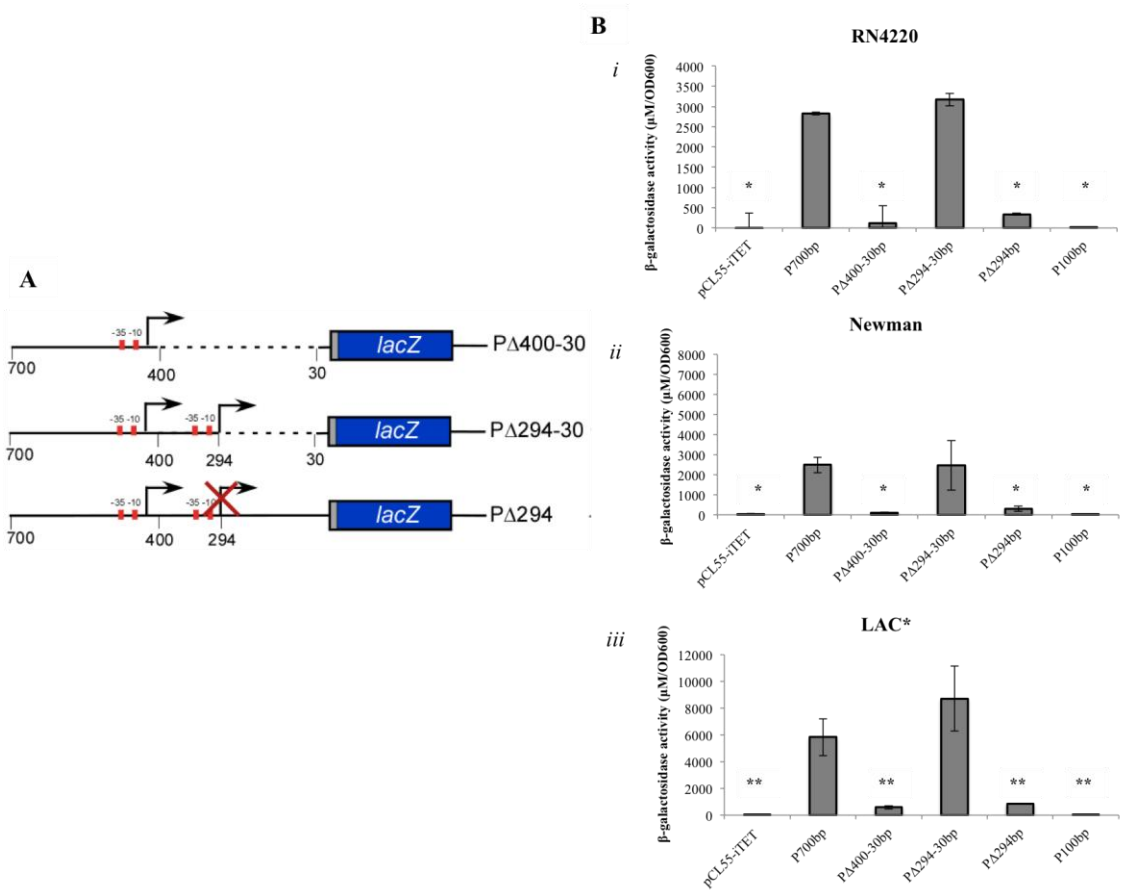

Figure 14 - Mapping and activity analysis of two *ltaS* promoters using a mutagenesis approach and assessed by *lacZ* fusions and β-galactosidase activity. (A) Schematic representation of the *lacZ* fusion constructs. The *ltaS* UTR region was fused to *lacZ* gene and cloned into pCL55i*TET*-*lacZ*. Three different constructions were made, where fragments with from the 700 bp *ltaS* UTR were fused to *lacZ:* a fragment with the region between -400 and -30 deleted, a fragment with the region between -294 and -30 deleted and a third construction with the P2 promoter mutated. **(B) Determination of β-galactosidase activity.** S. *aureus* strains RN4220Δ*spa* (*i*), Newman (*ii*) and LAC* (*iii*) containing pCL55i*TET* with the different fusions and the *S. aureus* strain RN4220Δ*spa* containing the empty vector pCL55i*TET* (negative control) were grown for 4 h at 37°C and samples were prepared as described in the Materials and Methods section. The assay was performed in triplicate and the mean and standard deviation are shown. Activity is given as Units per OD_{600nm}. A 2-tailed unequal variance T-test analysis was performed and results that are statistically different from the full-length UTR fusion (P700 bp) are indicated with asterisks (* $p<0.01$; ** $p<0.05$).

The results obtained seem to indicate that when the P2 promoter is deleted or mutated there is only a low level of activity even when the P1 promoter is present, as can be seen by the low activity in the PΔ400-30 and PΔ294 constructs, where the second promoter was deleted or mutated. This means that the P2 promoter is the main promoter useful for *ltaS* expression. Furthermore, when the region between the P2 promoter and the translational start site is deleted there is still a high level of expression.

This may suggest that under these circumstances this region is not important to activate expression.

3.2.2. LTA production is reduced under high salt conditions

It has been previously shown that LTA potentially has a role as an osmoprotectant under low osmolarity conditions (Oku *et al.*, 2009). Therefore, it was decided to investigate *S. aureus* cell viability in medium with different salt concentrations and the effect of altering *ltaS* expression and consequently LTA production. This was assessed using the inducible *ltaS* strains since it is known that these strains produce reduced amounts of LtaS compared to the wild-type strains (Wörmann *et al.*, 2011b), and consequently may resist less to osmotic stress.

LB medium was used for growth and the salt concentration adjusted by the addition of increasing amounts of NaCl. Since it is known that *S. aureus* cells can survive until approximately 7% of NaCl (Bruins *et al.*, 2007), LB medium containing 0% to 6% of NaCl was used to perform bacterial growth curves using the wild-type strains RN4220 and LAC*. The growth curves were performed by back diluting the overnight culture 1:100 into fresh medium and back diluting again after 4 h of growth to maintain the cells in exponential growth phase for an extended period of time.

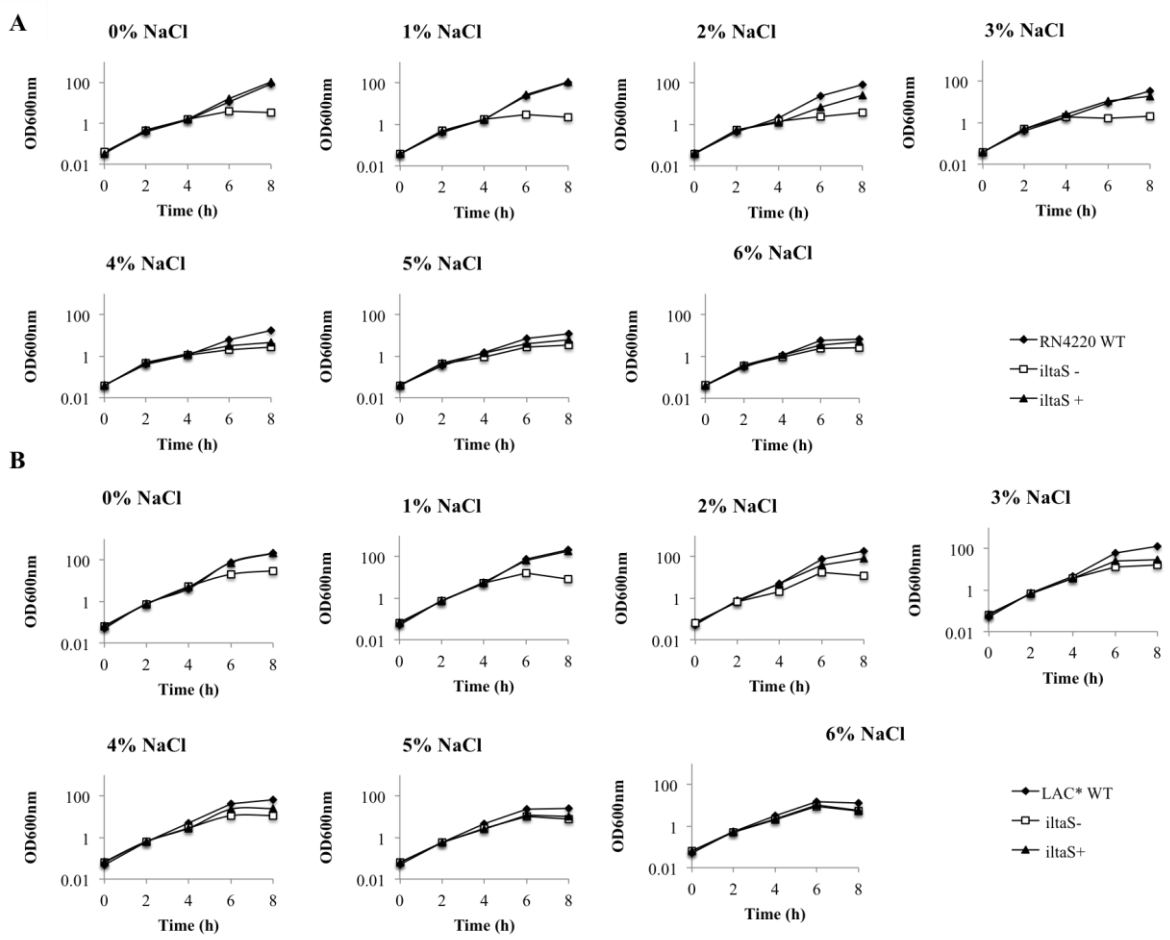

Figure 15 – Bacterial growth curves using wild-type and inducible *ltaS* strains in LB media containing a gradient of NaCl concentrations. The *S. aureus* RN4220 (A) and LAC* (B) inducible and wild-type strains were grown in LB media containing 0% to 6% NaCl and for the inducible strains in the absence (-) and presence (+) of 1mM IPTG. At the 4 h all strains were back-diluted 1:100. These experiments were performed in triplicate.

The results obtained indicate that in a range of 0% to 6% NaCl the wild-type strains RN4220 and LAC* both slow down their growth as the salt concentration increases. At 5% NaCl concentration both wild-type strains have a reduced growth rate and enter in stationary phase after growing for 4 h. Using the inducible strains there is also a growth reduction as the salt concentration increases even in the strains with inducer, which starts to occur at a lower NaCl concentration (around 2%) for both RN4220-i*ltaS* and LAC*-i*ltaS* strains (Figure 15). This may happen because the inducible *ltaS* strains produce less LtaS than the wild-type strains (Wörmann *et al.*, 2011b). This would also be reflected in a reduction of LTA production and a consequent reduction in resistance to high osmolarity.

In order to assess LTA production under these conditions, LTA was detected in samples isolated at the 4 h time point by western blot using a monoclonal anti-LTA antibody. Consistent with what was observed in the bacterial growth curves, as the NaCl percentage in the media increases a reduction in LTA production was observed for the i*ltaS* strains and the wild-type strains. This reduction was observed at higher concentrations for the wild-type strains when compared with the i*ltaS* strains (Figure 16A) and seems to be more drastic for the LAC* strains than for the RN4220 strains.

Given the fact that LtaS is produced in the i*ltaS* strains under the control of *spac* promoter, it could be hypothesised that these observations are due to an effect of NaCl on this promoter, causing alterations in LTA production. To analyse this possibility, the strains were grown under the same conditions and the protein LtaS detected by western blot using a polyclonal anti-LtaS antibody. LtaS is known to be cleaved at the linker region between the N-terminal transmembrane helices and the C-terminal extracellular domain (eLtaS), and eLtaS is released into the supernatant, though also retained within the whole cell fraction. On the other hand, full length LtaS is only detected in the whole cell fraction (Lu *et al.*, 2009; Wörmann *et al.*, 2011b) Therefore, a cell fractionation technique was employed and the cell fraction analysed. The uninduced i*ltaS* strains grown in 0% NaCl and the LTA negative strain 4S5 were used as negative controls. The results obtained show that full-length LtaS can be detected in high amounts both in wild-type and i*ltaS* strains in RN4220 and LAC* at any salt concentration (Figure 16B). In fact, it even seems possible that there is a slight increase in LtaS synthesis when there is an increase in NaCl percentage, which is opposite to what was observed for LTA production (Figure 16B).

Together, these results indicate that LTA production is reduced under high salt concentrations, which affects bacterial growth and this is possibly due to alterations in LtaS enzymatic activity, since LtaS levels are elevated even at high salt concentrations. Therefore, a strain with lower levels of LTA seems to not survive salt stress as well as a wild-type strain.

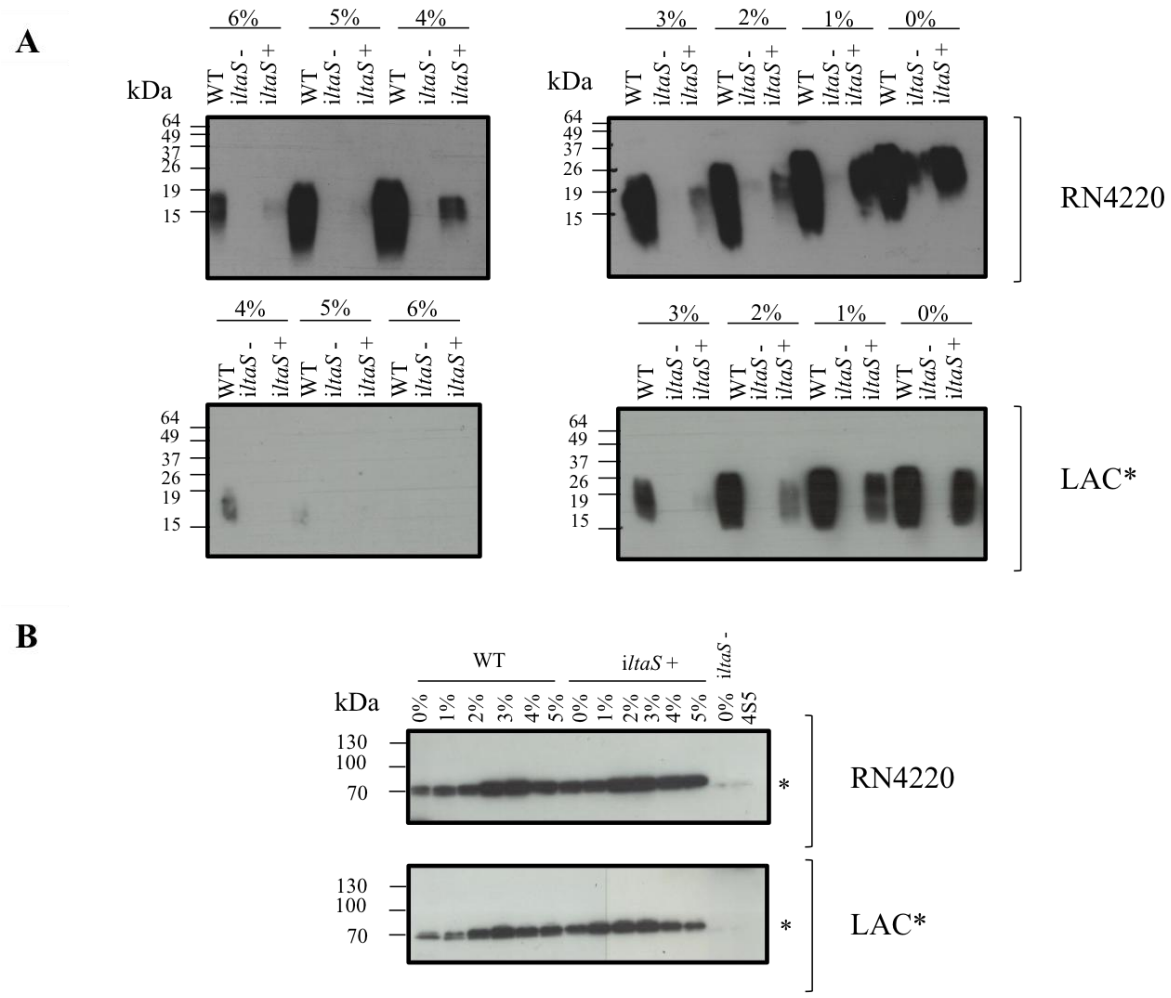

Figure 16 – LTA and LtaS production under different NaCl concentrations as assessed by western blot. (A) Detection of LTA by western blot. The *S. aureus* RN4220-i*ltaS* and LAC*-i*ltaS* strains were grown in absence (-) and presence (+) of 1mM IPTG in LB media containing 0% to 6% NaCl, while the RN4220 and LAC* wild-type strains were grown only in the absence of inducer in media with the same composition as for the i*ltaS* strains. Samples for western blot analysis were obtained after 4 h of growth. LTA was detected using a mouse monoclonal LTA antibody and HRP-conjugated anti-mouse IgG antibody at 1:5000 and 1:10000 dilutions, respectively (see section 2.Materials and Methods). **(B) Detection of LtaS by western blot.** *S. aureus* LAC* and LAC*-i*ltaS* strains were grown in the same way as for LTA detection and the LtaS protein detected by western blot using a rabbit polyclonal LtaS antibody and HRP-conjugated anti-rabbit IgG antibody at 1:20000 and 1:10000 dilutions, respectively (see section 2.Materials and Methods). The full-length protein is indicated with an asterisk (*). The experiments were performed in triplicate.

4. Discussion and Conclusions

LTA is a zwitterionic polymer that is widely distributed amongst Gram-positive bacteria, ranging from Actinobacteria to Firmicutes. Amongst these species emphasis has been given to researching LTA in the pathogenic bacteria *S. aureus* and *L. monocytogenes* and it has also been studied in the model organism *B. subtilis* (Reichmann & Gründling, 2011). The importance of LTA for adherence, host invasion, virulence and bacterial growth makes it appealing for further investigation as a promising target for new antimicrobials (Collins *et al.*, 2002; Doran *et al.*, 2005; Sheen *et al.*, 2010). This study is focused on *S. aureus*, where many roles for LTA are known, including roles in cell division, osmoprotection, regulation of enzymatic activity and ion scavenging (Archibald & Baddiley, 1966; Corrigan *et al.*, 2011; Gründling & Schneewind, 2007b; Heptinstall *et al.*, 1970; Oku *et al.*, 2009). Most importantly, LTA is essential for *S. aureus* growth and cells depleted of LTA become enlarged prior to cell lysis. The LTA synthase enzyme, LtaS, is the key enzyme involved in LTA synthesis, since it is responsible for the PGP chain polymerization. In the case of *S. aureus*, only one LTA synthase is encoded on the genome (Gründling & Schneewind, 2007b). LtaS is therefore essential for bacterial growth, and so until recently, investigations of the roles of LTA have been restricted to analysis of mutants synthesising the PGP chain, but with altered LTA glycolipid anchors (Fedtke *et al.*, 2007; Gründling & Schneewind, 2007a; Kiriukhin *et al.*, 2001). However, recent construction of a conditional depleted *ltaS* mutant (Gründling & Schneewind, 2007b) and a suppressor strain able to grow without LTA (Corrigan *et al.*, 2011) has enabled further investigations on the LTA roles on the cell, which was one of the overall aims of this study. Furthermore, the enzymes necessary for LTA synthesis are known but how this process is regulated and how this correlates with different growth conditions are largely unknown. Therefore, this study aimed to give new insights into the regulation of LTA synthesis, focusing on *ltaS* gene expression.

A previously proposed role for LTA is that of a donor of D-alanines for WTA. LTA D-alanylation is known to be an enzymatically catalysed process involving the Dlt proteins. However, a different process was previously proposed for WTA D-alanylation based on pulse-chase experiments using [^{14}C]-alanine, which demonstrated that

radioactive D-alanines are lost from the LTA fraction and increased in the WTA fraction (Haas *et al.*, 1984), indicating D-Ala-LTA is a donor for WTA D-alanylation. The disruption of the *dlt* operon results in a lack of D-alanines on both LTA and WTA (Perego *et al.*, 1995), but this observation in WTA could be directly due to the absence of Dlt proteins or the absence of D-Ala-LTA. Therefore, this mechanism was investigated in this study using a recently described *S. aureus* LTA negative strain with an intact *dlt* operon (Corrigan *et al.*, 2011). The result obtained here showed that the D-alanine content in WTA is drastically reduced in the absence of LTA (Figure 5), providing strong evidence that D-Ala-LTA is indeed the donor for D-Ala-WTA. However, these data also indicate that a small amount of D-alanine residues are still present in WTA in the LTA-negative strain. This might suggest that WTA polymers when on the outer leaflet of the membrane but still linked to the undecaprenyl phosphate membrane carrier can serve as an acceptor molecule for D-alanine modification by the Dlt system itself. If this is the case, it is likely to only happen inefficiently and transiently, though it would be enough to be detected by this method. On the other hand, we cannot rule out the possibility that the small degree of D-alanylation detected in the LTA-negative strain is due to cross contamination during the experimental procedure. This could be evaluated using a strain without an essential protein for D-alanylation, like DltB, where is known that D-alanylation does not occur and observe if the small amount of D-alanine residues would still be detected.

It is important to note that this result does not elucidate how and where at the cell surface the transfer of D-alanine residues from LTA to WTA occurs. D-alanine incorporation into WTA may happen when WTA is still linked to its membrane carrier or when it is already attached to the peptidoglycan. The occurrence at the membrane would be plausible since LTA and WTA are in close proximity. However, these results cannot distinguish between cell wall anchored WTA and WTA present at the cell membrane and only analysis of the D-alanine content in WTA still linked to the predicted undecaprenyl phosphate membrane carrier could answer this question. Furthermore, it is still not known if D-alanine transference from LTA to WTA is enzymatically catalysed and no proteins have been identified as being involved in this process. This unidentified enzyme or enzymatic complex would have to recognise both ribitol phosphate and glycerol phosphate, and to incorporate and remove D-alanines

from LTA. It is also possible that no enzyme is required for this process. In fact, it was already showed that D-alanines can be transferred between LTA molecules without requiring ATP, enzymatic activity or any Dlt protein (Childs *et al.*, 1985).

In conclusion, the results in this study establish a role for LTA as the D-alanine donor for WTA, indicating that the D-alanine modification of these two important polymers is closely linked. Given the importance of this modification for TAs roles in the cell, this may explain their overlapping functions. Additionally, it may also be an indication of coordination in synthesis and localisation between both TAs.

The importance of LTA in the cell is unquestionable, as this molecule is necessary for growth and cell division in *S. aureus*. However, the question we wished to answer was, if in the absence of LTA, cells only stop growing and enter starvation, which is reflected by early entrance into stationary phase (Gründling & Schneewind, 2007b), or whether the absence of LTA in fact causes such a large disruption to the cell that it leads to immediate cell death. For this purpose, and making use of a conditional *ltaS* depleted mutant, a live/dead staining procedure that distinguishes between living and dead cells was applied. This experiment showed that in the absence of LTA cells are actually dying (Figure 6), indicating that depletion of *ltaS* is bactericidal for *S. aureus* cells. These data may increase the interest in using LtaS as a possible target for new antimicrobials and, in fact, similar results were observed not only in the laboratory strain RN4220, but also in the MRSA strain LAC*, where the majority of the cells (around 80%) were dead 4 h after the removal of inducer. Moreover, a small molecule has already been discovered that works as an antibiotic for Gram-positive bacterial species, possibly by targeting LTA synthesis (Richter *et al.*, 2013). This molecule was shown not only to inhibit the growth of *S. aureus*, but also in other Gram-positive bacteria that produce polyglycerolphosphate LTA, and it would be interesting to investigate whether *ltaS* depletion is bactericidal in other species.

It is also important to note that besides this, the absence of LtaS may also result in the accumulation of PG lipid in the membrane. The PG serves as the donor for GroP in LTA synthesis by LtaS and it is estimated that the turn over in this reaction is more than twice in one bacterial doubling (Koch *et al.*, 1984) but, without LtaS, GroP is no longer hydrolysed from PG. This can result in significant changes in the membrane

stability causing membrane disruption.

Furthermore, and given these results, it was also investigated how *ltaS* depletion affects the membrane potential in *S. aureus* over time and how this could be correlated with the time course experiment performed using a live/dead bacterial viability assay. The close proximity of LTA to the membrane and its negatively charged PGP chain together with the variable degree of D-alanylation, could make this polymer an important component in maintaining the charge distribution at the cell surface and in cation binding (Hughes *et al.*, 1973). An assay using a membrane potential sensitive dye that shows increased levels of fluorescence when there is membrane depolarisation and decreased levels of fluorescence when there is membrane hyperpolarisation was used. Therefore, changes in the membrane potential due to the absence of LtaS could be assessed. Two hours after growth without inducer both uninduced RN4220-i*ltaS* and LAC*-i*ltaS* do not display a statistically significant increase in fluorescence (Figure 8). Based on the results from the live/dead staining assay, most of the cells (around 90%) are still alive at this time point, even in the uninduced strains. These results may indicate that the absence of LTA does not cause membrane depolarisation before cell death. On the other hand, it is possible that at this point the LtaS protein still present from the overnight culture is active and sufficient to maintain LTA production to a level that the membrane potential is not affected.

At the 4 h time point there is a significant increase in fluorescence, indicating membrane depolarisation, in the laboratory strain RN4220 and a less significant and more variable increase in the MRSA strain LAC*. At this point, however, it is known from the live/dead assay that the majority of the cells are dead. Since the live-dead assay is actually also detecting membrane depolarisation (propidium iodide is only able to enter cells with depolarised membranes), this indicates that although both assays show the same trend they still show subtle differences in the timing when the depolarisation is occurring. It is important to note that comparing these strains grown in the same conditions (Figure 6A, 6B), the non-induced LAC*-i*ltaS* enters growth arrest later (after growing for 4 h) when compared with the non-induced RN4200-i*ltaS* strain that stops growing after approximately 3 h. These differences may be reflected in the variances between the two assays. As the live/dead assay gives an indication at the

single cell level, using $DiSC_3(5)$ indicates an average between all the cells, which may influence the ability to compare both results.

Lastly, after 6 h of growth with depleted *ltaS*, both RN4220 and LAC* display increased fluorescence, indicating membrane depolarisation, which at this point is in agreement with the results from the live/dead assay, most likely reflecting the elevated fraction of dead cells.

In conclusion, it is now possible to say that the depletion of *ltaS* results in *S. aureus* cell death, which occurs approximately after 4 h of *ltaS* depletion. However, since the membrane depolarisation correlates with cell death, it is difficult to determine whether depletion of *ltaS* causes alterations in membrane potential prior to cell death.

As referred to above, another essential proposed role for LtaS is in cell division. In *B. subtilis*, UgtP (YpfP homologue) and LtaS were shown to localise in the septum, and the absence of LtaS results in delocalisation of FtsZ. (Schirner *et al.*, 2009; Weart *et al.*, 2007). Furthermore, in both *L. monocytogenes* and *B. subtilis ltaS* mutant strains present a filamentous phenotype (Schirner *et al.*, 2009; Webb *et al.*, 2009). Together, these data suggest a direct association between LTA synthesis and cell division and in order to further investigate this possibility, localisation studies involving the essential LTA synthase, LtaS, were performed in *S. aureus*. To perform these localisation studies a "superfast-folding" version of the green fluorescent protein (GFP), GFP_{P7} (Fisher & DeLisa, 2008) was fused to a less cleaved version of LtaS, $LtaS_{S218P}$ (Wörmann *et al.*, 2011b), and cloned under the native *ltaS* promoter or under an inducible promoter into a single copy chromosomal integration vector (Lee *et al.*, 1991). Integrative vectors provide stability in expression levels reducing the variability of the fluorescence signal between cells, making results more reliable.

LtaS is made up of transmembrane helices linked to an extracellular domain, which is cleaved by a signal peptidase named SpsB (Wörmann *et al.*, 2011b). Therefore, the utilisation of $LtaS_{S218P}$ variant was intended to reduce cleavage and subsequently reduce accumulation of cleaved products in the cytoplasm. The GFP_{P7} protein was used in order to reduce cytoplasmic fluorescence since this variant of GFP has been shown to keep its folded form more stably (Fisher & DeLisa, 2008). It was decided to clone the fusion under the expression control of two different promoters,

whereby the utilisation of the native promoter results in expression levels similar to the wild-type levels, while the inducible promoter allows expression levels to be varied in a controlled manner. In addition, the utilisation of an amino acid linker was explored. As an alternative to the direct fusion between GFP_{P7} and $LtaS_{S218P}$ an EAAAK linker repeated three times was used. This linker region increases the distance between the two proteins, and consequently increases the stability of the protein as well as the possibility of it being functional. Furthermore, it was shown previously that two functional proteins separated by this linker region had reduced interference with each other (Arai *et al.*, 2001).

These choices were made based on previous LtaS-GFP fusions constructed in our laboratory that showed very high cytoplasmic fluorescence and high levels of protein degradation and cleavage (Reichmann *et al*., unpublished results). While these full-length fusion proteins were detected by western blot analysis (Figure 10), there was still some cytoplasmic fluorescence signal (Figure 11), probably due to protein degradation. Furthermore, none of the constructed fusions were fully functional, because they did not result in wild-type production of LTA (Figure 10). Despite this, it is possible to see an accumulation of GFP_{P7}-$LtaS_{S218P}$ at the septum (Figure 11), indicating that LtaS possibly localises at the cell division site, and that the PGP backbone chain of LTA is mainly produced at the division site in *S. aureus*. Although these are just preliminary results, this supports the proposal of a role of LtaS in cell division. Apart from optimising the growth conditions for the microscopy experiment, it would also be of interest to study the timing of LtaS localisation during the cell cycle, in particular whether localisation occurs at an early stage during the division process or only at a late stage. For this, co-localisation studies with known early and late stage proteins such as EzrA and PBP4, respectively, would provide further information about the role of this protein during cell division. Additionally, it would be of interest to study localisation of the remaining proteins involved in LTA synthesis in *S. aureus*, including the proteins responsible the glycolipid anchor synthesis and of the DltABCD proteins that are responsible for D-alanylation, and how these different processes in LTA synthesis correlate with each other.

In conclusion, these data indicated that LtaS seems to localise at the cell division site in *S. aureus*. However it should be noted that even if new LTA is only synthesised

at the cell division, previous studies using immune electron microscopy indicate that LTA in *S. aureus* is distributed throughout the membrane (Aasjord & Grov, 1980). In addition, Matias & Beveridge identified a possible periplasmic space in *S. aureus* (Matias & Beveridge, 2006), and based on "mathematical analysis" this brings into question whether or not the PGP chain of LTA protrudes through the cell wall, as depicted in most papers.

The second overall aim of this study was to elucidate how LTA synthesis is regulated, by studying how LtaS production is regulated and how LTA and LtaS production is affected under stress conditions.

It was previously found in our laboratory that in two *S. aureus* strains, RN4220 and Newman, *ltaS* has two transcriptional start sites located 408 bp (P1 promoter) and 294 bp (P2 promoter) in front of the translation start site (Gründling, unpublished results). These findings are interesting not only because of the presence of two promoters, but also because the second promoter, at 294 bp distance from *ltaS* initiation codon, is still located very far away from the transcriptional start site, resulting in a long UTR. The UTR is a non-translated region, in this case upstream of the initiation codon (5'UTR or mRNA leader) that contains important regulatory elements (Papenfort & Vogel, 2010). Using a deep sequencing-based approach, Irnov and colleagues showed that the leader region length in *B. subtilis* is in average 35 nt long and the authors suggest that a likely explanation for a long 5' mRNA leader region is due to an inclusion of a *cis*-acting regulatory RNA (Irnov *et al.*, 2010). Since the *ltaS* UTR is much longer than the average 35 nt, transcriptional regulation may occur for this gene. However, using a bioinformatic approach it was not possible to identify any relevant RNA secondary structures, indicating that there may be another regulatory system involved. In order to study the relevance of both promoters and of the long UTR, different fragments from these regions were cloned upstream of the reporter gene *lacZ* (Figure 13A), which enabled the identification of the fragments able to activate expression, based on β-galactosidase activity. From the first set of fusions it was possible to see that upon removing the region upstream of the P1 promoter and the P1 promoter itself, there are still high levels of expression (Figure 13B), which indicated that under this experimental conditions the P1 promoter is not needed for expression.

Furthermore, no activity was detected following removal of P2 (Figure 13B), indicating that this promoter is essential for *ltaS* expression.

In order to confirm the relevance of the P2 promoter and investigate the possible function for the region between this promoter and the translation start site, further fusions to the *lacZ* gene were constructed (Figure 14A). The results confirmed that when *ltaS* is only under the control of the P1 promoter, there is no expression (Figure 14B). Furthermore, mutating the P2 promoter specifically indicated that there is no expression in its absence and this points to a scenario where the P2 promoter is not only sufficient, but also necessary for expression. However, these results do not give any information about the role of the P1 promoter, which seems to be irrelevant for expression under these conditions. Lastly, by removing the region between the P2 promoter and the *ltaS* initiation codon, it was possible to see that *lacZ* expression was not affected. These results pose two questions: why is the P1 promoter present if is not necessary for expression and why is there a large distance between the active promoter, P2, and *ltaS* initiation codon, which, as mentioned above, is rarely found. One explanation for the region between the -294 bp and the initiation codon could be the existence of a second open reading frame (ORF) similar to what was identified in the large UTR region of the *dlt* operon (Koprivnjak *et al.*, 2006), but none have been identified using bioinformatic prediction programmes.

For these assays *ltaS* expression was only evaluated when cells were in the exponential growth phase but these two regions in the UTR may have important roles in activation and/or repression of expression during different phases of growth. As shown above, LtaS seems to localise at the septum indicating a role in cell division and during exponential growth, cell division occurs most rapidly, which may affect *ltaS* expression levels during this phase. Therefore, it could be of interest to evaluate β-galactosidase activity of these fusions during different growth phases (lag phase, early exponential phase, mid-exponential phase, late exponential phase and stationary phase, for example) and in different conditions such as pH, salt concentration and temperature in order to look for a possible role for the P1 promoter and the region between the P2 promoter and the initiation codon at different phases and conditions. Additionally, it could also be of interest to look for possible *trans*-acting regulator factors like DNA or RNA binding proteins that may need a large region to bind to, justifying the large UTR found

upstream of *ltaS*. The possibility of factors being involved in up or down regulation of this gene could be further investigated performing a transposon mutant screen. The *ltaS* full-length promoter *lacZ* fusion could be used to perform this screen in order to identify factors up or down regulating *ltaS* through visual selection on plates containing the chromogenic 5-bromo-4-chloro-3-indolyl-β-D-galactopyranoside (X-gal).

In conclusion, the presence of two promoters upstream of *ltaS* was identified and only the promoter closer to the initiation codon is necessary and sufficient for expression. The large region between the active promoter and the initiation codon is not necessary to activate expression during exponential phase and so far no role for this region has been identified.

Lastly, osmolarity is an important factor for pathogenic bacteria, since differences between external and host associated environments, as well as between different environments within the host, are associated with variations in expression of virulence factors (Chowdhury *et al.*, 1996). Since LTA is important for virulence in *S. aureus*, its production under different osmolarity conditions and how this affects growth was assessed by performing growth curves using LB media containing 0% to 6% NaCl and western blot analysis to detect LTA and full-length LtaS under these conditions in the exponential growth phase. To assess the effect of varying levels of LtaS, both wild-type and inducible *ltaS* strains were used, where it is known that even in the presence of the inducer, the inducible strains produce reduced amounts of LTA (Wörmann *et al.*, 2011b). These experiments were intended to evaluate the importance of this polymer under high or low osmolarity conditions. It was observed that *S. aureus* growth rate is reduced under high osmolarity in both wild-type and inducible *ltaS* strains with inducer, however the effect was more accentuated in the inducible strains (Figure 15). This was observed in both the laboratory *S. aureus* strain RN4220 and in the MRSA strain LAC*. This result could be due to altered LTA levels, consequently having an impact on growth under high osmolarity conditions, and so LTA production was assessed by western blot analysis. The results obtained indicated that LTA production is reduced both in the wild-type and in the inducible *ltaS* strains with inducer when the salt concentration increases and the effect is again more accentuated for the inducible strains (Figure 16A). This analysis identified differences between the two *S. aureus* strains

used: while the wild-type RN4220 strain has wild-type levels of LTA when grown with 5% NaCl, the wild-type LAC* strain showed a decrease in LTA production from 2 to 3% NaCl, but the growth rate is only reduced at 5% NaCl. This suggests that LTA production does not correlate with growth reduction in the strain LAC*.

In order to determine whether the decrease in LTA synthesis was due to a decrease in LtaS production, full-length LtaS production was assessed by western blot. This demonstrated that expression of *ltaS* from the *spac* promoter was comparable to the wild-type strain in both RN4220 and LAC* strains. These results also showed that with the increase in salt concentration, full-length LtaS was produced at constant levels for both the wild-type and the inducible *ltaS* strains with inducer (Figure 16B), which also excludes the possibility that expression from the *spac* promoter was affected by the increase in salt concentration. Given that LtaS expression remains constant while LTA production is reduced, may indicates that there is a decrease in the enzymatic activity of the LtaS protein due to an increase in salt concentration, and LTA stability itself may be altered under these conditions.

These results suggest that LTA production and growth are both affected at high salt concentrations, while LtaS remains unaffected, indicating that this polymer is important to protect cells under high osmolarity conditions. However, this is not in accordance with previous data, where it has been shown that at 37°C LTA negative strains can only grow under high osmolarity conditions (7.5% NaCl or 40% sucrose) suggesting that LTA is more important under low osmolarity conditions (Oku *et al.*, 2009). Nevertheless it is important to note that this LTA negative mutant was not fully sequenced and it is known that suppressor mutations can change the need for LTA to be present (Corrigan *et al.*, 2011), which may affect the conclusions drawn from the phenotypic analysis of Oku and colleagues. In order to test if LTA it is indeed important as an osmoprotectant under low osmolarity conditions the inducible *ltaS* strain could be subjected to an osmotic down shock and the effect in cell death analysed through the live/dead assay referred above. Since the inducible strains even with inducer are known to produce less LtaS than the wild-type strains (Wörmann *et al.*, 2011b), an osmotic down shock could cause an increase in the number of dead cells comparing with the wild-type strains because reduced amounts of LTA would make cells more susceptible to the osmotic shock. An alternative possibility is that these observations are not due to

an osmotic effect, but instead due to an increase in ion concentrations since there are more Na^+ and Cl^- ions in solution. This could be assessed by performing similar assays using a range of sugar concentrations (sucrose, for example) instead of salt concentrations to distinguish between an osmotic or ionic effect.

In conclusion, it was possible to observe that an increase in NaCl alters the growth of *S. aureus* and also LTA production, but not LtaS production. However, whether these observations are due to an osmotic or ionic effect remains unknown.

This study aimed to give further insights into the roles of LTA and how LTA production is regulated under normal growth and stress conditions in *S. aureus*. It was possible to experimentally confirm that LTA is necessary for the efficient incorporation of D-alanine residues into WTA, which interconnects the roles of these two polymers closely related with their decoration with D-alanine residues. Furthermore, the absence of LTA was shown to be lethal resulting in cell membrane depolarisation. LtaS, essential for LTA synthesis, was suggested to localise in the cell site division. These results confirm that LTA might be a good target for new antimicrobials and highlight the multitude of processes for which LTA is important in the cell. Regarding LTA regulation, through transcriptional analysis it was shown that there are two promoters for *ltaS* expression and a large upstream UTR region, and although only one promoter was shown to be essential and sufficient for transcription, there is still the possibility that the other promoter is important under different conditions. Changes in NaCl concentration in the media seems to have an effect on LTA production, but not on LtaS synthesis, which may indicate an altered enzymatic activity of LtaS caused either by an osmotic or ionic effect. Once further elucidated the way LTA production can be affected, these can be used as new factors to arrest *S. aureus* growth.

5. Bibliographic references

Aasjord, P. & Grov, A. (1980). Immunoperoxidase and Electron-Microscopy Studies of Staphylococcal Lipoteichoic Acid. *Acta Path Micro Im B* **88**, 47-52.

Arai, R., Ueda, H., Kitayama, A., Kamiya, N. & Nagamune, T. (2001). Design of the linkers which effectively separate domains of a bifunctional fusion protein. *Protein Eng* **14**, 529-532.

Archibald, A. R. & Baddiley, J. (1966). The teichoic acids. *Adv Carbohydr Chem Biochem* **21**, 323-375.

Archibald, A. R., Baddiley, J. & Button, D. (1968). The membrane teichoic acid of *Staphylococcus lactis* I3. *Biochem J* **110**, 559-563.

Baddiley, J. & Neuhaus, F. C. (1960). The enzymic activation of D-alanine. *Biochem J* **75**, 579-587.

Badurina, D. S., Zolli-Juran, M. & Brown, E. D. (2003). CTP:glycerol 3-phosphate cytidylyltransferase (TarD) from *Staphylococcus aureus* catalyzes the cytidylyl transfer via an ordered Bi-Bi reaction mechanism with micromolar K(m) values. *Biochim Biophys Acta* **1646**, 196-206.

Barber, M. & Rozwadowska-Dowzenko, M. (1948). Infection by penicillin-resistant staphylococci. *Lancet* **2**, 641-644.

Barreteau, H., Kovac, A., Boniface, A., Sova, M., Gobec, S. & Blanot, D. (2008). Cytoplasmic steps of peptidoglycan biosynthesis. *FEMS Microbiol Rev* **32**, 168-207.

Beck, W. D., Berger-Bachi, B. & Kayser, F. H. (1986). Additional DNA in methicillin-resistant *Staphylococcus aureus* and molecular cloning of *mec*-specific DNA. *J Bacteriol* **165**, 373-378.

Bera, A., Biswas, R., Herbert, S., Kulauzovic, E., Weidenmaier, C., Peschel, A. & Gotz, F. (2007). Influence of wall teichoic acid on lysozyme resistance in *Staphylococcus aureus*. *J Bacteriol* **189**, 280-283.

Berger-Bachi, B. & Tschierske, M. (1998). Role of fem factors in methicillin resistance. *Drug Resist Updat* **1**, 325-335.

Bernal, P., Zloh, M. & Taylor, P. W. (2009). Disruption of D-alanyl esterification of *Staphylococcus aureus* cell wall teichoic acid by the β-lactam resistance modifier (-)-epicatechin gallate. *J Antimicrob Chemother* **63**, 1156-1162.

Bertram, K. C., Hancock, I. C. & Baddiley, J. (1981). Synthesis of teichoic acid by *Bacillus subtilis* protoplasts. *J Bacteriol* **148**, 406-412.

Boles, B. R., Thoendel, M., Roth, A. J. & Horswill, A. R. (2010). Identification of genes involved in polysaccharide-independent *Staphylococcus aureus* biofilm formation. *PLoS One* **5**, e10146.

Bondi, A., Jr. & Dietz, C. C. (1945). Penicillin resistant staphylococci. *Proc Soc Exp Biol Med* **60**, 55-58.

Boyd, D. A., Cvitkovitch, D. G., Bleiweis, A. S., Kiriukhin, M. Y., Debabov, D. V., Neuhaus, F. C. & Hamilton, I. R. (2000). Defects in D-alanyl-lipoteichoic acid synthesis in *Streptococcus mutans* results in acid sensitivity. *J Bacteriol* **182**, 6055-6065.

Brown, S., Zhang, Y. H. & Walker, S. (2008). A revised pathway proposed for *Staphylococcus aureus* wall teichoic acid biosynthesis based on in vitro reconstitution of the intracellular steps. *Chem Biol* **15**, 12-21.

Brown, S., Xia, G., Luhachack, L. G. & other authors (2012). Methicillin resistance in *Staphylococcus aureus* requires glycosylated wall teichoic acids. *Proc Natl Acad Sci U S A* **109**, 18909-18914.

Bruins, M. J., Juffer, P., Wolfhagen, M. J. & Ruijs, G. J. (2007). Salt tolerance of methicillin-resistant and methicillin-susceptible *Staphylococcus aureus*. *J Clin Microbiol* **45**, 682-683.

Chambers, H. F. (2003). Solving staphylococcal resistance to beta-lactams. *Trends Microbiol* **11**, 145-148.

Childs, W. C., Taron, D. J. & Neuhaus, F. C. (1985). Biosynthesis of D-alanyl-lipoteichoic acid by *Lactobacillus casei:* interchain transacylation of D-alanyl ester residues. *J Bacteriol* **162**, 1191-1195.

Chowdhury, R., Sahu, G. K. & Das, J. (1996). Stress response in pathogenic bacteria. *J Bioscience* **21**, 149-160.

Collins, L. V., Kristian, S. A., Weidenmaier, C., Faigle, M., Van Kessel, K. P., Van Strijp, J. A., Götz, F., Neumeister, B. & Peschel, A. (2002). *Staphylococcus aureus* strains lacking D-alanine modifications of teichoic acids are highly susceptible to human neutrophil killing and are virulence attenuated in mice. *J Infect Dis* **186**, 214-219.

Cormack, B. P., Valdivia, R. H. & Falkow, S. (1996). FACS-optimized mutants of the green fluorescent protein (GFP). *Gene* **173**, 33-38.

Corrigan, R. M., Abbott, J. C., Burhenne, H., Kaever, V. & Gründling, A. (2011). c-di-AMP is a new second messenger in *Staphylococcus aureus* with a role in controlling cell size and envelope stress. *PLoS Pathog* **7**, e1002217.

Corrigan, R. M., Campeotto, I., Jeganathan, T., Roelofs, K. G., Lee, V. T. & Gründling, A. (2013). Systematic identification of conserved bacterial c-di-AMP receptor proteins. *Proc Natl Acad Sci U S A* **110**, 9084-9089.

D'Elia, M. A., Millar, K. E., Beveridge, T. J. & Brown, E. D. (2006). Wall teichoic acid polymers are dispensable for cell viability in *Bacillus subtilis*. *J Bacteriol* **188**, 8313-8316.

de Jonge, B. L., Chang, Y. S., Gage, D. & Tomasz, A. (1992). Peptidoglycan composition of a highly methicillin-resistant *Staphylococcus aureus* strain. The role of penicillin binding protein 2A. *J Biol Chem* **267**, 11248-11254.

Doran, K. S., Engelson, E. J., Khosravi, A. & other authors (2005). Blood-brain barrier invasion by group B *Streptococcus* depends upon proper cell-surface anchoring of lipoteichoic acid. *The Journal of clinical investigation* **115**, 2499-2507.

Du, L., He, Y. & Luo, Y. (2008). Crystal structure and enantiomer selection by D-alanyl carrier protein ligase DltA from *Bacillus cereus*. *Biochemistry* **47**, 11473-11480.

Fabretti, F., Theilacker, C., Baldassarri, L., Kaczynski, Z., Kropec, A., Holst, O. & Huebner, J. (2006). Alanine esters of enterococcal lipoteichoic acid play a role in biofilm formation and resistance to antimicrobial peptides. *Infect Immun* **74**, 4164-4171.

Fedtke, I., Mader, D., Kohler, T. & other authors (2007). A *Staphylococcus aureus* ypfP mutant with strongly reduced lipoteichoic acid (LTA) content: LTA governs bacterial surface properties and autolysin activity. *Mol Microbiol* **65**, 1078-1091.

Fey, P. D., Said-Salim, B., Rupp, M. E., Hinrichs, S. H., Boxrud, D. J., Davis, C. C., Kreiswirth, B. N. & Schlievert, P. M. (2003). Comparative molecular analysis of community- or hospital-acquired methicillin-resistant *Staphylococcus aureus*. *Antimicrob Agents Chemother* **47**, 196-203.

Fischer, W., Rösel, P. & Koch, H. U. (1981). Effect of alanine ester substitution and other structural features of lipoteichoic acids on their inhibitory activity against autolysins of *Staphylococcus aureus*. *J Bacteriol* **146**, 467-475.

Fischer, W. (1988). Physiology of Lipoteichoic Acids in Bacteria. *Adv Microb Physiol* **29**, 233-302.

Fischer, W. (1994). Lipoteichoic Acid and Lipids in the Membrane of *Staphylococcus aureus*. *Med Microbiol Immun* **183**, 61-76.

Fisher, A. C. & DeLisa, M. P. (2008). Laboratory evolution of fast-folding green fluorescent protein using secretory pathway quality control. *PLoS One* **3**, e2351.

Foster, T. J. (2005). Immune evasion by Staphylococci. *Nat Rev Microbiol* **3**, 948-958.

Fournier, J. M., Vann, W. F. & Karakawa, W. W. (1984). Purification and characterization of *Staphylococcus aureus* type 8 capsular polysaccharide. *Infect Immun* **45**, 87-93.

Fournier, J. M., Hannon, K., Moreau, M., Karakawa, W. W. & Vann, W. F. (1987). Isolation of type 5 capsular polysaccharide from *Staphylococcus aureus*. *Ann Inst Pasteur Microbiol* **138**, 561-567.

Fuda, C. C., Fisher, J. F. & Mobashery, S. (2005). Beta-lactam resistance in *Staphylococcus aureus*: the adaptive resistance of a plastic genome. *Cell Mol Life Sci* **62**, 2617-2633.

Ghuysen, J. M. & Strominger, J. L. (1963). Structure of the Cell Wall of *Staphylococcus Aureus*, Strain Copenhagen I. Preparation of Fragments by Enzymatic Hydrolysis. *Biochemistry* **2**, 1110-1119.

Gotz, F., Bannerman, T. & Schleifer, K. H. (2006). The Genera *Staphylococcus* and *Macrococcus*. *Prokaryotes: A Handbook on the Biology of Bacteria, Vol 4, Third Edition*, 5-75.

Gross, M., Cramton, S. E., Götz, F. & Peschel, A. (2001). Key role of teichoic acid net charge in *Staphylococcus aureus* colonization of artificial surfaces. *Infect Immun* **69**, 3423-3426.

Gründling, A. & Schneewind, O. (2007a). Genes required for glycolipid synthesis and lipoteichoic acid anchoring in Staphylococcus aureus. *J Bacteriol* **189**, 2521-2530.

Gründling, A. & Schneewind, O. (2007b). Synthesis of glycerol phosphate lipoteichoic acid in *Staphylococcus aureus*. *Proc Natl Acad Sci U S A* **104**, 8478-8483.

Haas, R., Koch, H. U. & Fischer, W. (1984). Alanyl Turnover from Lipoteichoic Acid to Teichoic Acid in *Staphylococcus aureus*. *FEMS Microbiol Lett* **21**, 27-31.

Hartman, B. J. & Tomasz, A. (1984). Low-affinity penicillin-binding protein associated with beta-lactam resistance in *Staphylococcus aureus*. *J Bacteriol* **158**, 513-516.

Heaton, M. P. & Neuhaus, F. C. (1994). Role of the D-alanyl carrier protein in the biosynthesis of D-alanyl-lipoteichoic acid. *J Bacteriol* **176**, 681-690.

Heptinstall, S., Archibald, A. R. & Baddiley, J. (1970). Teichoic acids and membrane function in bacteria. *Nature* **225**, 519-521.

Herbert, S., Newell, S. W., Lee, C., Wieland, K. P., Dassy, B., Fournier, J. M., Wolz, C. & Doring, G. (2001). Regulation of *Staphylococcus aureus* type 5 and type 8 capsular polysaccharides by CO_2. *J Bacteriol* **183**, 4609-4613.

Hochkeppel, H. K., Braun, D. G., Vischer, W. & other authors (1987). Serotyping and electron microscopy studies of *Staphylococcus aureus* clinical isolates with monoclonal antibodies to capsular polysaccharide types 5 and 8. *J Clin Microbiol* **25**, 526-530.

Hofmann, K. (2000). A superfamily of membrane-bound O-acyltransferases with implications for Wnt signaling. *Trends Biochem Sci* **25**, 111-112.

Hughes, A. H., Hancock, I. C. & Baddiley, J. (1973). The function of teichoic acids in cation control in bacterial membranes. *Biochem J* **132**, 83-93.

Irnov, I., Sharma, C. M., Vogel, J. & Winkler, W. C. (2010). Identification of regulatory RNAs in *Bacillus subtilis*. *Nucleic Acids Res* **38**, 6637-6651.

Jorasch, P., Wolter, F. P., Zahringer, U. & Heinz, E. (1998). A UDP glucosyltransferase from *Bacillus subtilis* successively transfers up to four glucose residues to 1,2-diacylglycerol: expression of ypfP in *Escherichia coli* and structural analysis of its reaction products. *Mol Microbiol* **29**, 419-430.

Karatsa-Dodgson, M., Wörmann, M. E. & Gründling, A. (2010). In vitro analysis of the *Staphylococcus aureus* lipoteichoic acid synthase enzyme using fluorescently labeled lipids. *J Bacteriol* **192**, 5341-5349.

Kiriukhin, M. Y., Debabov, D. V., Shinabarger, D. L. & Neuhaus, F. C. (2001). Biosynthesis of the glycolipid anchor in lipoteichoic acid of *Staphylococcus aureus* RN4220: role of YpfP, the diglucosyldiacylglycerol synthase. *J Bacteriol* **183**, 3506-3514.

Koch, H. U., Haas, R. & Fischer, W. (1984). The role of lipoteichoic acid biosynthesis in membrane lipid metabolism of growing *Staphylococcus aureus*. *Eur J Biochem* **138**, 357-363.

Koch, H. U., Doker, R. & Fischer, W. (1985). Maintenance of D-alanine ester substitution of lipoteichoic acid by reesterification in *Staphylococcus aureus*. *J Bacteriol* **164**, 1211-1217.

Kohler, T., Weidenmaier, C. & Peschel, A. (2009). Wall teichoic acid protects *Staphylococcus aureus* against antimicrobial fatty acids from human skin. *J Bacteriol* **191**, 4482-4484.

Kopp, U., Roos, M., Wecke, J. & Labischinski, H. (1996). Staphylococcal peptidoglycan interpeptide bridge biosynthesis: a novel antistaphylococcal target? *Microb Drug Resist* **2**, 29-41.

Koprivnjak, T., Mlakar, V., Swanson, L., Fournier, B., Peschel, A. & Weiss, J. P. (2006). Cation-induced transcriptional regulation of the dlt operon of *Staphylococcus aureus*. *J Bacteriol* **188**, 3622-3630.

Kovács, M., Halfmann, A., Fedtke, I., Heintz, M., Peschel, A., Vollmer, W., Hakenbeck, R. & Brückner, R. (2006). A functional *dlt* operon, encoding proteins required for incorporation of D-alanine in teichoic acids in gram-positive bacteria, confers resistance to cationic antimicrobial peptides in *Streptococcus pneumoniae*. *J Bacteriol* **188**, 5797-5805.

Kramer, N. E., Hasper, H. E., van den Bogaard, P. T. & other authors (2008). Increased D-alanylation of lipoteichoic acid and a thickened septum are main determinants in the nisin resistance mechanism of *Lactococcus lactis*. *Microbiol* **154**, 1755-1762.

Kreiswirth, B. N., Lofdahl, S., Betley, M. J., Oreilly, M., Schlievert, P. M., Bergdoll, M. S. & Novick, R. P. (1983). The Toxic Shock Syndrome Exotoxin Structural Gene Is Not Detectably Transmitted by a Prophage. *Nature* **305**, 709-712.

Kristian, S. A., Datta, V., Weidenmaier, C., Kansal, R., Fedtke, I., Peschel, A., Gallo, R. L. & Nizet, V. (2005). D-alanylation of teichoic acids promotes group a *streptococcus* antimicrobial peptide resistance, neutrophil survival, and epithelial cell invasion. *J Bacteriol* **187**, 6719-6725.

Lazarevic, V., Soldo, B., Medico, N., Pooley, H., Bron, S. & Karamata, D. (2005). *Bacillus subtilis* alpha-phosphoglucomutase is required for normal cell morphology and biofilm formation. *Appl Environ Microbiol* **71**, 39-45.

Lee, C. Y., Buranen, S. L. & Ye, Z. H. (1991). Construction of single-copy integration vectors for *Staphylococcus aureus*. *Gene* **103**, 101-105.

Lee, J. C., Takeda, S., Livolsi, P. J. & Paoletti, L. C. (1993). Effects of in vitro and in vivo growth conditions on expression of type 8 capsular polysaccharide by *Staphylococcus aureus*. *Infect Immun* **61**, 1853-1858.

Li, M., Rigby, K., Lai, Y., Nair, V., Peschel, A., Schittek, B. & Otto, M. (2009). *Staphylococcus aureus* mutant screen reveals interaction of the human antimicrobial peptide dermcidin with membrane phospholipids. *Antimicrob Agents Chemother* **53**, 4200-4210.

Liu, G. Y., Essex, A., Buchanan, J. T., Datta, V., Hoffman, H. M., Bastian, J. F., Fierer, J. & Nizet, V. (2005). *Staphylococcus aureus* golden pigment impairs

neutrophil killing and promotes virulence through its antioxidant activity. *J Exp Med* **202**, 209-215.

Lowy, F. D. (2003). Antimicrobial resistance: the example of *Staphylococcus aureus*. *J Clin Invest* **111**, 1265-1273.

Lu, D., Wormann, M. E., Zhang, X. D., Schneewind, O., Grundling, A. & Freemont, P. S. (2009). Structure-based mechanism of lipoteichoic acid synthesis by *Staphylococcus aureus* LtaS. *Proc Natl Acad Sci U S A* **106**, 1584-1589.

Lu, M. & Kleckner, N. (1994). Molecular cloning and characterization of the *pgm* gene encoding phosphoglucomutase of *Escherichia coli*. *J Bacteriol* **176**, 5847-5851.

Matias, V. R. & Beveridge, T. J. (2005). Cryo-electron microscopy reveals native polymeric cell wall structure in *Bacillus subtilis* 168 and the existence of a periplasmic space. *Mol Microbiol* **56**, 240-251.

Matias, V. R. & Beveridge, T. J. (2006). Native cell wall organization shown by cryo-electron microscopy confirms the existence of a periplasmic space in *Staphylococcus aureus*. *J Bacteriol* **188**, 1011-1021.

Matias, V. R. & Beveridge, T. J. (2008). Lipoteichoic acid is a major component of the *Bacillus subtilis* periplasm. *J Bacteriol* **190**, 7414-7418.

McCormick, N. E., Halperin, S. A. & Lee, S. F. (2011). Regulation of D-alanylation of lipoteichoic acid in *Streptococcus gordonii*. *Microbiol* **157**, 2248-2256.

Memmi, G., Filipe, S. R., Pinho, M. G., Fu, Z. & Cheung, A. (2008). *Staphylococcus aureus* PBP4 is essential for beta-lactam resistance in community-acquired methicillin-resistant strains. *Antimicrob Agents Chemother* **52**, 3955-3966.

Meredith, T. C., Swoboda, J. G. & Walker, S. (2008). Late-stage polyribitol phosphate wall teichoic acid biosynthesis in *Staphylococcus aureus*. *J Bacteriol* **190**, 3046-3056.

Navarre, W. W. & Schneewind, O. (1999). Surface proteins of gram-positive bacteria and mechanisms of their targeting to the cell wall envelope. *Microbiol Mol Biol R* **63**, 174-229.

Neuhaus, F. C., Heaton, M. P., Debabov, D. V. & Zhang, Q. (1996). The *dlt* operon in the biosynthesis of D-alanyl-lipoteichoic acid in *Lactobacillus casei*. *Microb Drug Resist* **2**, 77-84.

Neuhaus, F. C. & Baddiley, J. (2003). A continuum of anionic charge: Structures and functions of D-Alanyl-Teichoic acids in gram-positive bacteria. *Microbiol Mol Biol R* **67**, 686-723.

Novitsky, T. J., Chan, M., Himes, R. H. & Akagi, J. M. (1974). Effect of temperature on the growth and cell wall chemistry of a facultative thermophilic *Bacillus*. *J Bacteriol* **117**, 858-865.

O'Riordan, K. & Lee, J. C. (2004). *Staphylococcus aureus* capsular polysaccharides. *Clinical microbiology reviews* **17**, 218-234.

Oku, Y., Kurokawa, K., Matsuo, M., Yamada, S., Lee, B. L. & Sekimizu, K. (2009). Pleiotropic roles of polyglycerolphosphate synthase of lipoteichoic acid in growth of *Staphylococcus aureus* cells. *J Bacteriol* **191**, 141-151.

Okuma, K., Iwakawa, K., Turnidge, J. D. & other authors (2002). Dissemination of new methicillin-resistant *Staphylococcus aureus* clones in the community. *J Clin Microbiol* **40**, 4289-4294.

Osman, K. T., Du, L., He, Y. & Luo, Y. (2009). Crystal structure of *Bacillus cereus* D-alanyl carrier protein ligase (DltA) in complex with ATP. *J Mol Biol* **388**, 345-355.

Pantucek, R., Doskar, J., Ruzickova, V., Kasparek, P., Oracova, E., Kvardova, V. & Rosypal, S. (2004). Identification of bacteriophage types and their carriage in *Staphylococcus aureus*. *Arch Virol* **149**, 1689-1703.

Papenfort, K. & Vogel, J. (2010). Regulatory RNA in bacterial pathogens. *Cell Host Microbe* **8**, 116-127.

Perego, M., Glaser, P., Minutello, A., Strauch, M. A., Leopold, K. & Fischer, W. (1995). Incorporation of D-alanine into lipoteichoic acid and wall teichoic acid in *Bacillus subtilis*. Identification of genes and regulation. *J Biol Chem* **270**, 15598-15606.

Pereira, S. F., Henriques, A. O., Pinho, M. G., de Lencastre, H. & Tomasz, A. (2009). Evidence for a dual role of PBP1 in the cell division and cell separation of *Staphylococcus aureus*. *Mol Microbiol* **72**, 895-904.

Peschel, A., Otto, M., Jack, R. W., Kalbacher, H., Jung, G. & Götz, F. (1999). Inactivation of the *dlt* operon in *Staphylococcus aureus* confers sensitivity to defensins, protegrins, and other antimicrobial peptides. *J Biol Chem* **274**, 8405-8410.

Pinho, M. G., de Lencastre, H. & Tomasz, A. (2001). An acquired and a native penicillin-binding protein cooperate in building the cell wall of drug-resistant staphylococci. *Proc Natl Acad Sci U S A* **98**, 10886-10891.

Pinho, M. G. & Errington, J. (2005). Recruitment of penicillin-binding protein PBP2 to the division site of *Staphylococcus aureus* is dependent on its transpeptidation substrates. *Mol Microbiol* **55**, 799-807.

Pooley, H. M., Paschoud, D. & Karamata, D. (1987). The *gtaB* marker in *Bacillus subtilis* 168 is associated with a deficiency in UDPglucose pyrophosphorylase. *J Gen Microbiol* **133**, 3481-3493.

Poutrel, B., Gilbert, F. B. & Lebrun, M. (1995). Effects of culture conditions on production of type 5 capsular polysaccharide by human and bovine *Staphylococcus aureus* strains. *Clin Diagn Lab Immunol* **2**, 166-171.

Poyart, C., Lamy, M. C., Boumaila, C., Fiedler, F. & Trieu-Cuot, P. (2001). Regulation of D-alanyl-lipoteichoic acid biosynthesis in *Streptococcus agalactiae* involves a novel two-component regulatory system. *J Bacteriol* **183**, 6324-6334.

Poyart, C., Pellegrini, E., Marceau, M., Baptista, M., Jaubert, F., Lamy, M. C. & Trieu-Cuot, P. (2003). Attenuated virulence of *Streptococcus agalactiae* deficient in D-alanyl-lipoteichoic acid is due to an increased susceptibility to defensins and phagocytic cells. *Mol Microbiol* **49**, 1615-1625.

Reichmann, N. T. & Gründling, A. (2011). Location, synthesis and function of glycolipids and polyglycerolphosphate lipoteichoic acid in Gram-positive bacteria of the phylum Firmicutes. *FEMS Microbiol Lett* **319**, 97-105.

Reichmann, N. T., Picarra Cassona, C. & Gründling, A. (2013). Revised mechanism of D-alanine incorporation into cell wall polymers in Gram-positive bacteria. *Microbiology* **159**, 1868-1877.

Richter, S. G., Elli, D., Kim, H. K., Hendrickx, A. P., Sorg, J. A., Schneewind, O. & Missiakas, D. (2013). Small molecule inhibitor of lipoteichoic acid synthesis is an antibiotic for Gram-positive bacteria. *Proc Natl Acad Sci U S A* **110**, 3531-3536.

Roghmann, M., Taylor, K. L., Gupte, A., Zhan, M., Johnson, J. A., Cross, A., Edelman, R. & Fattom, A. I. (2005). Epidemiology of capsular and surface polysaccharide in *Staphylococcus aureus* infections complicated by bacteraemia. *J Hosp Infect* **59**, 27-32.

Rowland, S. J. & Dyke, K. G. H. (1989). Characterization of the Staphylococcal Beta-Lactamase Transposon Tn552. *Embo Journal* **8**, 2761-2773.

Sanderson, A. R., Strominger, J. L. & Nathenson, S. G. (1962). Chemical structure of teichoic acid from *Staphylococcus aureus*, strain Copenhagen. *J Biol Chem* **237**, 3603-3613.

Sau, S., Bhasin, N., Wann, E. R., Lee, J. C., Foster, T. J. & Lee, C. Y. (1997). The *Staphylococcus aureus* allelic genetic loci for serotype 5 and 8 capsule expression contain the type-specific genes flanked by common genes. *Microbiology* **143 (Pt 7)**, 2395-2405.

Sauvage, E., Kerff, F., Terrak, M., Ayala, J. A. & Charlier, P. (2008). The penicillin-binding proteins: structure and role in peptidoglycan biosynthesis. *FEMS Microbiol Rev* **32**, 234-258.

Scheffers, D. J. & Pinho, M. G. (2005). Bacterial cell wall synthesis: new insights from localization studies. *Microbiol Mol Biol Rev* **69**, 585-607.

Schirner, K., Marles-Wright, J., Lewis, R. J. & Errington, J. (2009). Distinct and essential morphogenic functions for wall- and lipo-teichoic acids in *Bacillus subtilis*. *Embo J* **28**, 830-842.

Scott, J. R. & Barnett, T. C. (2006). Surface proteins of gram-positive bacteria and how they get there. *Annu Rev Microbiol* **60**, 397-423.

Sheen, T. R., Ebrahimi, C. M., Hiemstra, I. H., Barlow, S. B., Peschel, A. & Doran, K. S. (2010). Penetration of the blood-brain barrier by *Staphylococcus aureus*: contribution of membrane-anchored lipoteichoic acid. *J Mol Med (Berl)* **88**, 633-639.

Showsh, S. A., De Boever, E. H. & Clewell, D. B. (2001). Vancomycin resistance plasmid in *Enterococcus faecalis* that encodes sensitivity to a sex pheromone also produced by *Staphylococcus aureus*. *Antimicrob Agents Chemother* **45**, 2177-2178.

Sieradzki, K. & Tomasz, A. (1999). Gradual alterations in cell wall structure and metabolism in vancomycin-resistant mutants of *Staphylococcus aureus*. *J Bacteriol* **181**, 7566-7570.

Silhavy, T. J., Kahne, D. & Walker, S. (2010). The Bacterial Cell Envelope. *Csh Perspect Biol* **2**, 1-16.

Sip, M., Herman, P., Plasek, J. & Hrouda, V. (1990). Transmembrane Potential Measurement with Carbocyanine Dye Dis-C3-(5) - Fast Fluorescence Decay Studies. *J Photoch Photobio B* **4**, 321-328.

Sompolinsky, D., Samra, Z., Karakawa, W. W., Vann, W. F., Schneerson, R. & Malik, Z. (1985). Encapsulation and capsular types in isolates of *Staphylococcus aureus* from different sources and relationship to phage types. *J Clin Microbiol* **22**, 828-834.

Stranden, A. M., Ehlert, K., Labischinski, H. & Berger-Bachi, B. (1997). Cell wall monoglycine cross-bridges and methicillin hypersusceptibility in a *femAB* null mutant of methicillin-resistant *Staphylococcus aureus*. *J Bacteriol* **179**, 9-16.

Ton-That, H., Labischinski, H., Berger-Bachi, B. & Schneewind, O. (1998). Anchor structure of staphylococcal surface proteins. III. Role of the FemA, FemB, and FemX factors in anchoring surface proteins to the bacterial cell wall. *J Biol Chem* **273**, 29143-29149.

Tzagoloff, H. & Novick, R. (1977). Geometry of Cell-Division in *Staphylococcus aureus*. *J Bacteriol* **129**, 343-350.

Walter, J., Loach, D. M., Alqumber, M., Rockel, C., Hermann, C., Pfitzenmaier, M. & Tannock, G. W. (2007). D-alanyl ester depletion of teichoic acids in *Lactobacillus reuteri* 100-23 results in impaired colonization of the mouse gastrointestinal tract. *Environ Microbiol* **9**, 1750-1760.

Weart, R. B., Lee, A. H., Chien, A. C., Haeusser, D. P., Hill, N. S. & Levin, P. A. (2007). A metabolic sensor governing cell size in bacteria. *Cell* **130**, 335-347.

Webb, A. J., Karatsa-Dodgson, M. & Gründling, A. (2009). Two-enzyme systems for glycolipid and polyglycerolphosphate lipoteichoic acid synthesis in *Listeria monocytogenes*. *Mol Microbiol* **74**, 299-314.

Weidenmaier, C., Kokai-Kun, J. F., Kristian, S. A. & other authors (2004a). Role of teichoic acids in *Staphylococcus aureus* nasal colonization, a major risk factor in nosocomial infections. *Nat Med* **10**, 243-245.

Weidenmaier, C., Kokai-Kun, J. F., Kristian, S. A. & other authors (2004b). Role of teichoic acids in *Staphylococcus aureus* nasal colonization, a major risk factor in nosocomial infections. *Nat Med* **10**, 243-245.

Weidenmaier, C., Peschel, A., Xiong, Y. Q., Kristian, S. A., Dietz, K., Yeaman, M. R. & Bayer, A. S. (2005). Lack of wall teichoic acids in *Staphylococcus aureus* leads to reduced interactions with endothelial cells and to attenuated virulence in a rabbit model of endocarditis. *J Infect Dis* **191**, 1771-1777.

Weidenmaier, C. & Peschel, A. (2008). Teichoic acids and related cell-wall glycopolymers in Gram-positive physiology and host interactions. *Nature reviews Microbiology* **6**, 276-287.

White, D. C. & Frerman, F. E. (1967). Extraction, characterization, and cellular localization of the lipids of *Staphylococcus aureus*. *J Bacteriol* **94**, 1854-1867.

Wörmann, M. E., Corrigan, R. M., Simpson, P. J., Matthews, S. J. & Gründling, A. (2011a). Enzymatic activities and functional interdependencies of *Bacillus subtilis* lipoteichoic acid synthesis enzymes. *Mol Microbiol* **79**, 566-583.

Wörmann, M. E., Reichmann, N. T., Malone, C. L., Horswill, A. R. & Gründling, A. (2011b). Proteolytic Cleavage Inactivates the *Staphylococcus aureus* Lipoteichoic Acid Synthase. *J Bacteriol* **193**, 5279-5291.

Wyke, A. W., Ward, J. B., Hayes, M. V. & Curtis, N. A. (1981). A role in vivo for penicillin-binding protein-4 of *Staphylococcus aureus*. *Eur J Biochem* **119**, 389-393.

Xia, G., Kohler, T. & Peschel, A. (2010). The wall teichoic acid and lipoteichoic acid polymers of *Staphylococcus aureus*. *Int J Med Microbiol* **300**, 148-154.

6. Annex

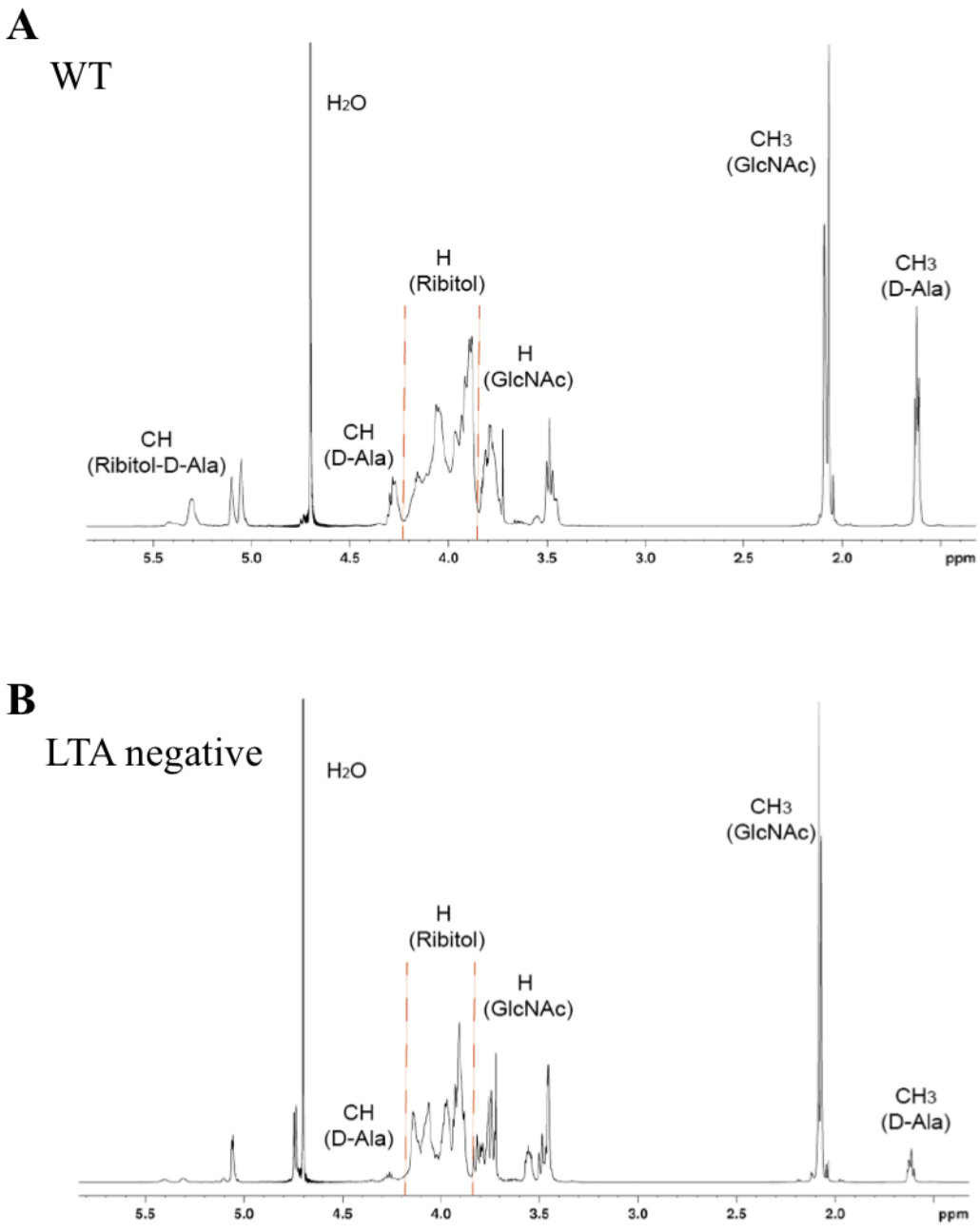

(Reichmann *et al.*, 2013)

Figure S1 – Full spectra from NMR analysis of WTA isolated from WT and LTA negative *S. aureus* strains. *S. aureus* strains WT and 4S5 (LTA negative) where grown to mid-log phase and WTA purified as described in the Materials and Methods section. Six mg of dried WTA were suspended in 99.99 % D_2O and 1-D proton spectra acquired at 600 MHz. The experiment was performed in triplicate and representative full spectra are shown. The ratio of the D-Ala to GlcNAc signal is 0.54 ± 0.08 for WTA isolated from a WT strain and 0.11 ± 0.01 for WTA isolated from the LTA negative strain. Peaks are annotated as previously described (Bernal et al, 2009).